# KINESIN-1 REGULATES SYNAPTIC STRENGTH BY MEDIATING DELIVERY, REMOVAL AND REDISTRIBUTION OF AMPARS

by

Dane Arthur Maxfield

A dissertation submitted to the faculty of
The University of Utah
in partial fulfillment of the requirements for the degree of

Doctor of Philosophy

Department of Biology

The University of Utah

May 2014

# The University of Utah Graduate School

## STATEMENT OF DISSERTATION APPROVAL

The dissertation of **Dane Arthur Maxfield**

has been approved by the following supervisory committee members:

| | | |
|---|---|---|
| **Andres Villu Maricq** | , Chair | **1/6/2014** Date Approved |
| **Michael Vershinin** | , Member | **1/6/2014** Date Approved |
| **Markus Babst** | , Member | **1/6/2014** Date Approved |
| **Julie Hollien** | , Member | **1/6/2014** Date Approved |
| **Erik Jorgensen** | , Member | **1/6/2014** Date Approved |

and by **Neil Vickers**, Chair of the Department of **Biology**

and by David B. Kieda, Dean of The Graduate School.

# ABSTRACT

The cellular processes that govern neuronal function are highly complex and tightly regulated in order to perform the elaborate information processing achieved by the brain. This is particularly evident in the trafficking of membrane proteins to and from synapses, which can travel long distances away from the cell body. Regulation of neurotransmitter receptors such as the AMPA-type glutamate receptor (AMPAR), the major excitatory neurotransmitter receptor in the brain, is a crucial mechanism for the modulation of synaptic transmission. Yet, the mechanisms by which AMPARs are transported over long distances are still unclear. We have addressed this question through genetic, cell biological and electrophysiological analysis of the *C. elegans* AMPAR GLR-1. This dissertation describes the role of long-range transport of AMPARs in the regulation of synaptic strength and provides insights into the cellular mechanisms underlying learning and memory.

The pair of interneurons AVA expresses GLR-1 and are part of a well-defined circuit regulating the forward and backward movement of *C. elegans* in response to sensory inputs. To determine the mechanism for GLR-1 delivery to a synapse, we monitored the real-time trafficking of a fluorescently tagged GLR-1 chimera in AVA. We show that UNC-116, the *C. elegans* homolog of the vertebrate kinesin-1 (KIF5), is responsible for mediating the rapid, bidirectional

transport of GLR-1. This motor-driven transport of GLR-1 modifies synaptic strength by mediating the rapid delivery, removal and redistribution of synaptic AMPARs. In the absence of *unc-116*, we found that although homomeric GLR-1 AMPARs can still diffuse to and accumulate at proximal synapses, glutamate-gated currents are decreased due to lack of heteromeric GLR-1/GLR-2-containing AMPARs. Furthermore, we show that transient expression of UNC-116 can rescue defective glutamatergic signaling in adult *unc-116* mutants, demonstrating that motor-dependent transport is ongoing in the adult nervous system and is involved in the regulation of synaptic strength. These data have allowed us to establish a link between motor-dependent transport of AMPARs and the strength of synaptic transmission.

To my parents, Karl and Joni, and my wife, Tabitha

for their constant support and encouragement.

TABLE OF CONTENTS

LIST OF FIGURES

# ACKNOWLEDGMENTS

A number of people have had a profound effect on my graduate school experience. First and foremost, I'd like to express my gratitude to my advisor, Dr. A. Villu Maricq. Thank you for taking a chance on this mathematician and for all your support and encouragement throughout the years. You have helped me to realize my scientific potential and pushed me to succeed both personally and professionally.

There are many members of the scientific community that I would like to acknowledge. Thank you to the members of my thesis committee: Dr. Markus Babst, Dr. Erik Jorgensen, Dr. Julie Holien and Dr. Michael Vershinin, for all of your guidance and enthusiasm throughout my graduate career. Additionally, I would like to thank Dr. James Keener and Dr. Paul Bressloff in the Mathematical Biology Program for initially bringing me to Utah and for their support and advice during my master's work. Finally, I'd like to extend a special thank you to Tony Cooke and Dr. Robin Battye for teaching me all aspects of microscopy and getting me into the "family."

Life in the lab would have not been the same without my awesome lab mates in the Maricq and Jorgenson laboratories. I am grateful for all your help and encouragement. I would like to thank Jerry Mellem, Penny Brockie, Fred Hörendli, Dave Madsen, Jann Gardner, Mike Jensen, Craig Walker, Rui Wang,

Colin Thacker, Angy Kallarackal, Randi Rawson, Rob Hobson and Christian Frøkjær-Jensen.

To my "work wife" and good friend, Amber Smith, thank you for your friendship and valuable advice throughout the years. No matter what the situation, everything from last minute text edits to sanity beverages, you have always been just a phone call away.

Finally, I would like to thank my friends and family for their never-ending encouragement throughout the years, especially my wife, Tabitha. Tabitha, you are my source of inspiration and a driving force in my life. This journey would not have been possible without you and your support.

# CHAPTER 1

# INTRODUCTION

## Overview

Learning and memory are essential for all aspects of life. The ability to process information and learn in response to experience is due to continual changes in the efficacy of neuronal communication. It is thought that experiences can modify neuronal communication by strengthening some neuronal pathways within a circuit and weakening others (Hebb, 1949). Identifying how these connections are modified, where in the brain the modifications occur, and how this leads to changes in behavior, learning and memory is a major goal of neuroscience.

The adult human brain contains over 100 billion neurons, which are interconnected with one another via trillions of specialized points of contact. These interconnected webs of neurons form networks of neural circuits that regulate the behavioral abilities and thought processes of an animal. The complex nervous system of humans and other vertebrates has hindered progress in understanding how the nervous system facilitates changes in the strength of neuronal communication at the circuit, cellular and molecular levels. To circumvent this, many studies have taken advantage of the simple nervous systems of model organisms such as the soil nematode *Caenorhabditis elegans*. Manipulation of this simple nervous system can be used to uncover the pathways regulating changes in the strength of synaptic communication.

We sought to uncover the gene products and pathways that regulate synaptic strength in *C. elegans* by using genetic, molecular and electrophysiological techniques. We first characterize the pathway required for

trafficking of molecules necessary for neuronal communication, then identify the gene products that regulate trafficking, and lastly determine the mechanism by which trafficking regulates synaptic strength. This work offers new insights into the mechanisms underlying experience-dependent changes in neuronal communication and the promise of novel strategies for the treatment of mental health and neurological disorders.

## Communication Between Neurons

Neurons send and receive information through specialized points of contact called synapses (Sudhof, 2004). At the synapse, a presynaptic neuron and a postsynaptic neuron are separated by a small gap called the synaptic cleft. Electrical activity in the presynaptic nerve terminal results in the rapid fusion of synaptic vesicles filled with small signaling molecules (neurotransmitters) with the plasma membrane. Consequently, the neurotransmitters contained in the synaptic vesicle are released into the synaptic cleft, diffuse across, bind to and activate the corresponding neurotransmitter receptors on the postsynaptic membrane (Figure 1.1). Binding of a neurotransmitter to its respective receptor initiates a signaling cascade that is specific to the type of neurotransmitter released (Sudhof, 2004).

There are two distinct classes of neurotransmitter receptors in the membrane of postsynaptic cells – metabotropic and ionotropic (Kew and Kemp, 2005). Metabotropic receptors are G-protein-coupled receptors that signal on a slow timescale through diverse second messenger pathways in cells.

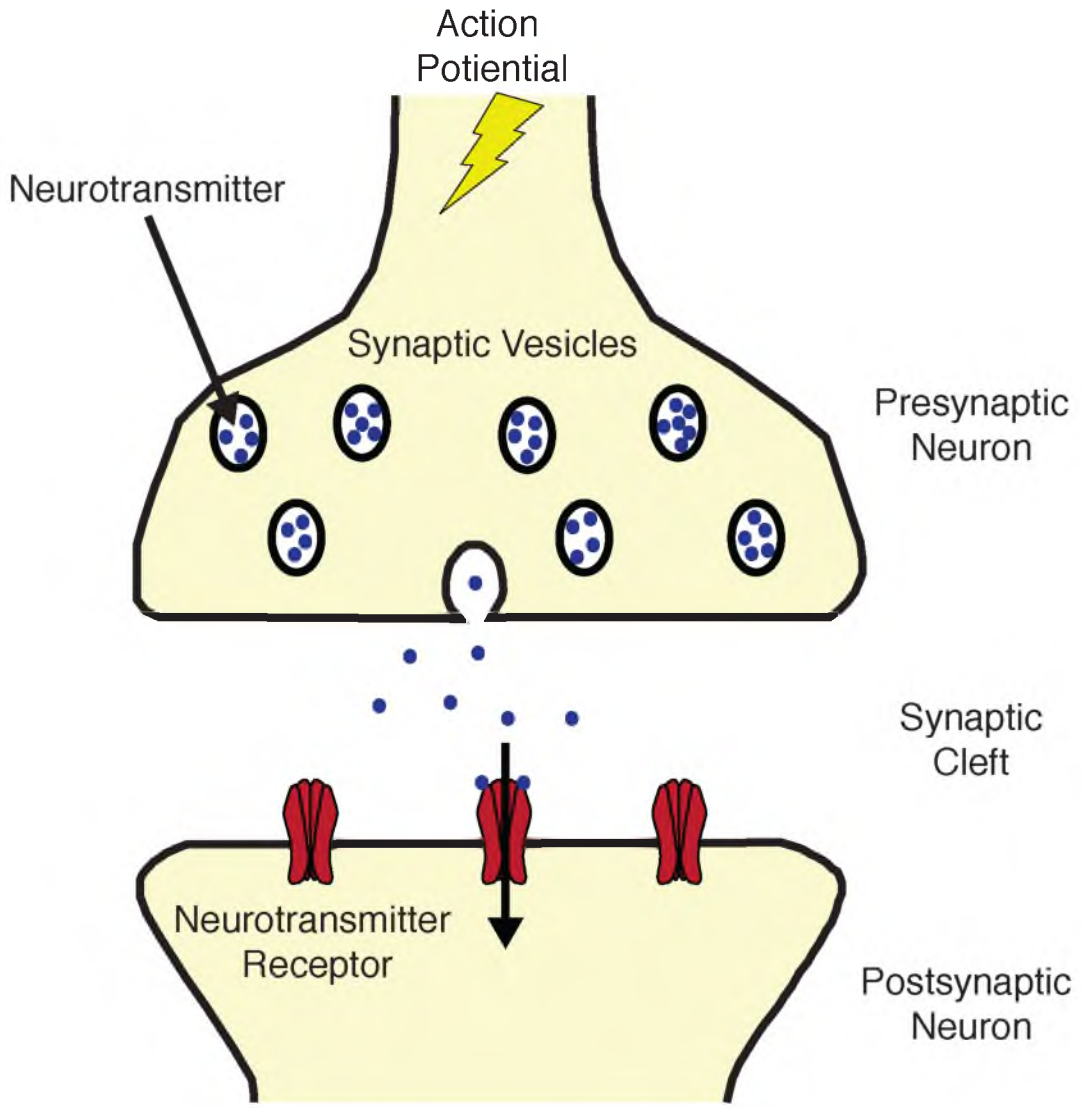


**Figure 1.1.** The chemical synapse. Depolarization of the presynaptic neuron by an action potential (lightning bolt) triggers synaptic vesicles filled with neurotransmitters to fuse to the presynaptic membrane, releasing neurotransmitters into the synaptic cleft. Neurotransmitters diffuse across the synaptic cleft and bind to the corresponding neurotransmitter receptors on the plasma membrane of the postsynaptic cell. Binding of neurotransmitter to its respective ionotropic neurotransmitter receptor gates open the ion pore, allowing charged ions (cations or anions) to pass through the postsynaptic membrane.

Conversely, ionotropic receptors are composed of several protein subunits that combine together to form either homomeric or heteromeric channels that contain an ion pore. Upon binding of the ligand, the pore of the ionotropic receptor gates open, allowing ions to traverse the cell membrane. This influx of ions causes a rapid change in the membrane potential of the cell. Ion channels that are permeable to cations ($Na^+$, $K^+$, $Ca^{2+}$) depolarize the cell membrane causing neuronal excitation, whereas channels permeable to anions ($Cl^-$) hyperpolarize the cell and are inhibitory. Glutamate is an excitatory neurotransmitter that controls a broad range of neuronal functions by activating a diverse set of ionotropic and metabotropic glutamate receptors (Kew and Kemp, 2005; Nakanishi, 1994).

## Vertebrate Ionotropic Glutamate Receptors

The neurotransmitter glutamate mediates the vast majority of fast excitatory neurotransmission in the brain (Brockie and Maricq, 2010). The importance of glutamatergic neurotransmission is illustrated by the wide range of neurological processes that glutamate influences and the variety of disorders that arise when it is disrupted. For example, glutamate receptors have been shown to have critical roles in development, learning and memory (reviewed in Chen and Tonegawa, 1997). In addition, the disruption of glutamatergic signaling has been implicated in a variety of neurological disorders including schizophrenia, Parkinson's disease, Alzheimer's disease, amyotrophic lateral sclerosis (ALS), and excitotoxicity associated with epileptic seizures and ischemic brain damage

(Meldrum, 1994; Mody, 1998; Montastruc et al., 1997; Nakajima et al., 2012; Ułas et al., 1994).

Eighteen ionotropic glutamate receptor (iGluR) subunits, which co-assemble to form functional receptors with highly varying properties, have been identified in the rat. Comparing the sequences of various iGluR subunits shows up to 80% similarity and the conservation of intron and exon structures (Suchanek et al., 1995; Wenthold et al., 1992). These different iGluR subunits can be separated into two different classes based on reactivity to the pharmacological agonist *N*-methyl-D-aspartate (NMDA): the NMDA and non-NMDA classes (reviewed in Dingledine et al., 1999). The 11 subunits of the non-NMDA class can be further subdivided based on their sensitivity to α-amino-3-hydroxy-5-methyl-4-isoxazolepropionic acid (AMPA) and those sensitive to kainate (KA) (reviewed in Dingledine et al., 1999). There is also an additional class of iGluRs, the delta class, which fail to respond to any known iGluR agonist yet show molecular identity to other iGluR subunits (Mayer, 2006; Watkins and Jane, 2006; Yamazaki et al., 1992; Zuo et al., 1997).

## Glutamate Receptor Topology, Stoichiometry and Kinetics

Ionotropic glutamate receptors are integral membrane proteins composed of four large subunits, each around 900 residues, which form an ion channel. Detailed crystallographic descriptions of iGluRs along with functional and biochemical data show that iGluRs form as tetrameric channels (Armstrong and Gouaux, 2000; Armstrong et al., 1998; Dingledine et al., 1999; Laube et al.,

1998; Rosenmund et al., 1998; Sobolevsky et al., 2009). A functional iGluR is formed when subunits of the same class co-assemble to create a ligand-gated ion channel, e.g., AMPA subunits assemble with other members of the AMPA subfamily (Ayalon and Stern-Bach, 2001; Laube et al., 1998; Mano and Teichberg, 1998; Rosenmund et al., 1998). These oligomeric combinations are formed in the endoplasmic reticulum (ER), possibly assembling as a dimer-of-dimers (Tichelaar et al., 2004). In addition to heteromeric receptors, some subunits are also capable of forming homomeric receptors. This diversity is further increased through posttranscriptional splice variants and RNA editing of iGluRs (Seeburg et al., 1998). These mechanisms result in a complex and diverse family of iGluRs that differ in kinetics, ion permeability and pharmacological specificity (detailed below); which are capable of regulating a wide range of neurological functions.

Due to the high sequence homology between the different iGluR subunits, all iGluRs are thought to have the same structure and topology (Figure 1.2A). Individual receptor subunits have discrete domains; an extracellular N-terminal domain; two extracellular domains, S1 and S2, that form the ligand binding site; four hydrophobic transmembrane domains (three true transmembrane domains and one re-entrant loop); and an intracellular C-terminal domain. Each of these domains plays a different role in receptor function. The N-terminal domain regulates the association between subunits (Ayalon and Stern-Bach, 2001; Ayalon et al., 2005), the S1 and S2 domains regulate desensitization

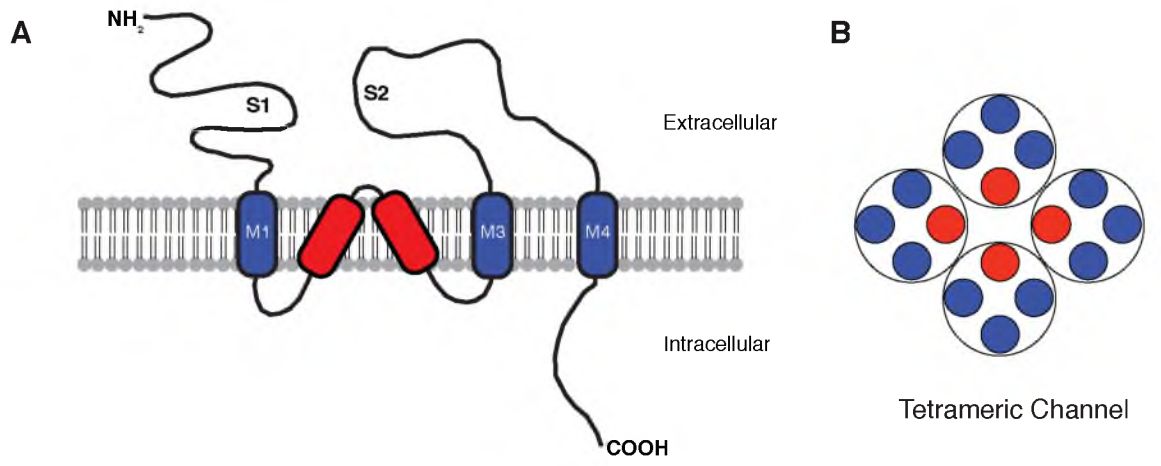


**Figure 1.2**. Glutamate receptor stoichiometry and structure. A) Ionotropic glutamate receptor subunits contain three transmembrane domains (blue) and a re-entrant loop (red). The binding site for glutamate is formed by the S1 domain in the extra-cellular N-terminus and S2 domain in the extracellular loop between M3 and M4. B) The iGluR channel is formed by a tetrameric assembly of subunits with the re-entrant loop lining the pore of the receptor (top view).

(Stern-Bach et al., 1994), and the C-terminal domain mediates receptor localization (Daw et al., 2000; Osten et al., 2000).

Once iGluRs have been assembled and localized, receptors can transduce the appropriate signal in response to glutamate binding. In the absence of the presynaptic release of glutamate, the iGluR channel remains in the closed state. Opening, and thus activation of the channel, can be achieved by glutamate binding to each receptor subunit in the S1 and S2 ligand-binding domain. To facilitate ligand binding, the S1 and S2 domains adopt a clamshell-like formation with each domain forming half of the clamshell and the agonist-binding pocket located between them (reviewed in Dingledine et al., 1999). When glutamate binds in this pocket, the resulting conformational change moves the S1 and S2 domains closer together. How this conformational change leads to the pore opening is still not fully understood.

The ion pore of the iGluR is formed by the amino acids of the M2 re-entrant loops of each of the four subunits (Figure 1.2B). The amino acids of the inner cavity of the pore determine the ion selectivity. All iGluRs are permeable to $Na^+$ and $K^+$, but $Ca^{2+}$ permeability is highly regulated due to its role in intracellular signaling cascades. The $Ca^{2+}$ permeability of iGluRs is largely dependent on the subunit composition of the channel and on a specific amino acid at the mouth of the pore, called the Q/R site. Both AMPA and kainate receptor subunits encode a glutamine (Q) at this site, which allows these subunits to have a high permeability to $Ca^{2+}$. However, posttranscriptional RNA editing can modify this site to an arginine (R) residue, resulting in decreased $Ca^{2+}$ permeability (Bass,

2002; Dingledine et al., 1999; Sommer et al., 1991). On the other hand, NMDA receptors (NMDAR) are $Ca^{2+}$ permeable when activated. However, the activation of NMDARs requires both presynaptic neurotransmitter release and post-synaptic depolarization (Ho et al., 2011).

Termination of synaptic signaling through iGluR channels is essential for proper synaptic signaling and can occur in one of two ways. The first is through agonist dissociation from the receptor. This allows the conformational change induced by agonist binding to be relaxed, thereby restoring the iGluR to the closed inactive state. Alternatively, the receptor can adopt an additional conformational state where the iGluR remains bound to glutamate yet the channel closes (Figure 1.3) (Jones and Westbrook, 1996). This is called a desensitized state and occurs during the continued presence of glutamate. Receptors can then recover from the desensitized state by releasing the agonist and again become competent for activation. Desensitization of receptors is an important process for maintaining the proper function and signaling of iGluRs. This step is of critical importance for the cessation of receptor signaling when glutamate clearance from the synaptic cleft is not achieved due to a high frequency of release events, multiple presynaptic inputs at a synapse, or spillover from nearby synapses (Jones and Westbrook, 1996; Otis et al., 1996; Stern-Bach et al., 1998; Trussell and Fischbach, 1989). Differential rates of desensitization and of receptor recovery from desensitization also play a role in the extent and duration of the postsynaptic response (Dingledine et al., 1999).

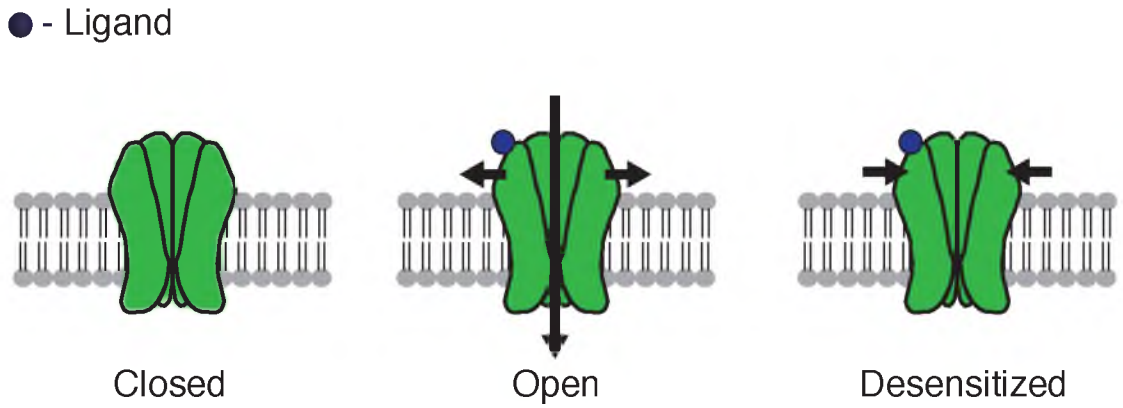


**Figure 1.3.** Desensitization of ionotropic glutamate receptors. The binding of ligand (blue) to a closed receptor causes a conformational change, opening the receptor (horizontal arrows) and allowing ions to flow through (vertical arrow). The receptor rapidly closes (horizontal arrows) in the presence of ligand, entering a desensitized state. Removal of the ligand returns the receptor to the closed state, allowing for activation upon ligand binding.

## Glutamate Receptor Localization in the Brain

Within the vertebrate central nervous system, iGluRs are expressed in almost all neurons and in some glial cells. Glutamate receptor expression is not static; rather, it varies in a cell-specific manner throughout development and in response to environmental factors. The level of expression of each iGluR subunit is determined at any particular time by a balance in the rates of gene transcription, mRNA translation, mRNA degradation, and protein degradation. Additional processes, such as receptor assembly in the ER and synaptic targeting, allow for further control over the levels of functional receptors in the cell. This is further complicated by the expression of several classes of iGluR subunits in most cells. Thus, the postsynaptic response is defined by the various iGluRs expressed within a particular cell and how they are arranged at individual synapses.

In the brain, iGluRs are required for the expression of synaptic plasticity, the cellular model of learning and memory (reviewed in Peng et al., 2011). There are two major types of synaptic plasticity, known as long-term potentiation (LTP) and long-term depression (LTD) (reviewed in Song and Huganir, 2002). LTP results in the strengthening of glutamatergic signaling between neurons, whereas LTD results in the weakening of this signal. Perturbations in glutamatergic signaling prevent the induction of LTP and LTD, leading to defects in learning and memory (Henley and Wilkinson, 2013; Huganir and Nicoll, 2013). Over the last 25 years, a myriad of studies have focused on the cellular trafficking of the AMPA-type glutamate receptor (AMPAR) due to its central role in synaptic

plasticity. These studies have proved useful in elucidating many of the cell biological processes involved in synaptic function.

## AMPAR Localization and Auxiliary Proteins

Proper AMPAR localization to a region of the synapse called the post-synaptic density (PSD) is crucial for efficient synaptic transmission. One of the major molecular mechanisms that controls the localization of AMPARs within the PSD is the interaction of the C-termini of AMPARs with PSD-95/DLG/ZO-1 (PDZ) containing intracellular scaffolding molecules. Several glutamate receptor-associated proteins containing PDZ domains have been identified, including PSD-95 family members GRIP1 and GRIP2, also known as ABP (AMPA receptor-binding protein) (Scannevin and Huganir, 2000; Tomita et al., 2001). These proteins have been shown to regulate the stability of AMPARs in the membrane through interactions of their respective PDZ domains (Daw et al., 2000; Osten et al., 2000). In the PSD, AMPARs are not uniformly distributed but are confined to subsynaptic domains and positioned near presynaptic release sites (Ehlers et al., 2007; Kerr and Blanpied, 2012; MacGillavry et al., 2013).

Once properly localized to the synapse, AMPARs must then be expressed on the cell surface and able to open in response to glutamate. Recently, it was discovered that AMPARs associate with auxiliary proteins, which regulate their surface expression and function at the synapse. The first AMPAR auxiliary protein was identified from a spontaneous mouse mutation in a gene encoding a multiple transmembrane protein called stargazin (Letts et al., 1998). Recordings

from cerebellar granule cells expressing the stargazin mutation revealed a significant loss of AMPA-mediated currents while showing normal NMDA-mediated currents (Chen et al., 2000), demonstrating that stargazin is critically required for surface expression of AMPARs. Stargazin and its closely related paralogs belong to a family of proteins that interact with AMPAR subunits termed transmembrane AMPA-receptor regulatory proteins (TARPs), which direct the proper expression and localization of AMPARs (Chen et al., 2000; Letts et al., 1998; Schnell et al., 2002; Tomita et al., 2003). In addition to regulating surface expression and localization, TARPs have also been shown to modify AMPAR function. AMPARs associated with TARPs show increased single-channel conductance, open probability and activation rates while having a reduced rate of desensitization and a slower deactivation time course (Priel et al., 2005; Tomita et al., 2005; Yamazaki et al., 2004).

More recently, an additional class of proteins, called cornichons, have been implicated as AMPAR auxiliary proteins (Schwenk et al., 2009). Cornichon was originally identified in Drosophila as a protein required for the ER export of the EGF-like ligand Gurken (Bökel et al., 2006; Roth et al., 1995). However, affinity purification of AMPARs from rat brain followed by mass spectroscopy analysis identified the cornichon proteins CNIH-2 and CNIH-3 as AMPAR-interacting proteins. When co-expressed with AMPARs in heterologous systems, CNIH-2 and CNIH-3 modified AMPAR desensitization, deactivation and surface expression (Coombs et al., 2012; Kato et al., 2010; Schwenk et al., 2009; Shi et al., 2010). Recently, two studies have shown that cornichons function to regulate

the trafficking of AMPARs in neurons (Brockie et al., 2013; Herring et al., 2013); yet, it is still unclear if cornichon functions as an auxiliary protein at synapses *in vivo.*

## AMPAR Trafficking at the Synapse

Changes in the number of AMPARs at the synapse tunes synaptic efficacy. Such modifications are dependent on the availability of receptor binding sites and on the equilibrium of receptor efflux and influx (Newpher and Ehlers, 2008; Shepherd and Huganir, 2007). Synaptic AMPARs are not stable, but rather are constantly diffusing in and out of the PSD and recycling between intracellular compartments and the postsynaptic membrane. This dynamic process controls the number of surface-expressed AMPARs and is of central importance for synaptic plasticity (Contractor and Heinemann, 2004; Malinow and Malenka, 2002; McGee and Bredt, 2003). The number of AMPARs at the synapse is estimated to be 50-100 by anatomical methods (Tanaka et al., 2005) and between 60-190 using physiological methods (Matsuzaki et al., 2001; Smith et al., 2003). Single molecule tracking and fluorescent recovery after photobleaching (FRAP) experiments revealed both mobile and immobile synaptic receptors numbering from 50-200 (Ashby et al., 2006; Tardin et al., 2003). The cell controls the number of surface expressed receptors through a dynamic balance of exocytosis, endocytosis and trapping of AMPARs in the PSD. AMPARs are first delivered to the surface via SNARE-dependent exocytosis (Lu et al., 2001). This process has been shown to be regulated in response to

synaptic activity (Yudowski et al., 2007). However, where these AMPAR exocytosis events take place is still a matter of debate. Some studies propose that AMPAR exocytosis occurs directly at the synapse (Gerges et al., 2006; Patterson et al., 2010), while others suggest exocytosis takes place in the dendrite near the synapse (Jaskolski et al., 2009; Makino and Malinow, 2009; Yudowski et al., 2007).

Once AMPARs are on the plasma membrane, they can move in and out of the synapse and between neighboring synapses via lateral diffusion (Borgdorff and Choquet, 2002; Groc et al., 2004; Opazo et al., 2010; Tardin et al., 2003). At the synapse, AMPARs exist in two populations: mobile and immobile. AMPARs inside the PSD show less mobility than AMPARs in the extrasynaptic space (Tardin et al., 2003). In addition, the mobility of AMPARs in the membrane is altered in response to synaptic activity. Active synapses capture diffusing AMPARs and inactive synapses release AMPARs to diffuse away (Ehlers et al., 2007; Lu et al., 2010; Makino and Malinow, 2009; Patterson et al., 2010; Tardin et al., 2003). This diffusional trapping is dependent on the interaction of the cytoskeletal protein PSD-95 with stargazin-bound AMPARs as they diffuse on the plasma membrane (Bats et al., 2007).

Surface-expressed AMPARs can be removed from the plasma membrane by endocytosis. Endocytic zones can be found in the lateral margins of excitatory synapses next to the PSD (Blanpied et al., 2002). Displacing endocytic zones disrupts AMPAR removal from the synapse and reduces the mobile pool of receptors at the surface (Petrini et al., 2009). After internalization,

AMPARs can be sorted into one of two pathways. Endocytosed AMPARs can be trafficked to early endosomes or to specialized recycling endosomes that allow for rapid reintroduction to the surface (Hanley, 2010). Alternatively, AMPARs can be sorted to late endosomes, which ultimately sends receptors to the lysosomes for degradation (Lee et al., 2004; Lu et al., 2007).

The trafficking of AMPARs at the synapse is also critically dependent on their subunit composition (Lu et al., 2009). In the hippocampus, it has been shown that the short-tailed subunits of the heteromeric GluA2/GluA3 AMPARs continuously cycle in and out of the synapse in an activity-independent manner (Passafaro et al., 2001; Shi et al., 2001). This process, termed constitutive recycling, is hypothesized to preserve the total number of AMPARs at the synapse and to maintain synaptic strength in the face of protein turnover (Zhu et al., 2000). Thus, in the absence of neuronal activity, AMPARs can go into synapses without changing the magnitude of synaptic transmission, suggesting a one-to-one exchange of AMPARs between extrasynaptic and synaptic sites (Kakegawa et al., 2004; Shi et al., 2001). Conversely, AMPARs with long-tailed subunits, such as GluA1, GluA2L (the long splice isoform of GluA2) or GluA4, are added to synapses in an activity-dependent manner during LTP (Hayashi et al., 2000; Kolleker et al., 2003; Makino and Malinow, 2009; Zhu et al., 2000). Formally, synaptic strengthening involves activity-dependent addition of long-tailed receptors, whereas synaptic weakening occurs through endocytosis of long-or short-tailed receptors.

## Models of Long-Range AMPAR Trafficking

Neurons pose a unique problem for the long-range trafficking of proteins due to their elaborate, highly polarized structure. Membrane proteins must travel extremely long distances and may be inserted at the plasma membrane far from their final destination. Although much is known about the local dynamics of AMPARs at the level of the synapse (discussed above), it is still an open question as to how AMPARs are trafficked to the synapse in the first place (Figure 1.4). It is generally accepted that AMPARs are synthesized in the cell body or soma of a neuron. Then, AMPARs must be trafficked to the synapse where they function, although this trafficking pathway is still unresolved. Given the central importance of AMPARs in synaptic plasticity, it is imperative to understand the molecular mechanisms governing the long-range transport of AMPARs in neurons. However, relatively few studies have addressed this fundamental question.

One model of how AMPARs are trafficked from the soma to the synapse is that AMPARs are inserted into the plasma membrane at the cell body and are then trafficked to synapses via lateral diffusion. This model is supported by work that used a membrane-impermeable, irreversible, photoreactive AMPAR agonist 6-azido-7-nitro-1,4-dihydroquinoxaline-2,3-dione (ANQX) (Chambers et al., 2004) to inactivate surface AMPARs. By monitoring the recovery of AMPA-mediated currents with electrophysiology after photoinactivation of surface AMPARs, Adesnik et al. showed that it took approximately 16 hours for AMPA-mediated currents to recover (Adesnik et al., 2005). These data suggest that most

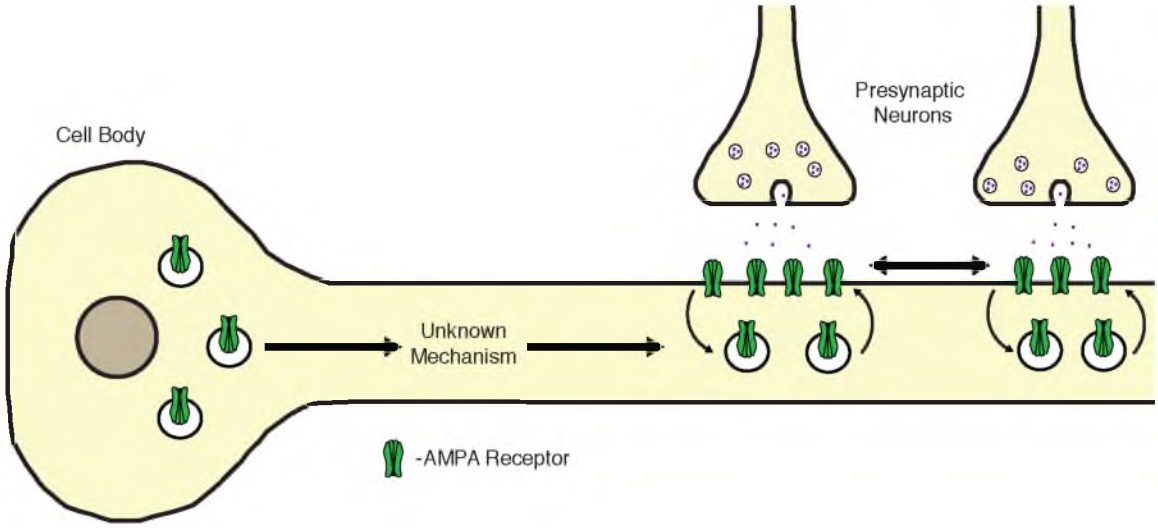


**Figure 1.4.** Overview of AMPAR transport. A cartoon schematic showing the trafficking pathways of AMPARs. At synapses, AMPARs can move via lateral diffusion in the plasma membrane between neighboring synapses. A dynamic balance of endocytosis and exocytosis regulates the level of surface-expressed receptors at synapses. The mechanism of long-range AMPAR transport to the synapse is unresolved.

long-range transport of AMPARs occurs by lateral diffusion in the membrane. Although the rapid recycling of AMPARs with internal stores does occur, it is not the major source of functional synaptic AMPARs (Adesnik et al., 2005). However, mathematical modeling studies of long-range AMPAR transport concluded that lateral diffusion alone would be insufficient for the delivery of AMPARs from the soma to distal dendrites (Earnshaw and Bressloff, 2008), suggesting there must be an additional active component to long-range AMPAR trafficking.

One such active process that would allow for the rapid delivery of proteins over long distances is molecular-motor-mediated transport. The molecular motors kinesin and dynein are part of a large family of proteins that move along microtubules (MTs) (Goldstein and Yang, 2000). Microtubules have defined polarity with a plus end and a minus end. In general, the motor protein family dynein moves towards the minus end of MTs, whereas the kinesin family moves to the plus end (Goldstein and Yang, 2000). Because dendrites contain MTs of mixed polarities (Baas, 1999), both dynein and kinesin could mediate transport of cargo from the soma into dendrites. In fact, disruption of both kinesin and dynein function with monoclonal antibodies has been shown to reduce AMPAR-mediated currents *in vitro* (Kim and Lisman, 2001), suggesting a role for motor-mediated transport in the delivery of AMPARs to synapses. Furthermore, yeast-two-hybrid experiments have shown that the AMPAR-interacting protein, GRIP1, can bind to the kinesin-1 KIF5 (Setou et al., 2002). The interaction between GRIP1 and KIF5 steers the motor complex into dendrites and is predicted to be

involved in the transport of AMPARs (Setou et al., 2002). However, direct measurements of AMPAR localization and trafficking after the disruption of motor-driven transport are not yet available.

Another model for the long-range transport of AMPARs to the synapse is that AMPARs are locally synthesized in the dendrite. Having AMPARs synthesized in proximity to the synapse provides a local pool of receptors, which can rapidly transport to nearby synapses via lateral diffusion. Protein synthesis was historically thought to occur exclusively in neuronal cell bodies. However, since the identification of poly-ribosomes in hippocampal dendrites (Steward and Levy, 1982), local translation of proteins in dendrites has become widely accepted. Studies of hippocampal slices in which the dendrites have been severed from the cell bodies were found to retain the ability to express LTP and LTD, indicating that local translation can mediate long-term modifications in synaptic strength (Huber et al., 2000; Kang and Schuman, 1996). In agreement with this, direct evaluation of AMPAR mRNA distribution (Grooms et al., 2006) and AMPAR local synthesis (Ju et al., 2004) have shown dendritic synthesis of AMPARs to be an effective regulator of the local abundance and composition of receptors.

To date, the question of how AMPARs are transported over long distances to synapses is still without a definitive answer. Multiple studies using various techniques have lead to differing results on the relative roles of lateral diffusion, motor-mediated transport and local synthesis in long-range AMPAR transport. These competing models derive almost exclusively from *in vitro* studies in

cultured neurons and may not accurately reflect AMPAR transport *in vivo*. Therefore, in order to elucidate how AMPARs are transported to the synapse *in vivo,* we investigated the long-range AMPAR transport in the model organism *Caenorhabditis elegans*.

## *Caenorhabditis elegans*

*C. elegans* is a free-living soil-dwelling nematode that has been used as a model organism for studies of the cellular and molecular mechanisms that regulate synaptic function for nearly 40 years (Brenner, 1974). As a relatively simple organism, the worm is comprised of approximately 1000 cells and its genome has been fully sequenced. *C. elegans* exists as a self-fertilizing hermaphrodite with a life cycle of approximately 4 days at 20°C and generates a typical brood size of 300 progeny. The ability of *C. elegans* to self propagate is a tremendous advantage for genetic studies as recessive homozygous mutations can be readily isolated and maintained. Hermaphroditic worms also have the ability to mate with male worms, aiding in genetic manipulation and also providing a simple way to achieve specific genetic backgrounds.

The *C. elegans* nervous system has many attributes that make it a perfect choice for neurobiological studies. Relative to the nervous system of rat, mouse and *Drosophila*, the *C. elegans* nervous system is extremely small, consisting of only 302 neurons. In addition, the neuronal circuitry and synaptic connectivity of the hermaphroditic nervous system has been fully reconstructed from serial section electron microscopy (White et al., 1986). The *C. elegans* nervous system

consists of several identifiable head and tail ganglia that send out neuronal processes, which run longitudinally along the ventral nerve cord (VNC). Since the neuronal lineage is invariant among animals, this allows for reproducible identification of individual neurons. Importantly, *C. elegans* can survive elimination of genes that are highly detrimental to the function of the nervous system.

Since the initial use of *C. elegans* as a model system by Sydney Brenner (1974), there have been tremendous advances in the techniques and methodology used to manipulate the worm for biological studies. Transgenic animals can be generated through injecting DNA directly into the gonad of the worm (Berkowitz et al., 2008; Evans, 2006). As the cuticle of the worm is transparent, fluorescently labeled proteins can easily be imaged in live animals (Boulin, 2006). Mutant alleles can be easily generated by screening through animals that have been exposed to chemical mutagens or x-rays (Jorgensen and Mango, 2002). RNA interference (RNAi) is an extremely powerful genetic tool used to knock down expression of specific gene products. In the worm, this can be achieved by feeding worms bacteria that expresses a vector containing double-stranded RNA (dsRNA) specific to a particular gene. Upon entering the cell, dsRNA is cleaved into small interfering RNAs (siRNAs) which then bind to the their mRNA targets, causing them to be degraded (Kamath et al., 2001; Mello and Conte, 2004). In addition, dsRNA can also be used for tissue specific knockdown of specific gene products. This is achieved by generating transgenic

animals that express dsRNA under a tissue specific promoter (Esposito et al., 2007).

To effectively study the function of particular genes in the nervous system, methods that access and monitor the electrical responses of individual neurons are essential. The nervous system of *C. elegans* spans the length of the worm. The nerve ring, generally regarded as the brain of the worm, is a large bundle of many axons that form numerous synapses in the head of the animal. Electrophysiological procedures have been developed to achieve neuronal access in live immobilized worms where electrical activity can be monitored (Mellem et al., 2002). This is done by dissecting the cuticle along the anterior portion of the worm, allowing for electrical access to the head neurons. In this way, individual neurons can be tested for their responses to agonists as well as the effect of mutations on neuronal function (Brockie et al., 2001a; Mellem et al., 2002).

## Glutamatergic Signaling in *C. elegans*

Similar to the vertebrate nervous system, *C. elegans* also uses glutamatergic signaling as a major component of synaptic communication. At least 10 putative iGluR subunits are expressed in *C. elegans* (Brockie et al., 2001b). As with vertebrate iGluRs, *C. elegans* iGluRs can be separated via pharmacology and sequence similarity into NMDA and non-NMDA classes of receptors. Members of the non-NMDA class (GLR-1 – GLR-8) include subunits most similar to the AMPA and kainate class of receptors, whereas NMR-1 and

NMR-2 make up the NMDA class of receptors (Brockie et al., 2001b). The large number of iGluRs expressed in *C. elegans* suggests that the worm has the potential to express a wide variety of functional iGluRs.

The expression of fusion proteins between iGluRs and the green fluorescent reporter GFP in transgenic worms has revealed a detailed map of the expression pattern for each subunit (Brockie et al., 2001b). All iGluR subunits in *C. elegans* are restricted to expression within the nervous system, with varying degrees of overlapping expression patterns. The kainate receptor subunits GLR-3 and GLR-6 have the most limited expression pattern, appearing in only a single pair of interneurons called RIA. The non-NMDA subunits GLR-1, GLR-2, GLR-4 and GLR-5 and the NMDA subunits NMR-1 and NMR-2 are expressed in many of the command interneurons – AVA, AVB, AVD, AVE and PVC – a circuit that has been shown to control worm forward and backward movement (Figure 1.5) (Brockie et al., 2001a; Chalfie et al., 1985). The remaining two subunits, GLR-7 and GLR-8, are expressed in the neurons of the pharyngeal nervous system (Brockie et al., 2001b). This suggests that iGluR subunits with overlapping expression patterns might function as heteromeric receptors in these neurons.

The first iGluR subunit to be characterized in *C. elegans* was the AMPAR subunit GLR-1. Mutations in *glr-1* disrupt the backward movement in response to nose touch stimulation (Hart et al., 1995; Maricq et al., 1995), resulting from defective glutamatergic signaling between sensory neurons and the command interneurons expressing GLR-1 (Mellem et al., 2002). In addition, the GLR-2 subunit is expressed in many of the same neurons that express GLR-1, including

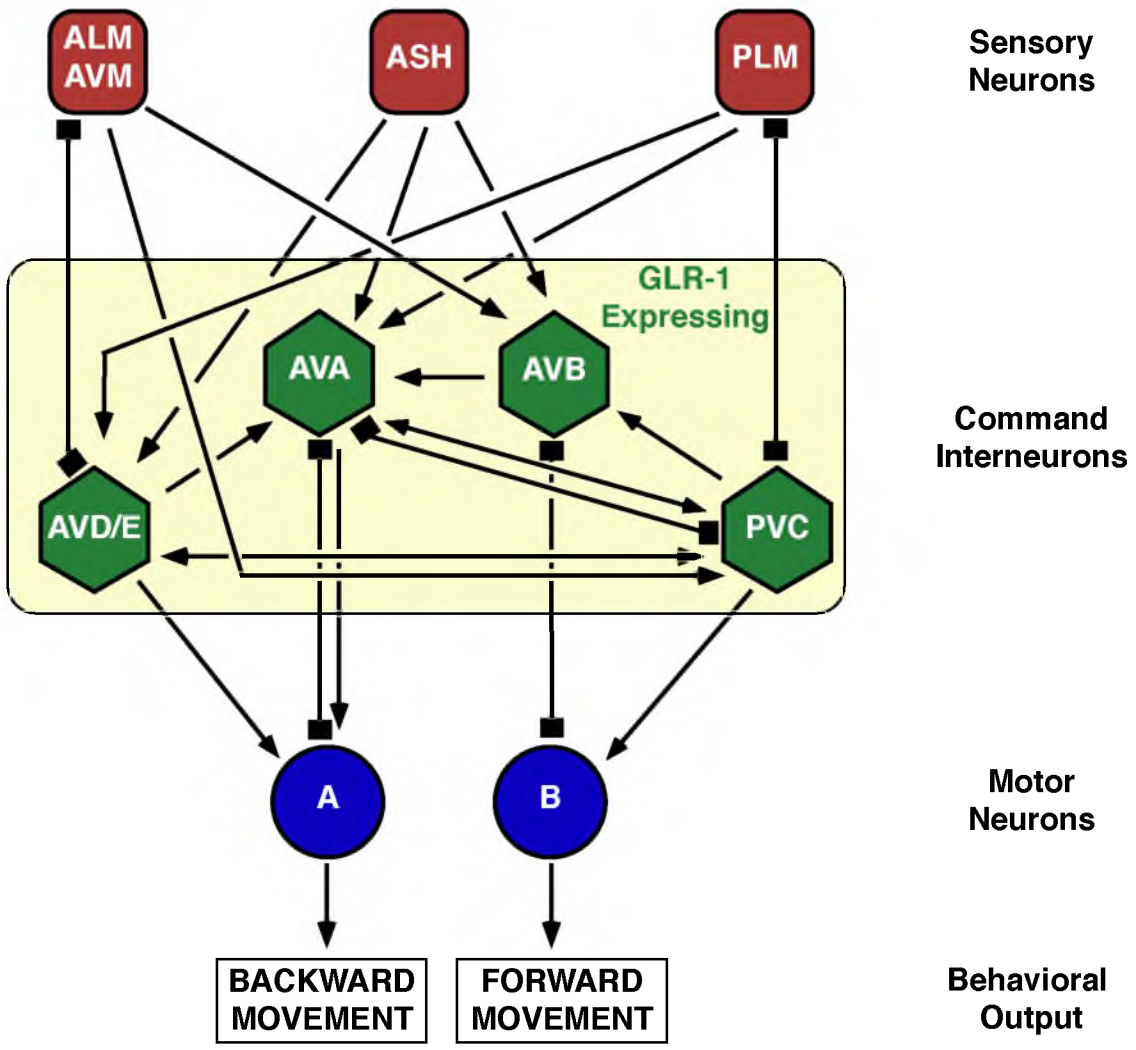


**Figure 1.5.** The *C. elegans* locomotory control circuit. The locomotory control circuit includes the sensory neurons ALM, AVM, ASH and PLM. These neurons receive sensory input from the external environment and relay this information to the GLR-1 expressing command interneurons AVA, AVB, AVD, AVE and PVC. The command interneurons process this information and activate VB or VA motor neurons to generate forward or backward movement, respectively. Chemical synapses are indicated by arrowheads and gap junctions by boxes.

the command interneurons. Mutations in *glr-1* and *glr-2* have the same behavioral defect, but are less severe in *glr-2* mutants (Mellem et al., 2002). Interestingly, glutamate-gated currents in the command interneuron AVA are completely absent in *glr-1* mutants. Yet, a small rapid current is still present in *glr-2* mutants, indicating that GLR-1 might form a homomeric receptor or a heteromeric receptor with other iGluR subunits (Mellem et al., 2002). Taken together, these data suggest that the vast majority of glutamatergic signaling in AVA is mediated by GLR-1/GLR-2 heteromeric AMPARs to facilitate backing in response to nose touch stimulation. In addition, this allows for the correlation between a known glutamate-dependent behavior and electrophysiology.

## GLR-1 Stability, Localization and Function at the Synapse

Which molecules are required for the proper trafficking of GLR-1 from the cell body to synaptic sites? To address this question, GLR-1::GFP fusion proteins have been used to observe the subcellular localization of GLR-1 (Brockie et al., 2001b; Burbea et al., 2002; Mellem et al., 2002; Rongo et al., 1998). These functional GLR-1::GFP proteins have proven to be invaluable for studies of GLR-1 trafficking, stability and localization to the synapse. In the neuronal process of transgenic animals, GLR-1::GFP is distributed in a punctate pattern. These GLR-1::GFP puncta have been shown to align with presynaptic markers and are likely to represent postsynaptic sites (Burbea et al., 2002; Rongo et al., 1998).

Since the initial identification of GLR-1 (Hart et al., 1995; Maricq et al., 1995), many gene products that regulate its localization have been identified. The first such discovery was the gene encoding *lin-10.* LIN-10 is a PDZ-domain protein involved in GLR-1 localization (Rongo et al., 1998). Mutations in *lin-10* change the distribution of GLR-1::GFP in the VNC, going from a punctate distribution in wild-type animals to a more uniform distribution in *lin-10* mutants (Rongo et al., 1998). Similar to *glr-1*, *lin-10* mutants are nose touch defective, further supporting the hypothesis that LIN-10 is involved in regulating GLR-1 localization and function (Rongo et al., 1998).

During *C. elegans* development, the density of GLR-1::GFP puncta remains constant despite a 10-fold increase in the size of the worm. The gene *unc-43*, which encodes the calmodulin-dependent protein kinase II (CaMKII), has been shown to be an important regulator of this process (Rongo and Kaplan, 1999). In *unc-43* loss-of-function mutants, the density of GLR-1::GFP puncta along the VNC is decreased and there is an observed increase of GLR-1::GFP in the cell body (Rongo and Kaplan, 1999). These findings suggest that UNC-43 functions during development to regulate trafficking of GLR-1 out of the cell body for the formation of new synapses (Rongo and Kaplan, 1999). Once the appropriate synaptic density has been established, UNC-43 might have an additional role at the synapse to maintain GLR-1 density (Rongo and Kaplan, 1999).

After GLR-1 has been localized to the synapse, endocytosis and membrane recycling play an important role in regulating the levels of GLR-1 at

the plasma membrane. An important regulator of this process is the *C. elegans* gene *unc-11*, which encodes an orthologue of the AP180 clathrin adaptor protein. Mutations in *unc-11* disrupt clathrin-mediated endocytosis (Nonet et al., 1999) and result in accumulations of GLR-1::GFP in the VNC (Burbea et al., 2002). GLR-1::GFP is also accumulated at synapses when ubiquitination of GLR-1 is blocked, suggesting that ubiquitinated GLR-1 receptors are endocytosed in an UNC-11-dependent manner (Burbea et al., 2002). In addition, GLR-1 can be recycled from the membrane via a clathrin-independent endocytosis pathway. In this pathway, the small GTPase RAB-10 and the PDZ-domain protein LIN-10 mediate the recycling of GLR-1 (Glodowski et al., 2007). GLR-1 trafficked through this pathway is thought to be mediated via the ubiquitin-conjugating enzyme *uev-1* (Kramer et al., 2010). In *uev-1* mutants, GLR-1 accumulates in RAB-10-containing endosomes and is predicted to have less surface-expressed GLR-1 based on behavioral data (Kramer et al., 2010).

Once at the synapse, GLR-1 must be competent to gate open in response to ligand binding. For years, iGluRs were thought to be stand-alone molecules; however, work in vertebrate systems and *C. elegans* has shown that this is not the case. The first AMPAR auxiliary protein identified in *C. elegans* was the CUB-domain transmembrane protein SOL-1 (Zheng et al., 2004). SOL-1 is required for GLR-1-dependent glutamate-gated currents and for behaviors that are dependent on GLR-1-mediated synaptic transmission (Zheng et al., 2004). Formally, SOL-1 functions to regulate GLR-1-mediated currents by modulating receptor desensitization (Walker et al., 2006a; Zheng et al., 2006). However,

GLR-1 function is not solely regulated by SOL-1, but also by the stargazin-like TARP proteins STG-1 and STG-2 (Walker et al., 2006b; Wang et al., 2008). That is, to form a fully functional GLR-1 complex that conducts physiologically relevant currents *in vivo*, the complex must contain the minimum set of proteins SOL-1, GLR-1, GLR-2 and either STG-1 or STG-2 (Figure 1.6) (Mellem et al., 2002; Walker et al., 2006a, 2006b; Wang et al., 2008; Zheng et al., 2004, 2006). Additional regulators of GLR-1-mediated currents *in vivo* have also recently been identified. SOL-2 is a CUB-domain protein related to SOL-1 that associates with both GLR-1 and SOL-1, and modifies GLR-1 desensitization and pharmacology (Wang et al., 2012).

## Regulation of the Long-Range Transport of GLR-1

The underlying molecular mechanisms regulating the long-range transport of the AMPAR subunit GLR-1 have yet to be discovered. However, many gene products implicated in regulating the transport of GLR-1 from the neuronal cell body to the synapse have been identified. One such proposed regulator of GLR-1 transport is the cyclin-dependent kinase CDK-5. Mutations in *cdk-5* decrease the amount of GLR-1::GFP in neuronal processes, whereas over-expression of CDK-5 results in an accumulation of GLR-1::GFP (Juo et al., 2007). This suggests that CDK-5 functions as a positive regulator of anterograde GLR-1 transport. Additional studies looking for suppressors of GLR-1 accumulation in CDK-5-overexpressing animals led to the identification of the kinesin-like protein KLP-4 (Monteiro et al., 2012). Mutations in *klp-4* decrease the amount of GLR-1

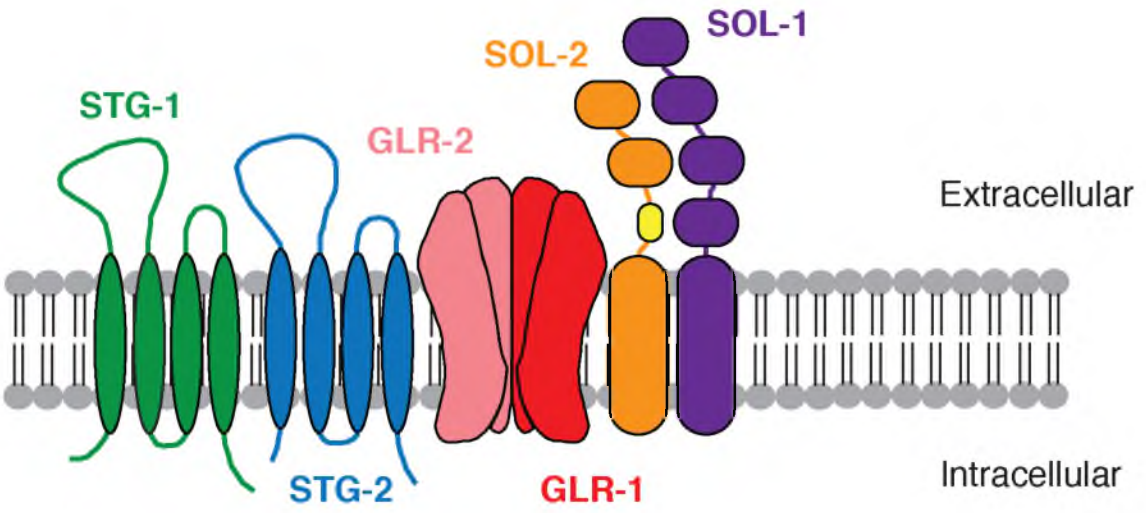


**Figure 1.6.** The GLR-1 signaling complex. GLR-1-mediated glutamate-gated currents *in vivo* require multiple auxiliary proteins. The vast majority of AMPARs in the AVA interneuron are GLR-1/GLR-2 heteromeric receptors. Channel opening requires the presence the TARP proteins STG-1 or STG-2. The CUB-domain proteins SOL-1 and SOL-2 modulate receptor desensitization and channel kinetics.

at synapses in the VNC (Monteiro et al., 2012). Further genetic studies suggest that KLP-4 and CDK-5 function in the same pathway in the cell body to regulate the anterograde transport of GLR-1 to synapses (Monteiro et al., 2012).

## Concluding Remarks

Throughout the nervous system, AMPARs mediate rapid excitatory signaling between neurons. The number of functional postsynaptic AMPARs at the synapse is involved in establishing the activity-induced changes in synaptic strength associated with learning and memory (Malinow and Malenka, 2002). Many studies have focused on how local processes such as exocytosis, endocytosis and lateral diffusion regulate the abundance of AMPARs in the postsynaptic membrane (Ashby et al., 2006; Borgdorff and Choquet, 2002; Kessels and Malinow, 2009; Passafaro et al., 2001; Shi et al., 2001; Yudowski et al., 2007); however, much less is known about the mechanisms involved in the trafficking of AMPARs from the cell body to the synapse (Bredt and Nicoll, 2003; Shepherd and Huganir, 2007; van der Sluijs and Hoogenraad, 2011).

To address this fundamental question, we have undertaken a comprehensive study to understand the molecular mechanisms governing the long-range trafficking of the AMPA-type glutamate receptor. This work utilizes the powerful genetic tools and simple nervous system of the model organism *C. elegans* to understand how AMPARs are transported *in vivo* (Chapter 2). To accomplish this, we took advantage of the clear worm cuticle and genetically engineered fluorescently tagged proteins and looked at AMPAR trafficking in the

unipolar process of the interneuron AVA. By looking at fluorescently tagged GLR-1 in AVA, we unequivocally show that AMPARs are transported by the molecular motor kinesin-1, encoded by the gene *unc-116*. Motor-based movement is required for the delivery of AMPARs to synapses, which occurs when a molecular motor stops near an existing synapse. We further demonstrate that AMPARs are not destined for a single synapse, but rather that GLR-1 can be reutilized at distant synapses through molecular motor-mediated removal and redistribution (Chapter 2).

To understand the role of kinesin-mediated transport of GLR-1 in AVA, we took advantage of multiple hypomorphic genetic mutations and RNAi knockdowns of *unc-116* (Chapter 2). In these mutants, AMPAR transport was severely disrupted in both anterograde and retrograde, suggesting that a single molecular motor can mediate the bidirectional transport of AMPARs. Unexpectedly, mutations in *unc-116* resulted in accumulations of surface-expressed GLR-1 at synapses. Despite these accumulations of GLR-1 in *unc-116* mutants, glutamate-gated currents were paradoxically decreased due to a preferential degradation of the GLR-2 AMPAR subunit in the absence of motor transport. Finally, we show that motor-mediated transport of GLR-1 in the adult nervous system plays a major role in maintaining synaptic transmission by providing a constant source of functional glutamate receptors.

Altogether, this work provides the first *in vivo* genetic, electrophysiological and cell biological characterization of AMPAR transport by molecular motors.

Given the conservation of the molecular mechanisms of neurotransmission between invertebrates and vertebrates, this work will aid in further understanding the role of motor-dependent transport in more complex nervous systems.

## References

Adesnik, H., Nicoll, R.A., and England, P.M. (2005). Photoinactivation of native AMPA receptors reveals their real-time trafficking. Neuron *48*, 977–985.

Armstrong, N., Sun, Y., Chen, G.Q., and Gouaux, E. (1998). Structure of a glutamate-receptor ligand-binding core in complex with kainate. Nature *395*, 913–917.

Armstrong, N., and Gouaux, E. (2000). Mechanisms for activation and antagonism of an AMPA-sensitive glutamate receptor: crystal structures of the GluR2 ligand binding core. Neuron *28*, 165–181.

Ashby, M.C., Maier, S.R., Nishimune, A., and Henley, J.M. (2006). Lateral diffusion drives constitutive exchange of AMPA receptors at dendritic spines and is regulated by spine morphology. J. Neurosci. Off. J. Soc. Neurosci. *26*, 7046–7055.

Ayalon, G., and Stern-Bach, Y. (2001). Functional assembly of AMPA and kainate receptors is mediated by several discrete protein-protein interactions. Neuron *31*, 103–113.

Ayalon, G., Segev, E., Elgavish, S., and Stern-Bach, Y. (2005). Two regions in the N-terminal domain of ionotropic glutamate receptor 3 form the subunit oligomerization interfaces that control subtype-specific receptor assembly. J. Biol. Chem. *280*, 15053–15060.

Baas, P.W. (1999). Microtubules and neuronal polarity: lessons from mitosis. Neuron *22*, 23–31.

Bass, B.L. (2002). RNA editing by adenosine deaminases that act on RNA. Annu. Rev. Biochem. *71*, 817–846.

Bats, C., Groc, L., and Choquet, D. (2007). The interaction between Stargazin and PSD-95 regulates AMPA receptor surface trafficking. Neuron *53*, 719–734.

Berkowitz, L.A., Knight, A.L., Caldwell, G.A., and Caldwell, K.A. (2008). Generation of stable transgenic C. elegans using microinjection. J. Vis. Exp. *18*, e833.

Blanpied, T.A., Scott, D.B., and Ehlers, M.D. (2002). Dynamics and regulation of clathrin coats at specialized endocytic zones of dendrites and spines. Neuron *36*, 435–449.

Bökel, C., Dass, S., Wilsch-Bräuninger, M., and Roth, S. (2006). Drosophila Cornichon acts as cargo receptor for ER export of the TGFalpha-like growth factor Gurken. Dev. Camb. Engl. *133*, 459–470.

Borgdorff, A.J., and Choquet, D. (2002). Regulation of AMPA receptor lateral movements. Nature *417*, 649–653.

Boulin, T. (2006). Reporter gene fusions. *WormBook.* ed. The C. elegans Research Community. https://www.wormbook.org.

Bredt, D.S., and Nicoll, R.A. (2003). AMPA receptor trafficking at excitatory synapses. Neuron *40*, 361–379.

Brenner, S. (1974). The genetics of Caenorhabditis elegans. Genetics *77*, 71–94.

Brockie, P.J., Mellem, J.E., Hills, T., Madsen, D.M., and Maricq, A.V. (2001a). The C. elegans glutamate receptor subunit NMR-1 is required for slow NMDA-activated currents that regulate reversal frequency during locomotion. Neuron *31*, 617–630.

Brockie, P.J., Madsen, D.M., Zheng, Y., Mellem, J., and Maricq, A.V. (2001b). Differential expression of glutamate receptor subunits in the nervous system of Caenorhabditis elegans and their regulation by the homeodomain protein UNC-42. J. Neurosci. Off. J. Soc. Neurosci. *21*, 1510–1522.

Brockie, P.J., and Maricq, A.V. (2010). In a pickle: is cornichon just relish or part of the main dish? Neuron *68*, 1017–1019.

Brockie, P.J., Jensen, M., Mellem, J.E., Jensen, E., Yamasaki, T., Wang, R., Maxfield, D., Thacker, C., Hoerndli, F., Dunn, P.J., et al. (2013). Cornichons control ER export of AMPA receptors to regulate synaptic excitability. Neuron *80*, 129–142.

Burbea, M., Dreier, L., Dittman, J.S., Grunwald, M.E., and Kaplan, J.M. (2002). Ubiquitin and AP180 regulate the abundance of GLR-1 glutamate receptors at postsynaptic elements in C. elegans. Neuron *35*, 107–120.

Chalfie, M., Sulston, J.E., White, J.G., Southgate, E., Thomson, J.N., and Brenner, S. (1985). The neural circuit for touch sensitivity in Caenorhabditis elegans. J. Neurosci. Off. J. Soc. Neurosci. *5*, 956–964.

Chambers, J.J., Gouda, H., Young, D.M., Kuntz, I.D., and England, P.M. (2004). Photochemically knocking out glutamate receptors in vivo. J. Am. Chem. Soc. *126*, 13886–13887.

Chen, C., and Tonegawa, S. (1997). Molecular genetic analysis of synaptic plasticity, activity-dependent neural development, learning, and memory in the mammalian brain. Annu. Rev. Neurosci. *20*, 157–184.

Chen, L., Chetkovich, D.M., Petralia, R.S., Sweeney, N.T., Kawasaki, Y., Wenthold, R.J., Bredt, D.S., and Nicoll, R.A. (2000). Stargazin regulates synaptic targeting of AMPA receptors by two distinct mechanisms. Nature *408*, 936–943.

Contractor, A., and Heinemann, S.F. (2004). AMPA receptor cycling in the synapse. Sci. STKE Signal Transduct. Knowl. Environ. *2004*, tr7.

Coombs, I.D., Soto, D., Zonouzi, M., Renzi, M., Shelley, C., Farrant, M., and Cull-Candy, S.G. (2012). Cornichons modify channel properties of recombinant and glial AMPA receptors. J. Neurosci. Off. J. Soc. Neurosci. *32*, 9796–9804.

Daw, M.I., Chittajallu, R., Bortolotto, Z.A., Dev, K.K., Duprat, F., Henley, J.M., Collingridge, G.L., and Isaac, J.T. (2000). PDZ proteins interacting with C-terminal GluR2/3 are involved in a PKC-dependent regulation of AMPA receptors at hippocampal synapses. Neuron *28*, 873–886.

Dingledine, R., Borges, K., Bowie, D., and Traynelis, S.F. (1999). The glutamate receptor ion channels. Pharmacol. Rev. *51*, 7–61.

Earnshaw, B.A., and Bressloff, P.C. (2008). Modeling the role of lateral membrane diffusion in AMPA receptor trafficking along a spiny dendrite. J. Comput. Neurosci. *25*, 366–389.

Ehlers, M.D., Heine, M., Groc, L., Lee, M.-C., and Choquet, D. (2007). Diffusional trapping of GluR1 AMPA receptors by input-specific synaptic activity. Neuron *54*, 447–460.

Esposito, G., Di Schiavi, E., Bergamasco, C., and Bazzicalupo, P. (2007). Efficient and cell specific knock-down of gene function in targeted C. elegans neurons. Gene *395*, 170–176.

Evans, T. (2006). Transformation and microinjection. *WormBook.* ed. The C. elegans Research Community. https://www.wormbook.org.

Gerges, N.Z., Backos, D.S., Rupasinghe, C.N., Spaller, M.R., and Esteban, J.A. (2006). Dual role of the exocyst in AMPA receptor targeting and insertion into the postsynaptic membrane. EMBO J. *25*, 1623–1634.

Glodowski, D.R., Chen, C.C.-H., Schaefer, H., Grant, B.D., and Rongo, C. (2007). RAB-10 regulates glutamate receptor recycling in a cholesterol-dependent endocytosis pathway. Mol. Biol. Cell *18*, 4387–4396.

Goldstein, L.S., and Yang, Z. (2000). Microtubule-based transport systems in neurons: the roles of kinesins and dyneins. Annu. Rev. Neurosci. *23*, 39–71.

Groc, L., Heine, M., Cognet, L., Brickley, K., Stephenson, F.A., Lounis, B., and Choquet, D. (2004). Differential activity-dependent regulation of the lateral mobilities of AMPA and NMDA receptors. Nat. Neurosci. *7*, 695–696.

Grooms, S.Y., Noh, K.-M., Regis, R., Bassell, G.J., Bryan, M.K., Carroll, R.C., and Zukin, R.S. (2006). Activity bidirectionally regulates AMPA receptor mRNA

abundance in dendrites of hippocampal neurons. J. Neurosci. Off. J. Soc. Neurosci. *26*, 8339–8351.

Hanley, J.G. (2010). Endosomal sorting of AMPA receptors in hippocampal neurons. Biochem. Soc. Trans. *38*, 460–465.

Hart, A.C., Sims, S., and Kaplan, J.M. (1995). Synaptic code for sensory modalities revealed by C. elegans GLR-1 glutamate receptor. Nature *378*, 82–85.

Hayashi, Y., Shi, S.H., Esteban, J.A., Piccini, A., Poncer, J.C., and Malinow, R. (2000). Driving AMPA receptors into synapses by LTP and CaMKII: requirement for GluR1 and PDZ domain interaction. Science *287*, 2262–2267.

Hebb, D.O. (1949). The Organization of Behavior: A Neuropsychological Theory (New York; Wiley), ISBN 9780471367277.

Henley, J.M., and Wilkinson, K.A. (2013). AMPA receptor trafficking and the mechanisms underlying synaptic plasticity and cognitive aging. Dialogues Clin. Neurosci. *15*, 11–27.

Herring, B.E., Shi, Y., Suh, Y.H., Zheng, C.-Y., Blankenship, S.M., Roche, K.W., and Nicoll, R.A. (2013). Cornichon proteins determine the subunit composition of synaptic AMPA receptors. Neuron *77*, 1083–1096.

Ho, V.M., Lee, J.-A., and Martin, K.C. (2011). The cell biology of synaptic plasticity. Science *334*, 623–628.

Huber, K.M., Kayser, M.S., and Bear, M.F. (2000). Role for rapid dendritic protein synthesis in hippocampal mGluR-dependent long-term depression. Science *288*, 1254–1257.

Huganir, R.L., and Nicoll, R.A. (2013). AMPARs and synaptic plasticity: the last 25 years. Neuron *80*, 704–717.

Jaskolski, F., Mayo-Martin, B., Jane, D., and Henley, J.M. (2009). Dynamin-dependent membrane drift recruits AMPA receptors to dendritic spines. J. Biol. Chem. *284*, 12491–12503.

Jones, M.V., and Westbrook, G.L. (1996). The impact of receptor desensitization on fast synaptic transmission. Trends Neurosci. *19*, 96–101.

Jorgensen, E.M., and Mango, S.E. (2002). The art and design of genetic screens: caenorhabditis elegans. Nat. Rev. Genet. *3*, 356–369.

Ju, W., Morishita, W., Tsui, J., Gaietta, G., Deerinck, T.J., Adams, S.R., Garner, C.C., Tsien, R.Y., Ellisman, M.H., and Malenka, R.C. (2004). Activity-dependent regulation of dendritic synthesis and trafficking of AMPA receptors. Nat. Neurosci. *7*, 244–253.

Juo, P., Harbaugh, T., Garriga, G., and Kaplan, J.M. (2007). CDK-5 regulates the abundance of GLR-1 glutamate receptors in the ventral cord of Caenorhabditis elegans. Mol. Biol. Cell *18*, 3883–3893.

Kakegawa, W., Tsuzuki, K., Yoshida, Y., Kameyama, K., and Ozawa, S. (2004). Input- and subunit-specific AMPA receptor trafficking underlying long-term potentiation at hippocampal CA3 synapses. Eur. J. Neurosci. *20*, 101–110.

Kamath, R.S., Martinez-Campos, M., Zipperlen, P., Fraser, A.G., and Ahringer, J. (2001). Effectiveness of specific RNA-mediated interference through ingested double-stranded RNA in Caenorhabditis elegans. Genome Biol. *2*, RESEARCH0002.

Kang, H., and Schuman, E.M. (1996). A requirement for local protein synthesis in neurotrophin-induced hippocampal synaptic plasticity. Science *273*, 1402–1406.

Kato, A.S., Gill, M.B., Ho, M.T., Yu, H., Tu, Y., Siuda, E.R., Wang, H., Qian, Y.-W., Nisenbaum, E.S., Tomita, S., et al. (2010). Hippocampal AMPA receptor gating controlled by both TARP and cornichon proteins. Neuron *68*, 1082–1096.

Kerr, J.M., and Blanpied, T.A. (2012). Subsynaptic AMPA receptor distribution is acutely regulated by actin-driven reorganization of the postsynaptic density. J. Neurosci. Off. J. Soc. Neurosci. *32*, 658–673.

Kessels, H.W., and Malinow, R. (2009). Synaptic AMPA receptor plasticity and behavior. Neuron *61*, 340–350.

Kew, J.N.C., and Kemp, J.A. (2005). Ionotropic and metabotropic glutamate receptor structure and pharmacology. Psychopharmacology (Berl.) *179*, 4–29.

Kim, C.H., and Lisman, J.E. (2001). A labile component of AMPA receptor-mediated synaptic transmission is dependent on microtubule motors, actin, and N-ethylmaleimide-sensitive factor. J. Neurosci. Off. J. Soc. Neurosci. *21*, 4188–4194.

Kolleker, A., Zhu, J.J., Schupp, B.J., Qin, Y., Mack, V., Borchardt, T., Köhr, G., Malinow, R., Seeburg, P.H., and Osten, P. (2003). Glutamatergic plasticity by synaptic delivery of GluR-B(long)-containing AMPA receptors. Neuron *40*, 1199–1212.

Kramer, L.B., Shim, J., Previtera, M.L., Isack, N.R., Lee, M.-C., Firestein, B.L., and Rongo, C. (2010). UEV-1 is an ubiquitin-conjugating enzyme variant that regulates glutamate receptor trafficking in C. elegans neurons. PloS One *5*, e14291.

Laube, B., Kuhse, J., and Betz, H. (1998). Evidence for a tetrameric structure of recombinant NMDA receptors. J. Neurosci. Off. J. Soc. Neurosci. *18*, 2954–2961.

Lee, S.H., Simonetta, A., and Sheng, M. (2004). Subunit rules governing the sorting of internalized AMPA receptors in hippocampal neurons. Neuron *43*, 221–236.

Letts, V.A., Felix, R., Biddlecome, G.H., Arikkath, J., Mahaffey, C.L., Valenzuela, A., Bartlett, F.S., 2nd, Mori, Y., Campbell, K.P., and Frankel, W.N. (1998). The mouse stargazer gene encodes a neuronal Ca2+-channel gamma subunit. Nat. Genet. *19*, 340–347.

Lu, J., Helton, T.D., Blanpied, T.A., Rácz, B., Newpher, T.M., Weinberg, R.J., and Ehlers, M.D. (2007). Postsynaptic positioning of endocytic zones and AMPA receptor cycling by physical coupling of dynamin-3 to Homer. Neuron *55*, 874–889.

Lu, W., Man, H., Ju, W., Trimble, W.S., MacDonald, J.F., and Wang, Y.T. (2001). Activation of synaptic NMDA receptors induces membrane insertion of new AMPA receptors and LTP in cultured hippocampal neurons. Neuron *29*, 243–254.

Lu, W., Shi, Y., Jackson, A.C., Bjorgan, K., During, M.J., Sprengel, R., Seeburg, P.H., and Nicoll, R.A. (2009). Subunit composition of synaptic AMPA receptors revealed by a single-cell genetic approach. Neuron *62*, 254–268.

Lu, W., Isozaki, K., Roche, K.W., and Nicoll, R.A. (2010). Synaptic targeting of AMPA receptors is regulated by a CaMKII site in the first intracellular loop of GluA1. Proc. Natl. Acad. Sci. U.S.A. *107*, 22266–22271.

MacGillavry, H.D., Song, Y., Raghavachari, S., and Blanpied, T.A. (2013). Nanoscale scaffolding domains within the postsynaptic density concentrate synaptic AMPA receptors. Neuron *78*, 615–622.

Makino, H., and Malinow, R. (2009). AMPA receptor incorporation into synapses during LTP: the role of lateral movement and exocytosis. Neuron *64*, 381–390.

Malinow, R., and Malenka, R.C. (2002). AMPA receptor trafficking and synaptic plasticity. Annu. Rev. Neurosci. *25*, 103–126.

Mano, I., and Teichberg, V.I. (1998). A tetrameric subunit stoichiometry for a glutamate receptor-channel complex. Neuroreport *9*, 327–331.

Maricq, A.V., Peckol, E., Driscoll, M., and Bargmann, C.I. (1995). Mechanosensory signalling in C. elegans mediated by the GLR-1 glutamate receptor. Nature *378*, 78–81.

Matsuzaki, M., Ellis-Davies, G.C., Nemoto, T., Miyashita, Y., Iino, M., and Kasai, H. (2001). Dendritic spine geometry is critical for AMPA receptor expression in hippocampal CA1 pyramidal neurons. Nat. Neurosci. *4*, 1086–1092.

Mayer, M.L. (2006). Glutamate receptors at atomic resolution. Nature *440*, 456–462.

McGee, A.W., and Bredt, D.S. (2003). Assembly and plasticity of the glutamatergic postsynaptic specialization. Curr. Opin. Neurobiol. *13*, 111–118.

Meldrum, B.S. (1994). The role of glutamate in epilepsy and other CNS disorders. Neurology *44*, S14–23.

Mellem, J.E., Brockie, P.J., Zheng, Y., Madsen, D.M., and Maricq, A.V. (2002). Decoding of polymodal sensory stimuli by postsynaptic glutamate receptors in C. elegans. Neuron *36*, 933–944.

Mello, C.C., and Conte, D., Jr (2004). Revealing the world of RNA interference. Nature *431*, 338–342.

Mody, I. (1998). Ion channels in epilepsy. Int. Rev. Neurobiol. *42*, 199–226.

Montastruc, J.L., Rascol, O., and Senard, J.M. (1997). Glutamate antagonists and Parkinson's disease: a review of clinical data. Neurosci. Biobehav. Rev. *21*, 477–480.

Monteiro, M.I., Ahlawat, S., Kowalski, J.R., Malkin, E., Koushika, S.P., and Juo, P. (2012). The kinesin-3 family motor KLP-4 regulates anterograde trafficking of GLR-1 glutamate receptors in the ventral nerve cord of Caenorhabditis elegans. Mol. Biol. Cell *23*, 3647–3662.

Nakajima, K., Yin, X., Takei, Y., Seog, D.-H., Homma, N., and Hirokawa, N. (2012). Molecular motor KIF5A is essential for GABA(A) receptor transport, and KIF5A deletion causes epilepsy. Neuron *76*, 945–961.

Nakanishi, S. (1994). Metabotropic glutamate receptors: synaptic transmission, modulation, and plasticity. Neuron *13*, 1031–1037.

Newpher, T.M., and Ehlers, M.D. (2008). Glutamate receptor dynamics in dendritic microdomains. Neuron *58*, 472–497.

Nonet, M.L., Holgado, A.M., Brewer, F., Serpe, C.J., Norbeck, B.A., Holleran, J., Wei, L., Hartwieg, E., Jorgensen, E.M., and Alfonso, A. (1999). UNC-11, a Caenorhabditis elegans AP180 homologue, regulates the size and protein composition of synaptic vesicles. Mol. Biol. Cell *10*, 2343–2360.

Opazo, P., Labrecque, S., Tigaret, C.M., Frouin, A., Wiseman, P.W., De Koninck, P., and Choquet, D. (2010). CaMKII triggers the diffusional trapping of surface AMPARs through phosphorylation of stargazin. Neuron *67*, 239–252.

Osten, P., Khatri, L., Perez, J.L., Köhr, G., Giese, G., Daly, C., Schulz, T.W., Wensky, A., Lee, L.M., and Ziff, E.B. (2000). Mutagenesis reveals a role for

ABP/GRIP binding to GluR2 in synaptic surface accumulation of the AMPA receptor. Neuron *27*, 313–325.

Otis, T., Zhang, S., and Trussell, L.O. (1996). Direct measurement of AMPA receptor desensitization induced by glutamatergic synaptic transmission. J. Neurosci. Off. J. Soc. Neurosci. *16*, 7496–7504.

Passafaro, M., Piëch, V., and Sheng, M. (2001). Subunit-specific temporal and spatial patterns of AMPA receptor exocytosis in hippocampal neurons. Nat. Neurosci. *4*, 917–926.

Patterson, M.A., Szatmari, E.M., and Yasuda, R. (2010). AMPA receptors are exocytosed in stimulated spines and adjacent dendrites in a Ras-ERK-dependent manner during long-term potentiation. Proc. Natl. Acad. Sci. U. S. A. *107*, 15951–15956.

Peng, S., Zhang, Y., Zhang, J., Wang, H., and Ren, B. (2011). Glutamate receptors and signal transduction in learning and memory. Mol. Biol. Rep. *38*, 453–460.

Petrini, E.M., Lu, J., Cognet, L., Lounis, B., Ehlers, M.D., and Choquet, D. (2009). Endocytic trafficking and recycling maintain a pool of mobile surface AMPA receptors required for synaptic potentiation. Neuron *63*, 92–105.

Priel, A., Kolleker, A., Ayalon, G., Gillor, M., Osten, P., and Stern-Bach, Y. (2005). Stargazin reduces desensitization and slows deactivation of the AMPA-type glutamate receptors. J. Neurosci. Off. J. Soc. Neurosci. *25*, 2682–2686.

Rongo, C., Whitfield, C.W., Rodal, A., Kim, S.K., and Kaplan, J.M. (1998). LIN-10 is a shared component of the polarized protein localization pathways in neurons and epithelia. Cell *94*, 751–759.

Rongo, C., and Kaplan, J.M. (1999). CaMKII regulates the density of central glutamatergic synapses in vivo. Nature *402*, 195–199.

Rosenmund, C., Stern-Bach, Y., and Stevens, C.F. (1998). The tetrameric structure of a glutamate receptor channel. Science *280*, 1596–1599.

Roth, S., Neuman-Silberberg, F.S., Barcelo, G., and Schüpbach, T. (1995). cornichon and the EGF receptor signaling process are necessary for both anterior-posterior and dorsal-ventral pattern formation in Drosophila. Cell *81*, 967–978.

Scannevin, R.H., and Huganir, R.L. (2000). Postsynaptic organization and regulation of excitatory synapses. Nat. Rev. Neurosci. *1*, 133–141.

Schnell, E., Sizemore, M., Karimzadegan, S., Chen, L., Bredt, D.S., and Nicoll, R.A. (2002). Direct interactions between PSD-95 and stargazin control synaptic AMPA receptor number. Proc. Natl. Acad. Sci. U.S.A. *99*, 13902–13907.

Schwenk, J., Harmel, N., Zolles, G., Bildl, W., Kulik, A., Heimrich, B., Chisaka, O., Jonas, P., Schulte, U., Fakler, B., et al. (2009). Functional proteomics identify cornichon proteins as auxiliary subunits of AMPA receptors. Science *323*, 1313–1319.

Seeburg, P.H., Higuchi, M., and Sprengel, R. (1998). RNA editing of brain glutamate receptor channels: mechanism and physiology. Brain Res. Brain Res. Rev. *26*, 217–229.

Setou, M., Seog, D.-H., Tanaka, Y., Kanai, Y., Takei, Y., Kawagishi, M., and Hirokawa, N. (2002). Glutamate-receptor-interacting protein GRIP1 directly steers kinesin to dendrites. Nature *417*, 83–87.

Shepherd, J.D., and Huganir, R.L. (2007). The cell biology of synaptic plasticity: AMPA receptor trafficking. Annu. Rev. Cell Dev. Biol. *23*, 613–643.

Shi, S., Hayashi, Y., Esteban, J.A., and Malinow, R. (2001). Subunit-specific rules governing AMPA receptor trafficking to synapses in hippocampal pyramidal neurons. Cell *105*, 331–343.

Shi, Y., Suh, Y.H., Milstein, A.D., Isozaki, K., Schmid, S.M., Roche, K.W., and Nicoll, R.A. (2010). Functional comparison of the effects of TARPs and cornichons on AMPA receptor trafficking and gating. Proc. Natl. Acad. Sci. U.S.A. *107*, 16315–16319.

Smith, M.A., Ellis-Davies, G.C.R., and Magee, J.C. (2003). Mechanism of the distance-dependent scaling of Schaffer collateral synapses in rat CA1 pyramidal neurons. J. Physiol. *548*, 245–258.

Sobolevsky, A.I., Rosconi, M.P., and Gouaux, E. (2009). X-ray structure, symmetry and mechanism of an AMPA-subtype glutamate receptor. Nature *462*, 745–756.

Sommer, B., Köhler, M., Sprengel, R., and Seeburg, P.H. (1991). RNA editing in brain controls a determinant of ion flow in glutamate-gated channels. Cell *67*, 11–19.

Song, I., and Huganir, R.L. (2002). Regulation of AMPA receptors during synaptic plasticity. Trends Neurosci. *25*, 578–588.

Stern-Bach, Y., Bettler, B., Hartley, M., Sheppard, P.O., O'Hara, P.J., and Heinemann, S.F. (1994). Agonist selectivity of glutamate receptors is specified by two domains structurally related to bacterial amino acid-binding proteins. Neuron *13*, 1345–1357.

Stern-Bach, Y., Russo, S., Neuman, M., and Rosenmund, C. (1998). A point mutation in the glutamate binding site blocks desensitization of AMPA receptors. Neuron *21*, 907–918.

Steward, O., and Levy, W.B. (1982). Preferential localization of polyribosomes under the base of dendritic spines in granule cells of the dentate gyrus. J. Neurosci. Off. J. Soc. Neurosci. *2*, 284–291.

Suchanek, B., Seeburg, P.H., and Sprengel, R. (1995). Gene structure of the murine N-methyl D-aspartate receptor subunit NR2C. J. Biol. Chem. *270*, 41–44.

Sudhof, T.C. (2004). The synaptic vesicle cycle. Annu. Rev. Neurosci. *27*, 509–547.

Tanaka, J., Matsuzaki, M., Tarusawa, E., Momiyama, A., Molnar, E., Kasai, H., and Shigemoto, R. (2005). Number and density of AMPA receptors in single synapses in immature cerebellum. J. Neurosci. Off. J. Soc. Neurosci. *25*, 799–807.

Tardin, C., Cognet, L., Bats, C., Lounis, B., and Choquet, D. (2003). Direct imaging of lateral movements of AMPA receptors inside synapses. EMBO J. *22*, 4656–4665.

Tichelaar, W., Safferling, M., Keinänen, K., Stark, H., and Madden, D.R. (2004). The three-dimensional structure of an ionotropic glutamate receptor reveals a dimer-of-dimers assembly. J. Mol. Biol. *344*, 435–442.

Tomita, S., Nicoll, R.A., and Bredt, D.S. (2001). PDZ protein interactions regulating glutamate receptor function and plasticity. J. Cell Biol. *153*, F19–24.

Tomita, S., Chen, L., Kawasaki, Y., Petralia, R.S., Wenthold, R.J., Nicoll, R.A., and Bredt, D.S. (2003). Functional studies and distribution define a family of transmembrane AMPA receptor regulatory proteins. J. Cell Biol. *161*, 805–816.

Tomita, S., Adesnik, H., Sekiguchi, M., Zhang, W., Wada, K., Howe, J.R., Nicoll, R.A., and Bredt, D.S. (2005). Stargazin modulates AMPA receptor gating and trafficking by distinct domains. Nature *435*, 1052–1058.

Trussell, L.O., and Fischbach, G.D. (1989). Glutamate receptor desensitization and its role in synaptic transmission. Neuron *3*, 209–218.

Ułas, J., Weihmuller, F.B., Brunner, L.C., Joyce, J.N., Marshall, J.F., and Cotman, C.W. (1994). Selective increase of NMDA-sensitive glutamate binding in the striatum of Parkinson's disease, Alzheimer's disease, and mixed Parkinson's disease/Alzheimer's disease patients: an autoradiographic study. J. Neurosci. Off. J. Soc. Neurosci. *14*, 6317–6324.

Van der Sluijs, P., and Hoogenraad, C.C. (2011). New insights in endosomal dynamics and AMPA receptor trafficking. Semin. Cell Dev. Biol. *22*, 499–505.

Walker, C.S., Francis, M.M., Brockie, P.J., Madsen, D.M., Zheng, Y., and Maricq, A.V. (2006a). Conserved SOL-1 proteins regulate ionotropic glutamate receptor desensitization. Proc. Natl. Acad. Sci. U.S.A. *103*, 10787–10792.

Walker, C.S., Brockie, P.J., Madsen, D.M., Francis, M.M., Zheng, Y., Koduri, S., Mellem, J.E., Strutz-Seebohm, N., and Maricq, A.V. (2006b). Reconstitution of invertebrate glutamate receptor function depends on stargazin-like proteins. Proc. Natl. Acad. Sci. U.S.A. *103*, 10781–10786.

Wang, R., Walker, C.S., Brockie, P.J., Francis, M.M., Mellem, J.E., Madsen, D.M., and Maricq, A.V. (2008). Evolutionary conserved role for TARPs in the gating of glutamate receptors and tuning of synaptic function. Neuron *59*, 997–1008.

Wang, R., Mellem, J.E., Jensen, M., Brockie, P.J., Walker, C.S., Hoerndli, F.J., Hauth, L., Madsen, D.M., and Maricq, A.V. (2012). The SOL-2/Neto auxiliary protein modulates the function of AMPA-subtype ionotropic glutamate receptors. Neuron *75*, 838–850.

Watkins, J.C., and Jane, D.E. (2006). The glutamate story. Br. J. Pharmacol. *147 Suppl 1*, S100–108.

Wenthold, R.J., Yokotani, N., Doi, K., and Wada, K. (1992). Immunochemical characterization of the non-NMDA glutamate receptor using subunit-specific antibodies. Evidence for a hetero-oligomeric structure in rat brain. J. Biol. Chem. *267*, 501–507.

White, J.G., Southgate, E., Thomson, J.N., and Brenner, S. (1986). The structure of the nervous system of the nematode Caenorhabditis elegans. Philos. Trans. R. Soc. Lond. B. Biol. Sci. *314*, 1–340.

Yamazaki, M., Araki, K., Shibata, A., and Mishina, M. (1992). Molecular cloning of a cDNA encoding a novel member of the mouse glutamate receptor channel family. Biochem. Biophys. Res. Commun. *183*, 886–892.

Yamazaki, M., Ohno-Shosaku, T., Fukaya, M., Kano, M., Watanabe, M., and Sakimura, K. (2004). A novel action of stargazin as an enhancer of AMPA receptor activity. Neurosci. Res. *50*, 369–374.

Yudowski, G.A., Puthenveedu, M.A., Leonoudakis, D., Panicker, S., Thorn, K.S., Beattie, E.C., and von Zastrow, M. (2007). Real-time imaging of discrete exocytic events mediating surface delivery of AMPA receptors. J. Neurosci. Off. J. Soc. Neurosci. *27*, 11112–11121.

Zheng, Y., Mellem, J.E., Brockie, P.J., Madsen, D.M., and Maricq, A.V. (2004). SOL-1 is a CUB-domain protein required for GLR-1 glutamate receptor function in C. elegans. Nature *427*, 451–457.

Zheng, Y., Brockie, P.J., Mellem, J.E., Madsen, D.M., Walker, C.S., Francis, M.M., and Maricq, A.V. (2006). SOL-1 is an auxiliary subunit that modulates the gating of GLR-1 glutamate receptors in Caenorhabditis elegans. Proc. Natl. Acad. Sci. U.S.A. *103*, 1100–1105.

Zhu, J.J., Esteban, J.A., Hayashi, Y., and Malinow, R. (2000). Postnatal synaptic potentiation: delivery of GluR4-containing AMPA receptors by spontaneous activity. Nat. Neurosci. *3*, 1098–1106.

Zuo, J., De Jager, P.L., Takahashi, K.A., Jiang, W., Linden, D.J., and Heintz, N. (1997). Neurodegeneration in Lurcher mice caused by mutation in delta2 glutamate receptor gene. Nature *388*, 769–773.

CHAPTER 2

# KINESIN-1 REGULATES SYNAPTIC STRENGTH BY MEDIATING DELIVERY, REMOVAL AND REDISTRIBUTION OF AMPARS

Reprinted from Neuron, 80 (6), Horendli, F., Maxfield, D.A., Brockie, P.J., Mellem, J.E., Jensen, E., Wang, R., Madsen, D.M. and Maricq, A.V., Kinesin-1 Regulates Synaptic Strength by Mediating Delivery, Removal and Redistribution of AMPARs, 1421-1437, Copyright (2013) with permission from Elsevier.

Neuron
Article

# Kinesin-1 Regulates Synaptic Strength by Mediating the Delivery, Removal, and Redistribution of AMPA Receptors

Frédéric J. Hoerndli,[1,2] Dane A. Maxfield,[1,2] Penelope J. Brockie,[1] Jerry E. Mellem,[1] Erica Jensen,[1] Rui Wang,[1] David M. Madsen,[1] and Andres V. Maricq[1,*]
[1]Department of Biology, Center for Cell and Genome Science, University of Utah, Salt Lake City, UT 84112, USA
[2]These authors contributed equally to this work
*Correspondence: maricq@biology.utah.edu
http://dx.doi.org/10.1016/j.neuron.2013.10.050

## SUMMARY

**A primary determinant of the strength of neurotransmission is the number of AMPA-type glutamate receptors (AMPARs) at synapses. However, we still lack a mechanistic understanding of how the number of synaptic AMPARs is regulated. Here, we show that UNC-116, the *C. elegans* homolog of vertebrate kinesin-1 heavy chain (KIF5), modifies synaptic strength by mediating the rapid delivery, removal, and redistribution of synaptic AMPARs. Furthermore, by studying the real-time transport of *C. elegans* AMPAR subunits in vivo, we demonstrate that although homomeric GLR-1 AMPARs can diffuse to and accumulate at synapses in *unc-116* mutants, glutamate-gated currents are diminished because heteromeric GLR-1/GLR-2 receptors do not reach synapses in the absence of UNC-116/KIF5-mediated transport. Our data support a model in which ongoing motor-driven delivery and removal of AMPARs controls not only the number but also the composition of synaptic AMPARs, and thus the strength of synaptic transmission.**

## INTRODUCTION

The number of functional postsynaptic glutamate receptors is a major determinant of the strength of synaptic signaling. Thus, experience-dependent changes in the number of receptors contribute to fundamental network properties such as learning and memory (Jackson and Nicoll, 2011; Kerchner and Nicoll, 2008; Malinow and Malenka, 2002). Because most neurons have long processes, synapses are often far removed from the cell body, imparting a major challenge for the modulation and maintenance of synaptic machinery. Although we have considerable insight into the local mechanisms that contribute to synaptic strength by regulating the recycling of α-amino-3-hydroxy-5-methyl-4-isoxazolepropionic acid-type glutamate receptors (AMPARs) between the postsynaptic membrane and endosomal compartments (Henley et al., 2011; Kennedy and Ehlers, 2011; Kessels and Malinow, 2009; Petrini et al., 2009; Rusakov et al., 2011; Shepherd and Huganir, 2007; Yudowski et al., 2006), we have far fewer mechanistic insights into the long-range transport of AMPARs and how transport impacts synaptic strength and plasticity. These questions are particularly timely, considering the strong association of transport defects with synaptopathies and neurodegenerative disorders such as Alzheimer's disease (Stokin and Goldstein, 2006).

At least three different mechanisms have been proposed for the long-range delivery of AMPARs to synapses, including local synthesis (Ho et al., 2011; Ju et al., 2004), lateral diffusion (Adesnik et al., 2005), and motor-dependent transport (Greger and Esteban, 2007; Kim and Lisman, 2001; Setou et al., 2002). However, it has been difficult to establish the relative contributions of these various processes to synaptic function. These competing models derive almost exclusively from in vitro studies in cultured neuronal preparations, and thus might not accurately reflect the effects of the local cellular environment, signaling molecules, and the extracellular matrix, all of which can influence neuronal development and synaptic function. Therefore, we developed techniques that allowed us to directly observe the in vivo delivery of AMPARs to synapses in a specific neuron in *C. elegans*.

Studying AMPAR delivery in *C. elegans* allows us to integrate in vivo cell biological and electrophysiological studies of synaptic function. *C. elegans* are transparent and have only 302 neurons, a subset of which communicate by the synaptic release of glutamate to mediate specific behaviors (de Bono and Maricq, 2005). Glutamate gates a variety of receptors, including the GLR-1 AMPAR signaling complex, which is expressed in interneurons that contribute to worm locomotion (de Bono and Maricq, 2005). Previous studies have identified the molecular components of the GLR-1 signaling complex (Brockie et al., 2001; Mellem et al., 2002; Walker et al., 2006; Wang et al., 2008, 2012; Zheng et al., 2004, 2006) and the mechanisms that regulate the localization and stability of synaptic GLR-1 (Burbea et al., 2002; Glodowski et al., 2007; Juo et al., 2007; Rongo and Kaplan, 1999; Rongo et al., 1998; Zhang et al., 2012).

We now demonstrate that the microtubule-dependent motor, UNC-116/KIF5, and the associated kinesin light chain, KLC-2, mediate the transport of GLR-1 to synapses. In a series of in vivo studies, we evaluated the relative contributions of motor transport, receptor diffusion, and local synthesis to the delivery of GLR-1 to synapses. We found that motor-mediated transport

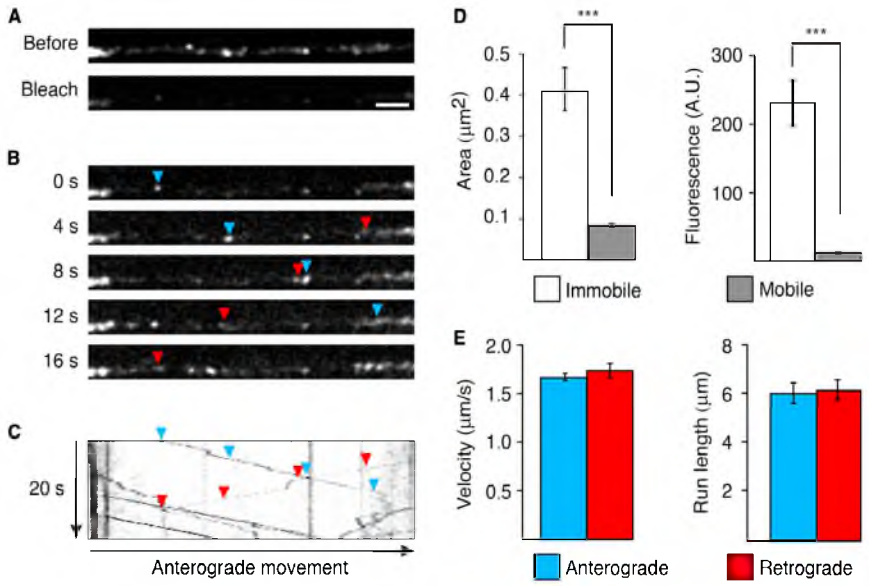


**Figure 1. GLR-1::GFP Is Transported in Both an Anterograde and a Retrograde Direction along the AVA Processes**

(A) Confocal images of GLR-1::GFP puncta in the proximal AVA processes before (top) and after (bottom) photobleaching. Scale bar represents 2.5 μm.

(B) Higher gain images of the region shown in (A) at various time points after photobleaching. The arrowheads indicate anterograde (blue) and retrograde (red) movement.

(C) Kymograph showing mobile and immobile GLR-1::GFP vesicles in the photobleached region shown in (A).

(D) Measurement of the area (left) and average total fluorescence (right) of immobile and mobile GLR-1::GFP. $n > 100$ immobile; $n > 450$ mobile; ***$p < 0.001$.

(E) Quantification of the velocity (left) and run length (right) of mobile GLR-1::GFP vesicles. $n > 450$ vesicles.

Error bars indicate SEM. See also Figure S1.

is the predominant mechanism for delivery, removal, and redistribution of GLR-1. In *unc-116* mutants, GLR-1 diffused out of the cell body to proximal synapses, where it reached higher than normal levels secondary to the loss of motor-driven removal of synaptic receptors. Despite the synaptic accumulation of GLR-1 in *unc-116* mutants, glutamate-gated currents were severely diminished because the AMPAR signaling complex lacked GLR-1/GLR-2 heteromeric receptors. Defective AMPAR signaling in *unc-116* mutants was rescued by transient expression of UNC-116 in the adult nervous system, demonstrating that ongoing motor-dependent transport is required for the regulation of synaptic strength.

## RESULTS

### In Vivo Measurement of GLR-1 Transport

In *C. elegans*, the two AVA interneurons are part of a well-defined circuit that regulates worm reversal behavior (Brockie et al., 2001). These neurons express the GLR-1 AMPAR subunit and each neuron extends a single process into the ventral cord that runs the length of the worm. We were able to specifically visualize these processes by using promoter sequences (*Prig-3* and *Pflp-18*) that limited transgene expression in the ventral cord to AVA (Figure S1A available online) (Feinberg et al., 2008; Wang et al., 2012). In transgenic worms that expressed a functional GFP-tagged variant of GLR-1 (GLR-1::GFP) in AVA, we observed discrete GFP puncta, which mark postsynaptic sites along the processes (Figure S1B) (Rongo et al., 1998). To address how GLR-1 receptors are delivered to these synapses, we used real-time streaming confocal microscopy to image receptor movement. Unless otherwise indicated, we imaged a region of the proximal AVA process of young adult worms (Figure S1A, boxed region). To better image receptor transport, we first reduced background fluorescence by photobleaching a region of interest that was approximately 45 μm in length (Figure 1A). Transport events were more apparent after photobleaching, and we noted no adverse effects of photobleaching on transport (Figures S1C and S1D). We then captured a series of confocal images that revealed numerous small, fluorescent GLR-1::GFP puncta that moved either anterogradely or retrogradely along the AVA processes. We refer to these as vesicles, given that their movement was consistent with known vesicular transport of transmembrane proteins (Figure 1B). The bidirectional vesicle transport, interrupted by occasional pauses or stops, is most apparent in kymographs generated from the full series of images (Figure 1C). The mobile vesicles were considerably smaller and dimmer than the large, immobile puncta (Figure 1D), which we refer to as synaptic puncta. Vesicles moved at approximately

1.6 μm/s in both anterograde and retrograde directions, with an average run length of approximately 6 μm (Figure 1E).

### Transport Vesicles Are Directed to Synapses

Most of the transport vesicles had brief pauses in their movement that were of variable duration (Figure 2A). A more detailed analysis of the kymographs revealed that stop events (defined as pauses in movement lasting at least 1.2 s) were clustered near existing GLR-1 synaptic puncta (Figures 2B and 2C). We also observed vesicles that stopped moving for extended periods, at times lasting many minutes. In one kymograph, we observed a vesicle moving anterogradely (Figure 2A, blue arrow) and another vesicle moving retrogradely (Figure 2A, red arrow) and observed both vesicles stop at the same synapse (Figure 2A, green box). Twenty minutes later, a kymograph of the same region revealed sustained recovery of GLR-1::GFP fluorescence at the synapse where the two vesicles stopped (Figure 2A, lower panel, filled arrowhead), suggesting that these stops might have been permanent delivery events. We also detected long-lived increases in fluorescence at additional synapses (Figure 2A, lower panel, open arrowheads), which we assume reflect stoppage events that occurred in the 20 min interval between kymographs.

We next asked whether vesicles were delivered directly to the surface membrane or first to a subsynaptic compartment. To simultaneously measure GLR-1 transport and surface delivery, we generated a transgenic strain that expressed a functional GLR-1 protein fused to both superecliptic pHluorin (SEP) and mCherry at the extracellular N-terminal domain (SEP::mCherry::GLR-1) (Kennedy and Ehlers, 2011) (Figure 2D). The SEP variant of GFP is pH sensitive and not appreciably fluorescent when localized to the relatively acidic environment of subcellular organelles in *C. elegans* (Dittman and Kaplan, 2006; Miesenböck et al., 1998; Wang et al., 2012). Thus, we rarely detect intracellular transport in the green channel (Figure 2E). Furthermore, photobleaching eliminates SEP fluorescence of surface GLR-1, but does not affect the SEP fluorophore on internalized receptors. Following photobleaching of both fluorophores, we acquired two-color streaming confocal movies to simultaneously monitor vesicle movement in the red channel and surface delivery of receptors that we detected by the appearance of a fluorescent signal in the green channel. Although we observed long-lived stops in vesicle movement, these were not immediately associated with GLR-1 surface delivery. However, we did observe insertion events occurring at variable intervals following vesicle stops (Figure 2E). This suggests that receptors were first delivered to a subsynaptic compartment rather than directly to the surface of the synapse and that stoppage and insertion are separable processes. Insertion events were observed most frequently at the same location as the synaptic puncta (Figures 2F and S2A).

These data indicate that delivery of GLR-1 to synapses occurs in at least two steps. First, transport vesicles stop and deliver GLR-1 to a subsynaptic compartment in the region of a synapse. Second, after some delay, receptors are inserted into the synaptic membrane. Interestingly, the insertion rate (Figure 2E) is a fraction of the stoppage rate (Figure 2C), even though the synaptic delivery (Figure S2B) and transport parameters (data not shown) were unaltered by the location of the fluorophore tag. This result suggests that not all longer-duration stops (>1.2 s) are destined for eventual insertion at a particular synapse.

### GLR-1 Receptors Are Redistributed between Synapses

To determine the fate of GLR-1 receptors at synapses, we fused a photoactivatable florophore (PAGFP) to GLR-1 and expressed the functional protein in the AVA neurons. Following photoactivation of GLR-1::PAGFP puncta, we occasionally observed vesicles leaving synaptic puncta and traveling in either an anterograde (Figure 3A) or a retrograde (Figure 3A, insert) direction. These observations raised the question of whether GLR-1 receptors could be utilized at multiple synapses. We therefore evaluated the source of synaptic receptors using a photoconversion strategy to follow the fate of receptors from the cell body, and from proximal and distal synapses. We tagged GLR-1 with Dendra2, a photoconvertible fluorophore that can be switched from green to red fluorescence using UV illumination (Gurskaya et al., 2006) and expressed the functional fusion protein in the AVA neurons. Four hours after photoconversion of GLR-1::Dendra2 in the AVA cell bodies, we found that approximately 25% of the fluorescent signal at distal synapses was red (Figure 3B). In contrast, we did not observe an appreciable red signal in the distal processes of sham-converted worms (Figure S3A).

Next, we photoconverted both synaptic puncta and interpunctal GLR-1::Dendra2 fluorescence in the proximal region of the AVA processes. Fours hours after photoconversion, we monitored the appearance of red fluorescence at distal synapses and found that red signal originating in the proximal processes had been redistributed to distal puncta (Figure 3C). In separate experiments, we photoconverted only the synaptic puncta in the proximal processes, leaving the interpuncta regions unconverted, and again observed red signal at distal synapses 4 hr after photoconversion (Figure 3D), but no red signal in sham-converted worms (Figure S3B). These data indicate that the red fluorescence, which appeared at distal synapses, was derived from receptors at proximal synapses rather than receptors that were photoconverted while in transit.

To further evaluate the redistribution of receptors, we photoactivated GLR-1::PAGFP in the distal half of the AVA processes. Fours hours after photoactivation, we observed GLR-1::PAGFP fluorescence at puncta in the proximal process (Figure 3E), but no signal in sham photoactivated controls (Figure S3C). Together, these data indicate that most synaptic GLR-1 receptors are delivered from the cell body to synapses, but receptors at a given synapse can be redistributed to other synapses.

### UNC-116/KIF5 Mediates GLR-1 Transport

The speed and processivity of vesicle transport strongly suggested an energy-dependent, motor-driven process. In support of this hypothesis, we did not observe vesicle movement following treatment with Na-azide, a potent inhibitor of mitochondrial respiration and ATP production (Bowler et al., 2006), or nocodazole, an inhibitor of microtubule polymerization (Figure S3D), suggesting that microtubule-dependent motors drive the movement of GLR-1 vesicles. There are 21 known kinesin-like motors encoded by the *C. elegans* genome (Siddiqui, 2002), but only a few have been studied in detail, including OSM-3, UNC-104/KIF1, KLP-4, and UNC-116/KIF5. Of these,

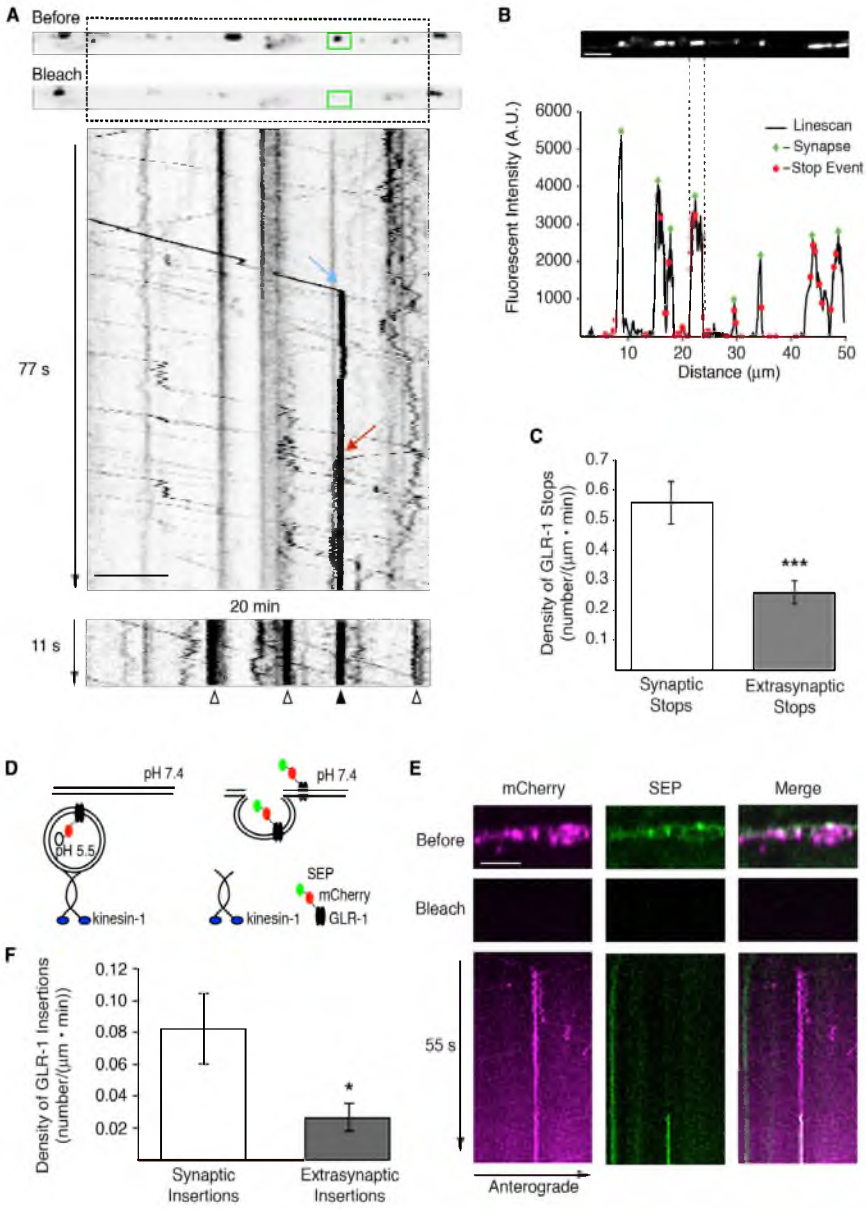


**Figure 2. GLR-1 Is Preferentially Delivered to Synaptic Puncta in the AVA Processes**

(A) Single-plane confocal images before and after photobleaching GLR-1::GFP in the AVA processes with the corresponding kymograph showing anterograde (blue arrow) and retrograde (red arrow) delivery events to a synaptic puncta (green box). A second kymograph (bottom), taken 20 min after the first, shows the stable delivery event from the first kymograph (filled arrowhead), as well as additional delivery events during the interval between the two kymographs (open arrowheads).

(B) Confocal image of synaptic GLR-1::GFP puncta in AVA (top) and the corresponding linescan of fluorescence intensity (bottom). Green diamonds mark the peak fluorescence of synaptic puncta and red dots mark the relative positions of GLR-1::GFP vesicle stops from a 5 min movie.

(C) Quantification of GLR-1::GFP vesicle stops in synaptic and extrasynaptic regions. n = 7.

*(legend continued on next page)*

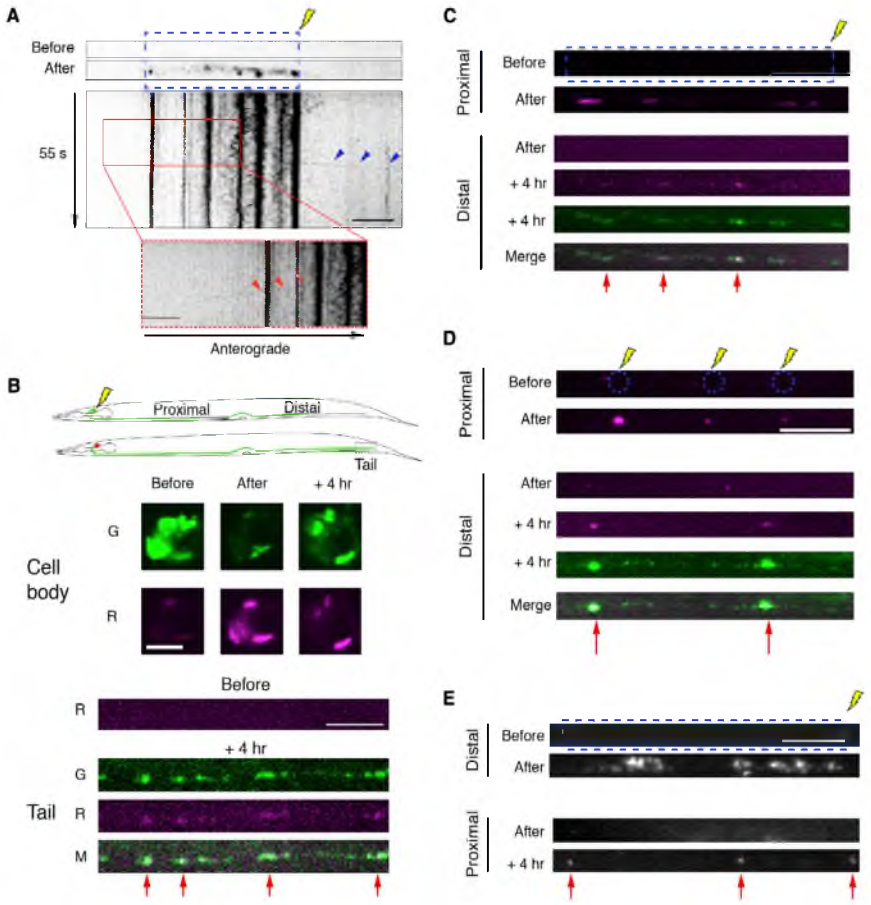


**Figure 3. GLR-1 Is Redistributed between Synapses**

(A) Photoactivation of GLR-1::PAGFP expressed in AVA before and after UV photoactivation (blue, dashed box) with the corresponding kymograph. Arrowheads show anterograde (blue arrowheads) and retrograde (inset, red arrowheads) departure of a GLR-1 vesicle from converted synaptic puncta.

(B–E) All confocal images were taken before, immediately after, or 4 hr after photoconversion or photoactivation. (B) Schematic of GLR-1::Dendra2 photoconversion in the cell body (top). Images of GLR-1::Dendra2 in the cell body and in the distal processes (tail). Red arrowheads highlight synapses that received photoconverted GLR-1::Dendra2 from the cell body. (C and D) Images of GLR-1::Dendra2 after photoconversion of total fluorescence (C) or puncta fluorescence only (D) in the proximal processes (only the red signal is shown). Red arrows indicate the appearance of photoconverted GLR-1::Dendra2 at distal synapses (red and green signal shown). (E) Images of GLR-1::PAGFP before and after photoactivation. Red arrows indicate the appearance of photoactivated GLR-1::PAGFP at proximal synapses.

Scale bars represent 5 μm. See also Figure S3.

only UNC-104/KIF1 (kinesin-3), KLP-4 (a protein related to UNC-104), and UNC-116/KIF5 are known to be expressed in the AVA interneurons (http://www.wormbase.org) (Siddiqui, 2002).

To determine the identity of the molecular motor(s) that transport GLR-1 receptors, we measured the in vivo transport of GLR-1::GFP vesicles in candidate motor protein mutants and found

(D) Cartoon schematic of the double-tagged SEP::mCherry::GLR-1 in transport vesicles and on the cell surface.

(E) Simultaneous two-color confocal imaging of SEP::mCherry::GLR-1. Single-plane confocal images taken before and after photobleaching (top) and the corresponding kymograph (bottom) showing GLR-1 transport (mCherry signal) and GLR-1 insertion into the membrane (SEP signal).

(F) Quantification of GLR-1 insertion events in synaptic and extrasynaptic regions. n = 10.

*$p < 0.05$, ***$p < 0.001$. Scale bars represent 5 μm. Error bars indicate SEM. See also Figure S2.

that both anterograde and retrograde GLR-1 transport were dramatically disrupted in *unc-116* loss-of-function mutants (Figures 4A–4D). In contrast, we observed normal velocity and run length in *klp-4(ok3537)* null mutants and only mild disruption of transport in *unc-104(e1265)* null mutants (Figures S4A and S4B).

Interestingly, we observed an *unc-116* allelic series with respect to GLR-1::GFP transport. Thus, the severity of the defects in GLR-1 transport speed, run length, and the number of transport events progressively increased from *unc-116(e2310)* to *unc-116(rh24)* (Figures 4A–4D; Table S1). The defective GLR-1 transport observed in these *unc-116* partial loss-of-function mutants suggested that transport might be eliminated by a complete loss of UNC-116/KIF5 function. Unfortunately, we were unable to measure GLR-1 transport in null mutants because the *unc-116* null allele is lethal (Byrd et al., 2001). We therefore generated transgenic worms that expressed a dominant-negative (DN) variant of UNC-116 (E160A) that is predicted to trap the protein in a rigor state (Klumpp et al., 2003). The rapid movement of GLR-1::GFP vesicles was eliminated in worms that expressed UNC-116(E160A) solely in AVA (Figures 4A–4D). We also failed to observe vesicle movement in transgenic worms where UNC-116 was knocked down specifically in AVA using double-stranded RNAi (*unc-116(RNAi)*; Figures 4A–4D). We could rescue the defective transport of GLR-1::GFP in *unc-116(wy270)* mutants by specifically expressing a wild-type *unc-116* transgene in AVA (Figures 4A–4D), indicating a cell-autonomous role for UNC-116-mediated transport of GLR-1.

Kinesin-1 motors are tetrameric proteins composed of two heavy chains (UNC-116) and two light chains. In *C. elegans*, the genes encoding the kinesin light chains (*klc-1* and *klc-2*) are broadly expressed (Sakamoto et al., 2005) (http://www.wormbase.org). Light chains regulate the binding of cargo to the motor and are involved in the recruitment of the motor to microtubule tracks (Hirokawa et al., 2010). To determine whether KLC-1 or KLC-2 light chains regulate GLR-1 transport, we examined GLR-1::GFP movement in light chain mutants. Transport was severely disrupted in *klc-2*, but not *klc-1* mutants (Figures 4E and 4F), indicating that GLR-1 transport is dependent on a specific isoform of kinesin-1.

To determine the subcellular distribution of UNC-116, we coexpressed fluorescently labeled UNC-116::mCherry with GLR-1::GFP in the AVA neurons. Although UNC-116 was detected throughout the processes, we noted that it appeared to accumulate at synapses (Figure 4G). We also simultaneously measured the movement of GLR-1::mCherry and UNC-116::GFP using two-color streaming confocal movies. As predicted for kinesin-driven transport of GLR-1, we found that the two signals colocalized in a subset of transport events, including retrograde movement toward the cell body (Figure 4H).

Kinesin-1 motors direct movement toward the plus-end of microtubules, which are typically oriented plus-end out, i.e., toward the distal ends of axonal processes (Stepanova et al., 2003). Because we observed bidirectional movement of GLR-1::GFP, we asked whether microtubules in AVA were of mixed polarity, similar to what has been observed in *Drosophila* dendrites (Stone et al., 2008; Zheng et al., 2008). Examination of microtubule growth dynamics in transgenic worms that expressed the microtubule end-binding protein EBP-2 (Stepanova et al., 2003; Zheng et al., 2008) fused to GFP revealed both plus-end-out and minus-end-out microtubules, consistent with bidirectional transport by UNC-116/KIF5 (Figures S4C and S4D). Additionally, we did not find that microtubule orientation or dynamics were disrupted in *unc-116* mutants (Figures S4C and S4D), indicating that the disrupted transport of GLR-1 in *unc-116* mutants was not an indirect effect of altered microtubules.

## GLR-1 Removal from Synapses Is Reduced in *unc-116* Mutants

Although GLR-1 transport was severely disrupted in *unc-116* mutants, we still observed accumulations of GLR-1::GFP in the proximal AVA processes (Figure 5A). Surprisingly, the average fluorescence intensity of synaptic puncta was considerably increased in *unc-116* mutants compared to wild-type (Figures 5A and 5B) and with the same allelic dependence we observed for GLR-1 transport (Figure 4). The increased fluorescence in *unc-116* mutants was not secondary to possible presynaptic defects, as we found that the intensity of synaptic GLR-1::GFP puncta was rescued by the selective expression of UNC-116 in AVA (Figures 5A and 5B).

To determine whether *C. elegans* kinesin-1 could also mediate the transport of vertebrate AMPARs, we expressed the vertebrate AMPAR subunit GluA1 fused to GFP in the AVA neurons. GluA1::GFP is functional and localized to puncta in the neural processes (Figure S5) (Brockie et al., 2013). Similar to what we observed for GLR-1, transport of GluA1::GFP was significantly impaired and the receptor accumulated at synaptic puncta in *unc-116* mutants compared to wild-type worms (Figure S5).

We reasoned that the accumulations of GLR-1 in *unc-116* mutants might be secondary to defective removal of synaptic receptors. To test this hypothesis, we photoconverted GLR-1::Dendra 2 at single synapses (Figure 5C). Following photoconversion, the red fluorescence decreased in wild-type worms with approximately 25% remaining 4 hr after conversion (Figure 5D). In contrast, decay was significantly reduced in *unc-116* mutants, with the slowest decay observed in *unc-116(RNAi)*. These results indicate that the removal of synaptic receptors is dependent on UNC-116/KIF5, consistent with the observed increase in synaptic GLR-1::GFP in *unc-116* mutants.

## UNC-116/KIF5 Is Required for the Delivery of Synaptic GLR-1

In contrast to the increased GLR-1::GFP fluorescence in the proximal processes of *unc-116* mutants, fluorescence intensity in distal regions of the AVA processes was decreased compared to that in wild-type worms (Figures 5E, 5F, and S6A). This finding, along with our analysis of vesicle stoppage and insertion (Figure 2), suggests that UNC-116/KIF5 is also required for the normal delivery of GLR-1 to synapses. Because diffusion depends on the square root of time, it is inefficient over long distances. Although the young adult worms we study are approximately 96 hr old, the number of synaptic GLR-1 receptors at more distal synapses was reduced in the absence of UNC-116/KIF5-mediated transport (Figure 5E). Assuming that the diffusion constant for receptors in the cell membrane is approximately 0.1 $\mu m^2/s$ (Earnshaw and Bressloff, 2008), we estimate that 96 hr is sufficient time for GLR-1 receptors to diffuse to

Neuron
UNC-116/KIF5 Mediates Transport of Synaptic AMPARs

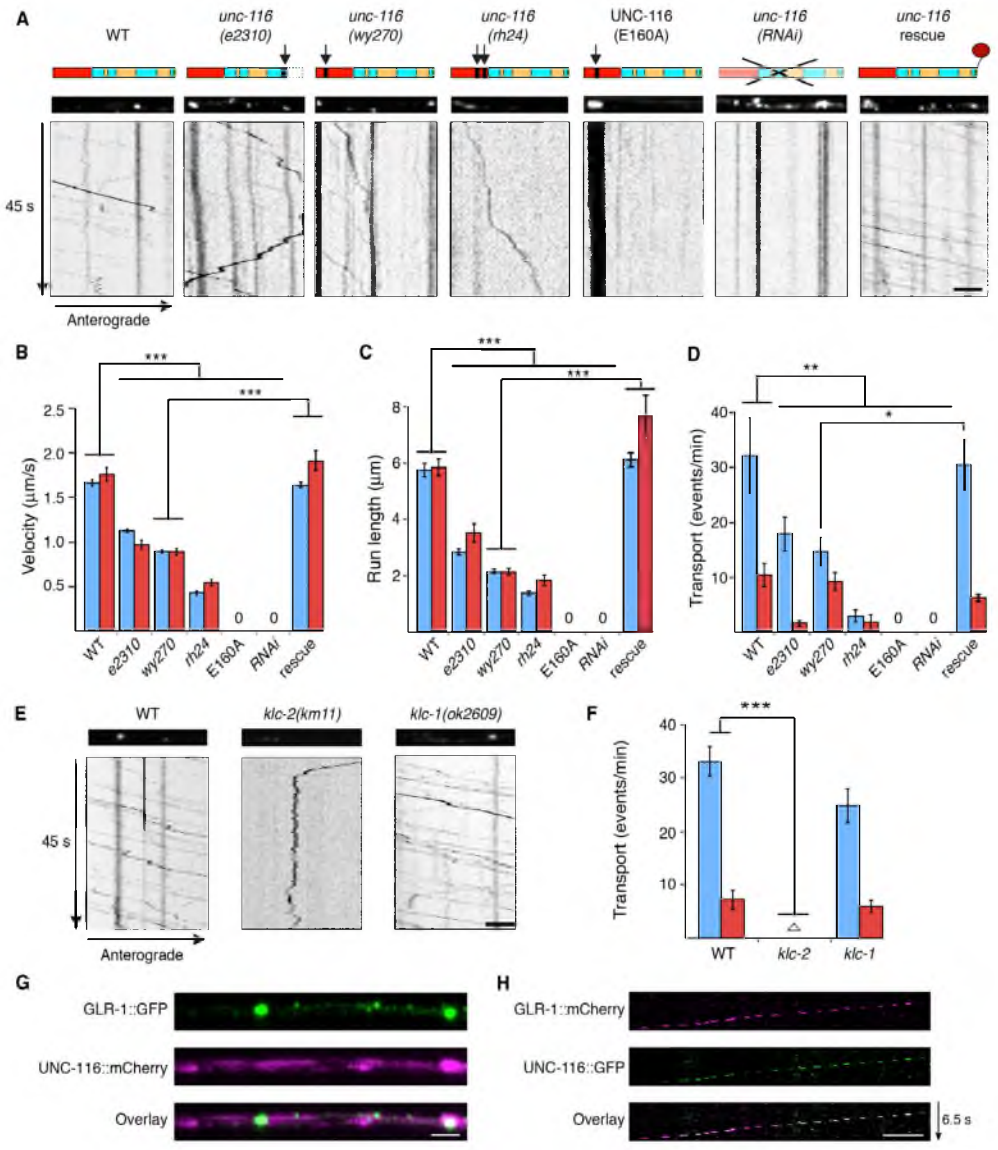


**Figure 4. Bidirectional Transport of GLR-1 Is Dependent on UNC-116/KIF5**

(A) Schematic of UNC-116/KIF5 (top). Arrows and black bar indicate the location of the mutation for each allele (Table S1). Red and yellow boxes represent the motor domain and coiled coil domains, respectively. Confocal images (middle) and kymographs (bottom) of GLR-1::GFP in the AVA processes. Scale bar represents 2.5 μm.

(B–D) Quantification of anterograde (blue) and retrograde (red) vesicle velocity (B), run length (C), and the frequency of transport events (D). n = 10 worms; "0" indicates no measurable mobile vesicles.

(E) Confocal images (top) and kymographs (bottom) of GLR-1::GFP in the AVA processes in wild-type (WT), *klc-2(km11)*, and *klc-1(ok2809)*. Scale bar represents 5 μm.

(F) Quantification of the frequency of transport events. Empty triangle in *klc-2* represents anterograde = 0.22 events/min and retrograde = 0.17 events/min. n = 5.

(G) Images of GLR-1::GFP and UNC-116::mCherry in the AVA processes of a transgenic worm. Scale bar represents 2 μm.

(H) Kymograph showing retrograde comovement of GLR-1::mCherry and UNC-116::GFP in AVA. The breaks in fluorescence are secondary to limited streaming capacity. Scale bar represents 2.5 μm.

*p < 0.05, **p < 0.01, ***p < 0.001. Error bars indicate SEM. See also Figures S3–S5.

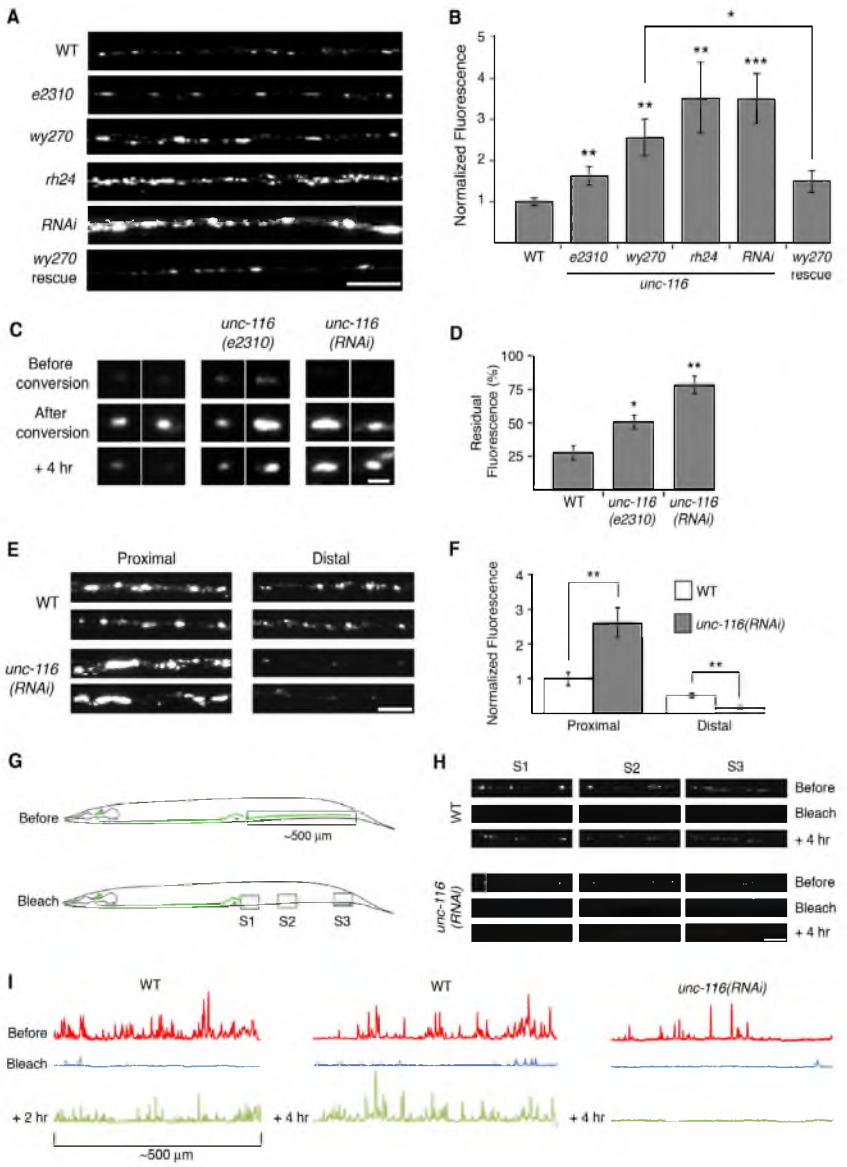


**Figure 5. Delivery and Removal of Synaptic GLR-1 Is Mediated by UNC-116/KIF5**

(A) Confocal images of GLR-1::GFP puncta in the proximal region of the AVA processes in various transgenic worms.

(B) Quantification of GLR-1::GFP synaptic puncta fluorescence normalized to WT. For all genotypes, $n \geq 10$ worms.

(C) Confocal images of GLR-1::Dendra2 synaptic puncta (red signal only) before and after photoconversion. Scale bar represents 1 µm.

(D) Quantification of the red signal remaining 4 hr after photoconversion. $n = 15$ puncta per genotype.

(E and F) Images (E) and quantification (F) of synaptic GLR-1::GFP puncta in AVA normalized to the proximal region of WT. $n = 10$ worms. Scale bar represents 5 µm.

(G) Cartoon schematic of the distal photobleach experiment.

(H) GLR-1::GFP images before, immediately after, and 4 hr after photobleaching in the regions indicated in (G). Scale bar represents 5 µm.

(I) Linescans of GLR-1::GFP fluorescence intensity in the distal half of AVA before and after photobleaching.

$^*p < 0.05$, $^{**}p < 0.01$, $^{***}p < 0.001$. Error bars indicate SEM. See also Figures S4–S8.

proximal synapses, but not long enough to reach distal synapses. In support of this, line scans of GLR-1::GFP fluorescence in *unc-116(RNAi)* and *unc-116(rh24)* mutants revealed dramatically reduced fluorescence in the distal processes when compared to fluorescence in more proximal regions, a pattern consistent with a diffusion-driven process (Figure S6A). We considered whether other motors might contribute to GLR-1 transport earlier in development, thereby confounding the interpretation of our line-scan analysis. However, in larval L2 stage *unc-116* mutants (Figures S6B and S6C), we found defects in GLR-1 puncta and transport similar to those of adult *unc-116* mutants (Figures 4 and 5).

To directly test the contribution of motor-mediated delivery of GLR-1 to synapses, we photobleached the entire distal half of the AVA processes and monitored the return of GFP fluorescence in three regions within the photobleached area (Figure 5G). Four hours after photobleaching, we observed significant fluorescence recovery in all distal regions in wild-type worms (67.5% ± 8.2%, n = 4; Figures 5H and 5I). In contrast, essentially no recovery was observed in *unc-116(RNAi)* mutants (3.5% ± 1.4%, n = 4, $p < 0.01$). Thus, in *unc-116* mutants, receptors diffused out of the cell body to proximal synapses where they accumulated secondary to defective removal.

### Blocking Protein Synthesis Does Not Appreciably Alter Delivery of GLR-1 to Synapses

While our data indicate that UNC-116/KIF5 has a critical role in receptor removal and delivery, other mechanisms, such as local synthesis of GLR-1, might also contribute to the number of synaptic receptors. For example, UNC-116/KIF5 might transport mRNA encoding GLR-1 to distal synapses, thus complicating the interpretation of our photobleaching studies. To evaluate the role of local GLR-1 synthesis, we blocked protein synthesis by acutely treating worms with the drug cycloheximide (CHX) for 6 hr (Jensen et al., 2012; Kourtis and Tavernarakis, 2009). We reasoned that if local synthesis of GLR-1 contributed to new synaptic receptors, treatment with CHX should significantly slow fluorescence recovery following photobleaching of GLR-1::GFP. Although CHX blocked new protein synthesis (Figure S7A), it did not disrupt existing GLR-1::GFP puncta or motor-mediated transport of GLR-1 (Figures S7B and S7C). Importantly, we did not observe an appreciable difference in the recovery of CHX-treated and untreated wild-type worms (Figure S7C). These data indicate that the repopulation of synaptic GLR-1 during the 4 hr following photobleaching is primarily dependent on motor-driven transport.

### The Intensity of GLR-1::GFP Puncta Is Decreased in *klp-4* Mutants

Although we did not observe any transport in *unc-116(RNAi)* worms, it is possible that additional kinesin motors might contribute to GLR-1 transport. In contrast to the accumulation of receptors in *unc-116* mutants, we observed a decrease in synaptic GLR-1::GFP fluorescence in mutants that lacked the Kinesin-3 motor KLP-4 (Figures S8A and S8B), which is consistent with an earlier report on *klp-4* mutants (Monteiro et al., 2012). Further analysis revealed that GLR-1::GFP puncta intensities were similarly diminished in *klp-4* mutants and *unc-116; klp-4* double mutants, indicating that *klp-4* is epistatic to *unc-116* and suggesting that KLP-4 functions upstream of UNC-116/KIF5-mediated transport of GLR-1. Although GLR-1::GFP synaptic puncta were smaller in *klp-4* mutants, analysis of the kymographs revealed apparently normal transport of vesicles in the AVA processes compared to the severely disrupted transport in *unc-116* mutants and *unc-116; klp-4* double mutants (Figures S8C and S8D). Additionally, we did not detect any apparent difference in the intensity of GLR-1::GFP transport vesicles in *klp-4* mutants (data not shown). Our data suggest that KLP-4 motors likely act in the cell body to regulate the number of exported GLR-1, but they apparently do not have a direct role in the long-range transport of GLR-1 vesicles in neuronal processes.

### GLR-1 Surface Expression Is Increased in *unc-116* Mutants

In *unc-116* mutants, the intensity of synaptic GLR-1::GFP fluorescence in the proximal processes was increased compared to wild-type. However, two populations of GLR-1 contribute to this fluorescent signal, i.e., receptors at the surface and receptors localized to subcellular compartments. To determine whether the number of surface receptors was modified by motor transport, we examined the relative levels of GLR-1 tagged with SEP (SEP::GLR-1) in wild-type and *unc-116* mutants. Interestingly, we found that surface SEP::GLR-1 fluorescence was considerably increased following RNAi knockdown of UNC-116 in AVA compared to that observed in wild-type (Figures 6A and 6B).

Since both the total pool of GLR-1 (GLR-1::GFP) and surface-expressed GLR-1 (SEP::GLR-1) were increased in *unc-116* mutants, we next asked whether the ratio of surface to total receptors was modified. We examined SEP::mCherry::GLR-1 at synapses and found that the ratio of surface to total receptors was considerably increased in *unc-116* mutants compared to wild-type (Figures 6C and 6D). This increase was similar to that in transgenic worms that expressed SEP::mCherry::GLR-1(4KR)—an ubiquitination-defective variant of GLR-1 that is predicted to increase the number of cell-surface synaptic receptors (Burbea et al., 2002; Grunwald et al., 2004).

Together, our data suggest a model in which GLR-1 receptors in *unc-116* mutants diffuse within the membrane to synaptic sites, where they preferentially remain at the surface. The altered ratio of surface to internal receptors might reflect a decreased rate of local receptor endocytosis, or an increased rate of receptor recycling to the cell surface. To distinguish between these possibilities, we photobleached SEP::mCherry::GLR-1 in either transgenic wild-type worms or *unc-116* mutants and quantified the rate of GLR-1 surface insertion by the appearance of SEP fluorescence. In transgenic wild-type worms that expressed either SEP::mCherry::GLR-1 or SEP::mCherry::GLR-1(4KR), we were able to detect insertion events, with GLR-1(4KR) having a higher rate of insertion (Figures 6E and 6F). In contrast, we did not observe any insertion events in *unc-116* mutants (Figures 6E and 6F). The observed defects in receptor removal and recycling in *unc-116* mutants suggest that UNC-116/KIF5 might also be required for the delivery of endosomal machinery.

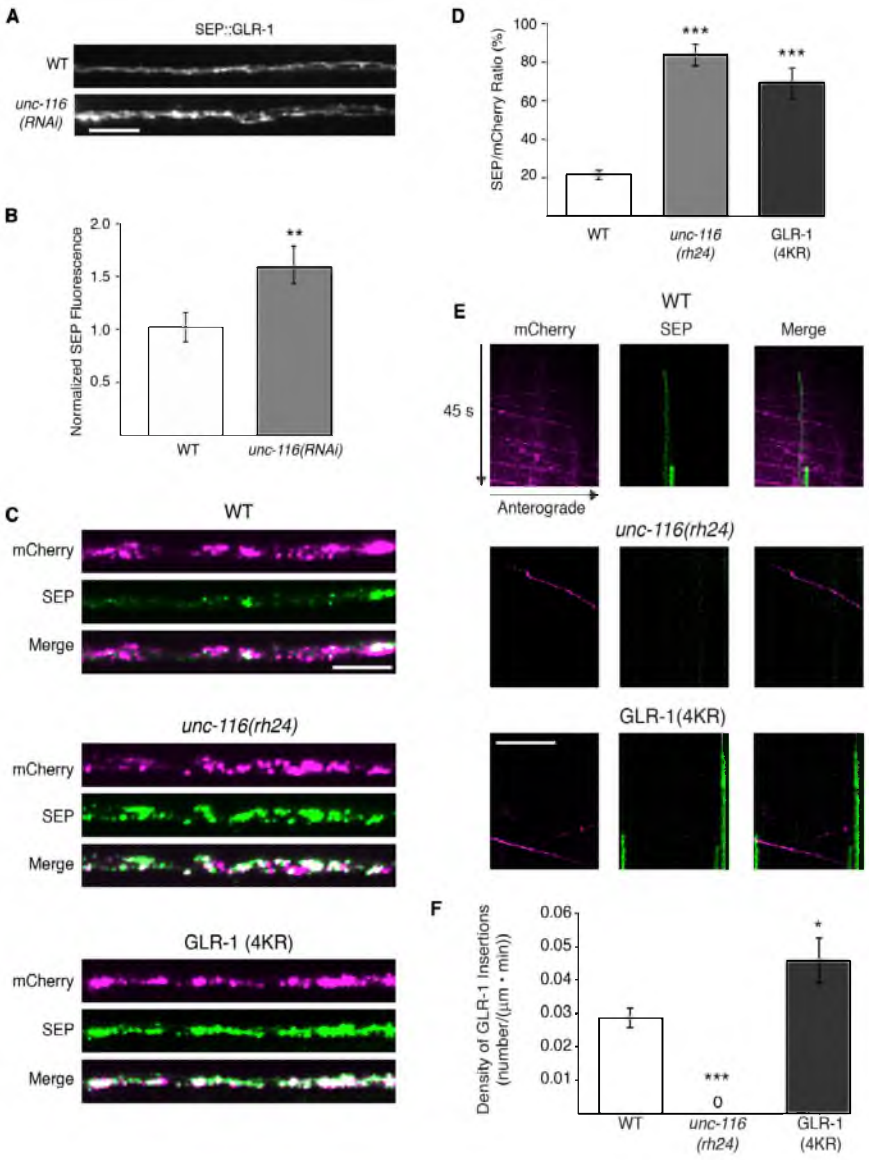


**Figure 6. Surface Expression of GLR-1 Is Increased in *unc-116* Mutants**

(A and B) Images of SEP::GLR-1 fluorescence (A) and quantification (B) of total fluorescence intensity normalized to WT. n = 10 worms.

(C) Confocal images of SEP::mCherry::GLR-1 and SEP::mCherry::GLR-1(4KR).

(D) Ratio quantification of total synaptic SEP and mCherry signals from SEP::mCherry::GLR-1 in WT and *unc-116* mutants, and SEP::mCherry::GLR-1(4KR). For all genotypes, n > 15 worms.

(E) Kymographs from simultaneous two-color streaming confocal movies of SEP::mCherry::GLR-1 in WT and *unc-116(rh24)*, and SEP::mCherry::GLR-1(4KR).

(F) Quantification of the overall insertion events. "0" indicates no measurable insertion events. For all genotypes, n > 15 worms.

Scale bars represent 5 µm. *p < 0.05, **p < 0.01, ***p < 0.001. Error bars indicate SEM.

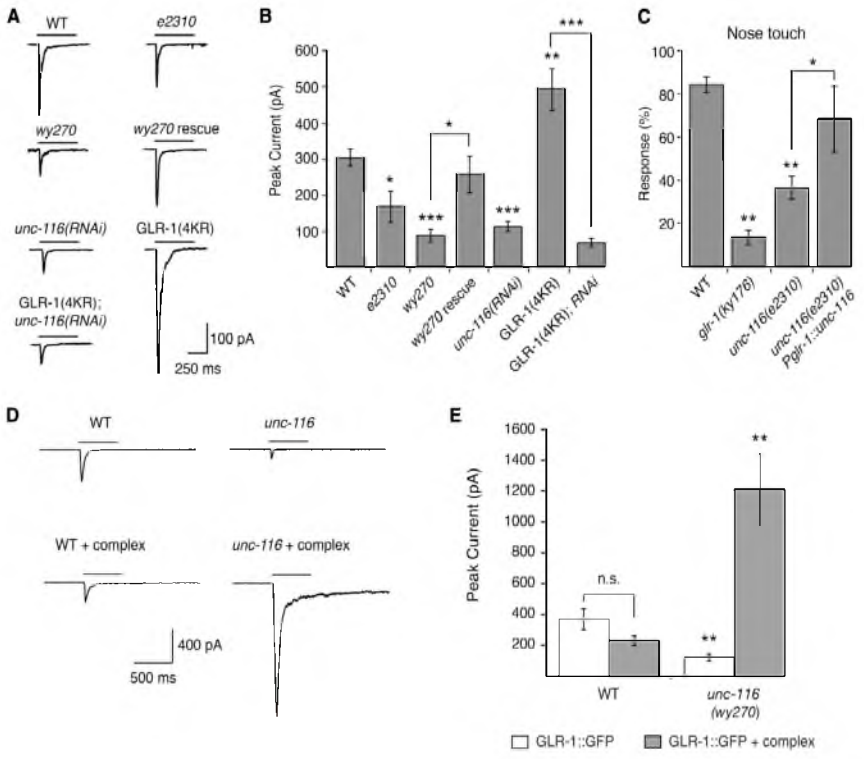


**Figure 7. Glutamate-Gated Currents Are Reduced in *unc-116* Mutants**

(A) Representative traces of glutamate-gated currents in AVA of transgenic worms that expressed GLR-1::GFP or GLR-1(4KR)::GFP.

(B) Quantification of glutamate-gated currents. For all genotypes, n ≥ 6 worms.

(C) Response to nose touch stimulation. n = 10 worms.

(D) Glutamate-gated currents in AVA of transgenic worms that overexpressed GLR-1::GFP either with or without overexpression of the GLR-1 signaling complex (complex = SOL-1 + SOL-2 + STG-2 + GLR-2).

(E) Quantification of glutamate-gated currents. For all genotypes, n ≥ 5 worms.

*p < 0.05; **p < 0.01; ***p < 0.001. For all recordings, cells were held at −60 mV. Bars indicate 3 mM glutamate application. Error bars indicate SEM. See also Figure S9.

## Glutamate-Gated Currents Are Decreased in *unc-116* Mutants

Based on our finding that loss of UNC-116/KIF5 function is associated with an increase in GLR-1::GFP surface expression, we predicted that voltage-clamp recordings from the proximal processes of AVA in these transgenic *unc-116* mutant worms would reveal an increase in glutamate-gated currents. Instead, we found that glutamate-gated currents in AVA were significantly decreased. This defect was cell autonomous as we could rescue the current by specifically expressing UNC-116 in the AVA neurons (Figures 7A and 7B). This decrease in current was independent of the GLR-1::GFP transgene as we found similar decreases in current when recording from *unc-116(RNAi)* or *unc-116(wy270)* mutants that did not express the transgene (Figure S9). In contrast, the increased surface expression of GLR-1(4KR) resulted in larger glutamate-gated currents compared to wild-type GLR-1 (Figures 7A and 7B). However, current amplitudes in transgenic *unc-116(RNAi)* mutants that expressed either GLR-1::GFP or GLR-1(4KR)::GFP were both indistinguishable and dramatically reduced compared to wild-type transgenic worms (Figures 7A and 7B). Thus, although surface GLR-1 was increased in *unc-116* mutants, glutamate-gated currents were paradoxically decreased.

Because of the diminished GLR-1-mediated currents in *unc-116* mutants, we asked whether a known GLR-1-mediated behavior was also disrupted. Similar to *glr-1* mutants (Hart et al., 1995; Maricq et al., 1995), we found that *unc-116(e2310)* mutants were defective in their avoidance response to tactile stimulation of the nose (Figure 7C). We could partially rescue this response in transgenic *unc-116* mutants that expressed a wild-type *unc-116* transgene under control of the *glr-1* promoter (*Pglr-1::unc-116*).

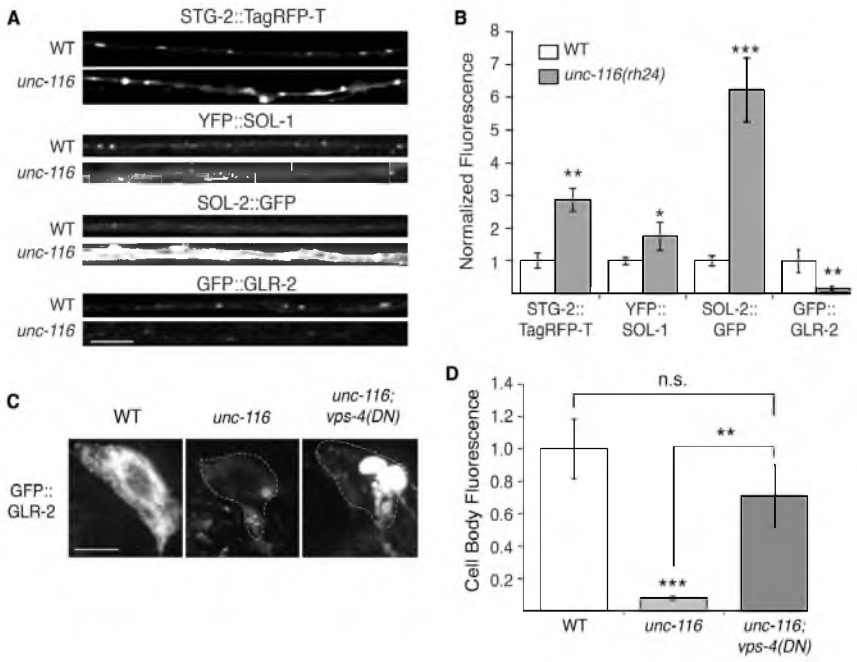


**Figure 8. GLR-2 Is Decreased in *unc-116* Mutants**

(A) Confocal images of STG-2::TagRFP-T, YFP::SOL-1, SOL-2::GFP, and GFP::GLR-2 in the AVA processes in transgenic WT and *unc-116(rh24)* mutants.

(B) Quantification of synaptic puncta fluorescence normalized to WT, n > 15 worms.

(C and D) Confocal images of GFP::GLR-2 in the AVA cell bodies (C) and corresponding quantification (D) in WT, *unc-116(rh24)*, and *unc-116(rh24); vps-4(DN)* double mutants. For all genotypes, n ≥ 8 worms.

*p < 0.05, **p < 0.01, ***p < 0.001. Scale bars represent 5 μm. Error bars indicate SEM.

## Overexpressing the AMPAR Signaling Complex Restored Current in *unc-116* Mutants

We speculated that the diminished glutamate-gated current in *unc-116* mutants, despite increased GLR-1 surface expression, was secondary to defects in the GLR-1 signaling complex. Perhaps the delivery of a key postsynaptic component was limited in the absence of motor function. To test this possibility, we measured glutamate-gated currents in transgenic wild-type worms and *unc-116* mutants that expressed GLR-1::GFP either with or without a second multitransgene array that encoded all of the additional known components of the GLR-1 signaling complex (GLR-2, SOL-1, SOL-2, and STG-2) (Brockie et al., 2001; Mellem et al., 2002; Walker et al., 2006; Wang et al., 2008, 2012; Zheng et al., 2004, 2006). Remarkably, overexpressing the signaling complex was sufficient to restore glutamate-gated currents in transgenic *unc-116* mutants (Figure 7D and 7E). Furthermore, currents in *unc-116* mutants were several-fold larger than those observed in transgenic wild-type worms. Presumably, this increase in *unc-116* mutants was secondary to a change in the composition of the GLR-1 signaling complex in addition to the observed increase in surface expression of GLR-1 (Figure 7). In contrast, the number of surface GLR-1 signaling complexes is well-regulated in wild-type worms, and therefore currents did not appreciably change with overexpression of the signaling complex (Figures 7D and 7E). These results indicate that in the absence of overexpression, the levels of one or more components of the GLR-1 signaling complex are diminished in *unc-116* mutants, thus limiting the number of functional receptors.

To determine the missing component(s) of GLR-1 signaling complexes in *unc-116* mutants, we used confocal microscopy to evaluate the distribution of the components in the proximal processes of AVA. Similar to GLR-1, we found increased synaptic accumulations of STG-2, SOL-1, and SOL-2 in *unc-116* mutants compared to wild-type (Figures 8A and 8B). In contrast, we found the opposite pattern with GLR-2 and observed a considerable decrease in GLR-2 levels in *unc-116* mutants compared to wild-type (Figures 8A and 8B).

These results suggest that the decrease in glutamate-gated current in *unc-116* mutants was secondary to decreased GLR-2 at synapses. Thus, although GLR-1 receptors accumulate at synapses in *unc-116* mutants, synaptic transmission is impaired because the signaling complex lacks the GLR-2 subunit. In support of this conclusion, in a previous study we found that currents in *glr-2* mutants are decreased in amplitude (Mellem et al., 2002).

One possible explanation for the decreased synaptic GLR-2 in *unc-116* mutants is that in the absence of UNC-116/KIF5-mediated transport, GLR-2-containing receptors are diverted to the lysosome for degradation. Consistent with this possibility, we found that the levels of GLR-2 were greatly reduced in the AVA cell bodies in *unc-116* mutants (Figures 8C and 8D). To evaluate the contribution of possible lysosomal degradation, we examined GLR-2 levels in transgenic worms that expressed a DN variant of the AAA-type adenosine triphosphatase, VPS-4, that mediates sorting of cargo from endosomes to the multivesicular body (Babst et al., 2002; Chun et al., 2008). In *vps-4(DN); unc-116* double mutants, we found that the GFP::GLR-2 signal was significantly increased compared to that in *unc-116* single mutants (Figures 8C and 8D). This result is consistent with increased lysosomal-mediated degradation of GLR-2 in *unc-116* mutants.

### Heat-Shock Expression of UNC-116/KIF5 in Adult Mutants Rescued Synaptic Defects

We next asked whether the GLR-1 transport and synaptic defects in *unc-116* mutants could be rescued in adult worms by expressing UNC-116/KIF5 specifically at the adult stage. Using a heat-shock promoter to induce expression of a wild-type *unc-116* transgene in adult *unc-116* mutants, we found that both the number of GLR-1::GFP transport events and synaptic puncta intensity were restored to near wild-type levels (Figures 9A–9C). Consistent with the normalization of synaptic puncta intensity following heat shock, we also found that glutamate-gated currents were significantly increased (Figures 9D and 9E). These data demonstrate that transport and redistribution of GLR-1 in the adult nervous system is ongoing and dependent on UNC-116/KIF5.

## DISCUSSION

### UNC-116/KIF5 Mediates the Delivery, Removal, and Redistribution of Synaptic AMPARs

We have demonstrated that kinesin-1 (UNC-116/KIF5) mediates the delivery, removal, and redistribution of GLR-1 AMPARs in *C. elegans* neurons, and that this motor-driven transport is of critical importance for synaptic function in the adult nervous system. Our in vivo studies have also shed light on the relative roles of diffusion, local synthesis, and motor-dependent transport in the establishment and maintenance of glutamatergic synapses. Defective motor-driven transport of AMPARs leads to an accumulation of dysfunctional AMPARs at synapses that lack the GLR-2 subunit; however, even after chronic loss of motor function, the synaptic defects could be corrected by transient expression of functional kinesin-1 motors.

Streaming movies of GLR-1::GFP revealed bidirectional motor-driven transport of AMPARs along the AVA processes that was dependent on UNC-116/KIF5. Although diffusion of GLR-1 in *unc-116* mutants is sufficient to populate proximal synaptic sites over a developmental time course of 4 days, receptors do not reach distal synapses, i.e., those greater than ~600 μm from the cell body. In contrast, motor-driven transport allows for the rapid delivery of receptors along the entire length of the processes. Thus, after photobleaching synaptic GLR-1::GFP, motor-dependent delivery of new receptors occurred within minutes and was the dominant process in the recovery of the fluorescent signal. Because neither diffusion nor local translation appeared to significantly contribute to fluorescence recovery in this time period, we conclude that delivery of new receptors is primarily dependent on kinesin-mediated transport. Although AMPARs labeled with quantum dots in cultured neurons have been observed moving between neighboring synapses by diffusing in the cell membrane (Ehlers et al., 2007), we now show that AMPARs are actively redistributed to distant synapses. This indicates that receptors are not simply destined for a single synapse, but rather can be utilized at multiple synapses.

GLR-1-mediated currents were reduced in *unc-116* mutants even though levels of the GLR-1 subunit and auxiliary proteins were increased. In *unc-116* mutants, we found an increased number of GLR-1 receptors at the surface, suggesting defective endocytosis and removal of GLR-1. Thus, kinesin-1 might deliver endosomal machinery to synapses that is required for the removal of GLR-1 receptors. In addition, we found that GLR-2-containing AMPARs appear to be more dependent on kinesin-mediated transport. Because the majority of the glutamate-gated current in wild-type worms is mediated by GLR-1/GLR-2 heteromers (Mellem et al., 2002), the current is reduced in *unc-116* mutants even though surface expression of GLR-1 is increased. Alternatively, if GLR-2 is required for the endocytosis of GLR-1/GLR-2 heteromers, then the increased synaptic GLR-1 in *unc-116* mutants might be secondary to the relative lack of synaptic GLR-2. However, the surface to internal ratio of SEP::mCherry::GLR-1 in *glr-2* mutants was not appreciably different from wild-type (data not shown).

Of particular interest was our observation that glutamate-gated currents in *unc-116* mutants that overexpressed all components of the signaling complex were far larger than those measured in either *unc-116* mutants or wild-type worms. In contrast, current magnitudes in wild-type worms either with or without overexpression of all components of the signaling complex were identical. These findings indicate that the balance between kinesin-dependent delivery and removal of AMPARs is critical for regulating synaptic strength, and that regulation of these transport processes could provide an additional mechanism for the homeostatic scaling of synaptic signaling (Davis, 2006; Goold and Nicoll, 2010; Tatavarty et al., 2013; Turrigiano, 2008). A recent paper from the Nicoll and Roche groups addressed distance-dependent scaling and demonstrated increased surface levels of AMPARs in distal synapses compared to proximal synapses (Shipman et al., 2013). Although we have not directly addressed this question, we found that the SEP::mCherry::GLR-1 ratio varied along the length of the AVA processes. Thus, the percentage of GLR-1 at the surface increased proximally to distally (data not shown).

### UNC-116/KIF5 Transport: Implications for Synaptic Plasticity

How the strength of synaptic communication between neurons is modified by experience-dependent neural activity is still an open question. The synaptic tag and capture hypothesis posits that synaptic activity leads to molecular changes that "tag" a synapse to enhance the probability of capturing plasticity-related proteins (PRPs) required for changes in synaptic strength. Thus, early long-term potentiation (LTP) of a synapse

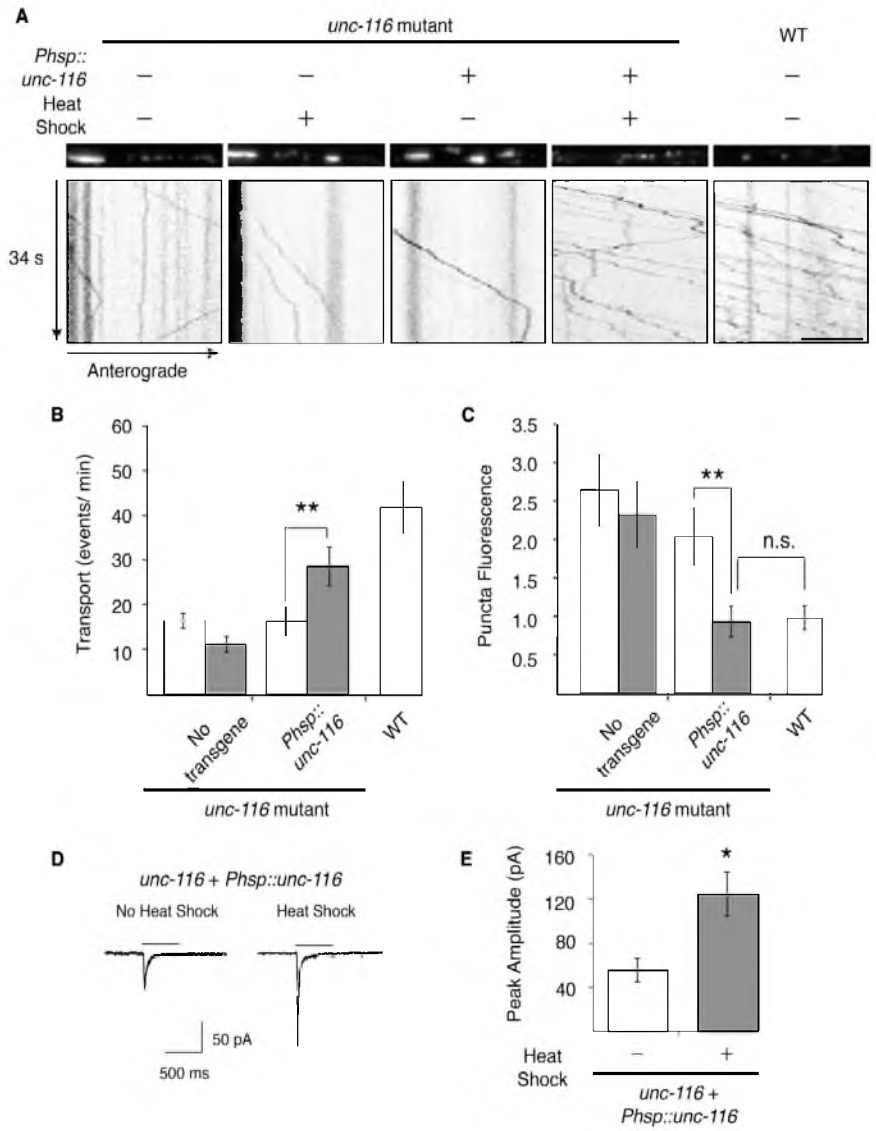


**Figure 9. Transient Expression of UNC-116/KIF5 in Adult *unc-116* Mutants Rescues GLR-1 Transport and Synaptic Transmission**

(A) GLR-1::GFP confocal images (top) and kymographs (bottom) in WT and *unc-116(wy270)* mutants in various treatment conditions.

(B and C) Quantification of GLR-1::GFP transport events per minute (B) and synaptic puncta fluorescence intensity (C) in worms with (gray) or without (white) heat-shock treatment normalized to WT. n = 15 worms. Scale bar represents 5 μm.

(D) Representative traces of glutamate-gated currents in AVA in transgenic *unc-116(wy270); Phsp::unc-116* worms either with (right) or without (left) heat-shock treatment. Bars indicate 3 mM glutamate application. Cells were held at −60 mV.

(E) Quantification of glutamate-gated currents in worms with (gray) or without (white) heat-shock treatment. For all genotypes, n ≥ 5 worms.

*p < 0.05, **p < 0.01. Error bars indicate SEM.

leads to local molecular changes (synaptic tagging) and the local synthesis of diffusible PRPs that are then captured by the tagged synapse (Redondo and Morris, 2011).

Our experiments suggest a model of synaptic capture in which activity-dependent synaptic tagging increases the probability of motor-dependent delivery of AMPARs. We found that receptor movement is highly dynamic in the AVA neurons, which have a large pool of motor-transported receptors. This ensures that any given synapse is only a few seconds removed from a motor carrying AMPARs, allowing for rapid, activity-dependent changes in synaptic AMPARs that are independent of new protein synthesis. We suggest that synaptic tagging and motor-dependent delivery can also contribute to longer-timescale, protein-synthesis-dependent plasticity. Protein synthesis associated with late LTP might fortify the synaptic tag, thus maintaining the probability of motor-dependent receptor delivery. In this process, the tagged synapse can become self-sustaining as long as motor transport is unimpaired.

Our studies raise several important questions. First, what are the local signals for kinesin-mediated delivery and removal of synaptic AMPARs? We can imagine that these processes are regulated by synaptic activity and, thus, could serve as a mechanism for local strengthening or weakening of synapses, i.e., LTP or long-term depression. Although the nature of the synaptic tag has not yet been identified (Redondo and Morris, 2011), we expect that genetic analysis in *C. elegans* will distinguish among possible mechanisms for synaptic tagging, including local modification of microtubules, recruitment of actin for hand off to myosin-class motors, local increases in intracellular $Ca^{2+}$, and local depletion of ATP causing stalling of motors at synapses (Guillaud et al., 2008; Kapitein et al., 2013; Maas et al., 2009; Newby and Bressloff, 2009, 2010). Second, what distinguishes GLR-1 homomers from GLR-1/GLR-2 heteromers with respect to motor-mediated transport? In the absence of kinesin-1, heteromers are selectively degraded, suggesting the involvement of a possible GLR-2-specific cargo adaptor protein. Third, how are the other components of the GLR-1 signaling complex delivered and removed from synapses? Fourth, what are the relevant cargo adaptors? An early report implicated the GRIP1 scaffolding protein in kinesin-dependent trafficking (Setou et al., 2002), but conditional knockout of glutamate receptor interacting proteins did not appear to disrupt the steady state trafficking or endocytosis of AMPARs (Mao et al., 2010). Finally, although our results clearly demonstrate that UNC-116/KIF5 is required for the long-range transport of GLR-1, we would expect that additional motors such as dynein, other kinesins, or unconventional myosins might contribute to this process, as well as to other aspects of delivery such as switching of transport direction and short-range transport at the synapse.

Altered transport is found in a variety of neurological disorders and presumably contributes to the disrupted synaptic function that is evident at all stages of diseases such as Alzheimer's (Hirokawa et al., 2010; Ittner and Götz, 2011; Stokin and Goldstein, 2006). Our results demonstrate a critical role of kinesin in the establishment and maintenance of glutamatergic synapses and suggest that defective synaptic signaling secondary to altered transport might be restored by repairing the underlying transport defect.

## EXPERIMENTAL PROCEDURES

### Strains and Genetics

All *C. elegans* strains were raised under standard conditions on the *E. coli* strain OP50 at 20°C unless otherwise noted. Wild-type worms were the Bristol N2 strain. Transgenic worms were generated by gonadal microinjection of *lin-15(n765ts)* mutants, wild-type, or appropriate mutant worms. Transgenic animals were selected by rescue of the *lin-15(n765ts)* mutant phenotype or expression of a fluorescent coinjection marker. Plasmids, transgenic arrays, and strains are described in the Supplemental Experimental Procedures. All fluorescently labeled proteins were found to be functional in transgenic rescue experiments of the mutant phenotype.

### Spinning Disk Confocal Imaging

One-day-old adult worms were mounted on 10% agarose pads with 1 µl of 30 mM muscimol, unless otherwise indicated. Images were acquired using a spinning disk confocal. Transport images were acquired by taking a streaming movie in a single Z-plane with 100 ms exposure time unless otherwise stated. GLR-1 was tagged with GFP, SEP, mCherry, or SEP::mCherry either at the N terminus (SEP::GLR-1 and SEP::mCherry::GLR-1) or near the C terminus (GLR-1::GFP and GLR-1::mCherry) as described previously (Rongo et al., 1998). The trajectory of moving GLR-1::GFP particles was quantified on kymographs in MetaMorph 7.7.7 (Molecular Devices) or MATLAB 2012a (MathWorks) and analyzed with a custom written MATLAB script to yield velocity, run length, flux, pause time, and stopping/insertion location. Fluorescence intensities of synaptic puncta were measured using a linescan measurement in MetaMorph and analyzed with a custom written MATLAB script (based on http://terpconnect.umd.edu/~toh/spectrum/PeakFindingandMeasurement.htm).

All other image analysis was performed in MetaMorph or ImageJ. A more detailed description of these procedures can be found in the Supplemental Experimental Procedures.

### Photobleaching, Photoconversion, and Photoactivation

Photobleaching was achieved using an argon laser (Coherent) set to 1.6 W total power output and/or a 561 nm laser (CNI Lasers) set to 600 mW total power output. GLR-1::Dendra2 and GLR-1::PAGFP were photoconverted and photoactivated, respectively, using a 405 nm laser (Coherent) set at 35 mW total power output. Lasers and laser merge module were provided by Spectral Applied Research. Regions of interest for photobleaching, photoconversion, and photoactivation were selected using a Mosaic II digital mirror device (Andor) controlled through MetaMorph. After photobleaching the distal region of the processes (Figure 5), the worms were transferred from the agarose pad on a microscope slide to a standard agar dish for 4 hr where they could move freely and feed. The worms were then transferred back to agarose pads for imaging. For photoconversion and redistribution experiments, worms were mounted on 10% agarose pads with 1.5 µl polystyrene beads (Kim et al., 2013). A detailed description of the quantification and procedures for fluorescence recovery after photobleaching, photoconversion, and redistribution experiments can be found in the Supplemental Experimental Procedures.

### Na-Azide and Nocodazole Treatments

For Na-azide treatment, worms were incubated in 40 mM Na-azide in M9 buffer on agar pads for 20 min at room temperature before imaging GLR-1 transport. For nocodazole treatment, 30 mM nocodazole in DMSO, or DMSO alone as control, was injected into the pseudocoelome of worms 1 hr prior to imaging.

### Heat Shock Treatment

Induction of *Phsp::unc-116::mCherry* expression was achieved by two heat-shock treatments of 1 hr each at 33°C separated by 12 hr at room temperature. Worms were imaged 4 hr following the second heat shock. For electrophysiology experiments, currents were recorded in worms with high expression of UNC-116::mCherry in AVA 12 hr after heat shock.

### Electrophysiology

Electrophysiological recordings were performed blind to genotype and treatment using previously described voltage-clamp techniques (Mellem et al.,

2002). With the exception of Figure S9, all worms expressed either GLR-1::GFP or GLR-1(4KR)::GFP in AVA.

### Behavioral Analysis

Nose touch response assays were performed as described in Mellem et al. (2002). All assays were performed blind to genotype.

### Statistical Analysis

The results were analyzed using an unpaired Student's t test.

## SUPPLEMENTAL INFORMATION

Supplemental Information includes Supplemental Experimental Procedures, nine figures, and one table and can be found with this article online at http://dx.doi.org/10.1016/j.neuron.2013.10.050.

## ACKNOWLEDGMENTS

We thank members of the Maricq laboratory for comments on the manuscript, Aleksander Maricq for assistance with data analysis, Amit Mukherjee for his assistance with kymograph analysis, and Linda Hauth for generating transgenic strains. We thank Josh Kaplan, Kang Shen, and Yishi Jin for providing worm strains. Some strains were provided by the *Caenorhabditis* Genetics Center, which is funded by National Institutes of Health (NIH) Office of Research Infrastructure Programs (P40 OD010440). This research was made possible by support from NIH grant NS35812 (to A.V.M.), a Human Frontier Science Program grant (to A.V.M.), and by postdoctoral fellowships from the Swiss National Science Foundation (to F.J.H.).

Accepted: October 18, 2013
Published: December 18, 2013

## REFERENCES

Adesnik, H., Nicoll, R.A., and England, P.M. (2005). Photoinactivation of native AMPA receptors reveals their real-time trafficking. Neuron *48*, 977–985.

Babst, M., Katzmann, D.J., Snyder, W.B., Wendland, B., and Emr, S.D. (2002). Endosome-associated complex, ESCRT-II, recruits transport machinery for protein sorting at the multivesicular body. Dev. Cell *3*, 283–289.

Bowler, M.W., Montgomery, M.G., Leslie, A.G., and Walker, J.E. (2006). How azide inhibits ATP hydrolysis by the F-ATPases. Proc. Natl. Acad. Sci. USA *103*, 8646–8649.

Brockie, P.J., Mellem, J.E., Hills, T., Madsen, D.M., and Maricq, A.V. (2001). The C. elegans glutamate receptor subunit NMR-1 is required for slow NMDA-activated currents that regulate reversal frequency during locomotion. Neuron *31*, 617–630.

Brockie, P.J., Jensen, M., Mellem, J.E., Jensen, E., Yamasaki, T., Wang, R., Maxfield, D., Thacker, C., Hoerndli, F., Dunn, P.J., et al. (2013). Cornichons control ER export of AMPA receptors to regulate synaptic excitability. Neuron *80*, 129–142.

Burbea, M., Dreier, L., Dittman, J.S., Grunwald, M.E., and Kaplan, J.M. (2002). Ubiquitin and AP180 regulate the abundance of GLR-1 glutamate receptors at postsynaptic elements in C. elegans. Neuron *35*, 107–120.

Byrd, D.T., Kawasaki, M., Walcoff, M., Hisamoto, N., Matsumoto, K., and Jin, Y. (2001). UNC-16, a JNK-signaling scaffold protein, regulates vesicle transport in C. elegans. Neuron *32*, 787–800.

Chun, D.K., McEwen, J.M., Burbea, M., and Kaplan, J.M. (2008). UNC-108/Rab2 regulates postendocytic trafficking in Caenorhabditis elegans. Mol. Biol. Cell *19*, 2682–2695.

Davis, G.W. (2006). Homeostatic control of neural activity: from phenomenology to molecular design. Annu. Rev. Neurosci. *29*, 307–323.

de Bono, M., and Maricq, A.V. (2005). Neuronal substrates of complex behaviors in C. elegans. Annu. Rev. Neurosci. *28*, 451–501.

Dittman, J.S., and Kaplan, J.M. (2006). Factors regulating the abundance and localization of synaptobrevin in the plasma membrane. Proc. Natl. Acad. Sci. USA *103*, 11399–11404.

Earnshaw, B.A., and Bressloff, P.C. (2008). Modeling the role of lateral membrane diffusion in AMPA receptor trafficking along a spiny dendrite. J. Comput. Neurosci. *25*, 366–389.

Ehlers, M.D., Heine, M., Groc, L., Lee, M.C., and Choquet, D. (2007). Diffusional trapping of GluR1 AMPA receptors by input-specific synaptic activity. Neuron *54*, 447–460.

Feinberg, E.H., Vanhoven, M.K., Bendesky, A., Wang, G., Fetter, R.D., Shen, K., and Bargmann, C.I. (2008). GFP Reconstitution Across Synaptic Partners (GRASP) defines cell contacts and synapses in living nervous systems. Neuron *57*, 353–363.

Glodowski, D.R., Chen, C.C., Schaefer, H., Grant, B.D., and Rongo, C. (2007). RAB-10 regulates glutamate receptor recycling in a cholesterol-dependent endocytosis pathway. Mol. Biol. Cell *18*, 4387–4396.

Goold, C.P., and Nicoll, R.A. (2010). Single-cell optogenetic excitation drives homeostatic synaptic depression. Neuron *68*, 512–528.

Greger, I.H., and Esteban, J.A. (2007). AMPA receptor biogenesis and trafficking. Curr. Opin. Neurobiol. *17*, 289–297.

Grunwald, M.E., Mellem, J.E., Strutz, N., Maricq, A.V., and Kaplan, J.M. (2004). Clathrin-mediated endocytosis is required for compensatory regulation of GLR-1 glutamate receptors after activity blockade. Proc. Natl. Acad. Sci. USA *101*, 3190–3195.

Guillaud, L., Wong, R., and Hirokawa, N. (2008). Disruption of KIF17-Mint1 interaction by CaMKII-dependent phosphorylation: a molecular model of kinesin-cargo release. Nat. Cell Biol. *10*, 19–29.

Gurskaya, N.G., Verkhusha, V.V., Shcheglov, A.S., Staroverov, D.B., Chepurnykh, T.V., Fradkov, A.F., Lukyanov, S., and Lukyanov, K.A. (2006). Engineering of a monomeric green-to-red photoactivatable fluorescent protein induced by blue light. Nat. Biotechnol. *24*, 461–465.

Hart, A.C., Sims, S., and Kaplan, J.M. (1995). Synaptic code for sensory modalities revealed by C. elegans GLR-1 glutamate receptor. Nature *378*, 82–85.

Henley, J.M., Barker, E.A., and Glebov, O.O. (2011). Routes, destinations and delays: recent advances in AMPA receptor trafficking. Trends Neurosci. *34*, 258–268.

Hirokawa, N., Niwa, S., and Tanaka, Y. (2010). Molecular motors in neurons: transport mechanisms and roles in brain function, development, and disease. Neuron *68*, 610–638.

Ho, V.M., Lee, J.A., and Martin, K.C. (2011). The cell biology of synaptic plasticity. Science *334*, 623–628.

Ittner, L.M., and Götz, J. (2011). Amyloid-β and tau—a toxic pas de deux in Alzheimer's disease. Nat. Rev. Neurosci. *12*, 65–72.

Jackson, A.C., and Nicoll, R.A. (2011). The expanding social network of ionotropic glutamate receptors: TARPs and other transmembrane auxiliary subunits. Neuron *70*, 178–199.

Jensen, M., Hoerndli, F.J., Brockie, P.J., Wang, R., Johnson, E., Maxfield, D., Francis, M.M., Madsen, D.M., and Maricq, A.V. (2012). Wnt signaling regulates acetylcholine receptor translocation and synaptic plasticity in the adult nervous system. Cell *149*, 173–187.

Ju, W., Morishita, W., Tsui, J., Gaietta, G., Deerinck, T.J., Adams, S.R., Garner, C.C., Tsien, R.Y., Ellisman, M.H., and Malenka, R.C. (2004). Activity-dependent regulation of dendritic synthesis and trafficking of AMPA receptors. Nat. Neurosci. *7*, 244–253.

Juo, P., Harbaugh, T., Garriga, G., and Kaplan, J.M. (2007). CDK-5 regulates the abundance of GLR-1 glutamate receptors in the ventral cord of Caenorhabditis elegans. Mol. Biol. Cell *18*, 3883–3893.

Kapitein, L.C., van Bergeijk, P., Lipka, J., Keijzer, N., Wulf, P.S., Katrukha, E.A., Akhmanova, A., and Hoogenraad, C.C. (2013). Myosin-V opposes microtubule-based cargo transport and drives directional motility on cortical actin. Curr. Biol. *23*, 828–834.

**Neuron, Volume *80***

# Supplemental Information

# Kinesin-1 Regulates Synaptic Strength by Mediating the Delivery, Removal, and Redistribution of AMPA Receptors

**Frédéric J. Hoerndli, Dane A. Maxfield, Penelope J. Brockie, Jerry E. Mellem, Erica Jensen, Rui Wang, David M. Madsen, and Andres V. Maricq**

Supplemental text and figures: Hoerndli et al.

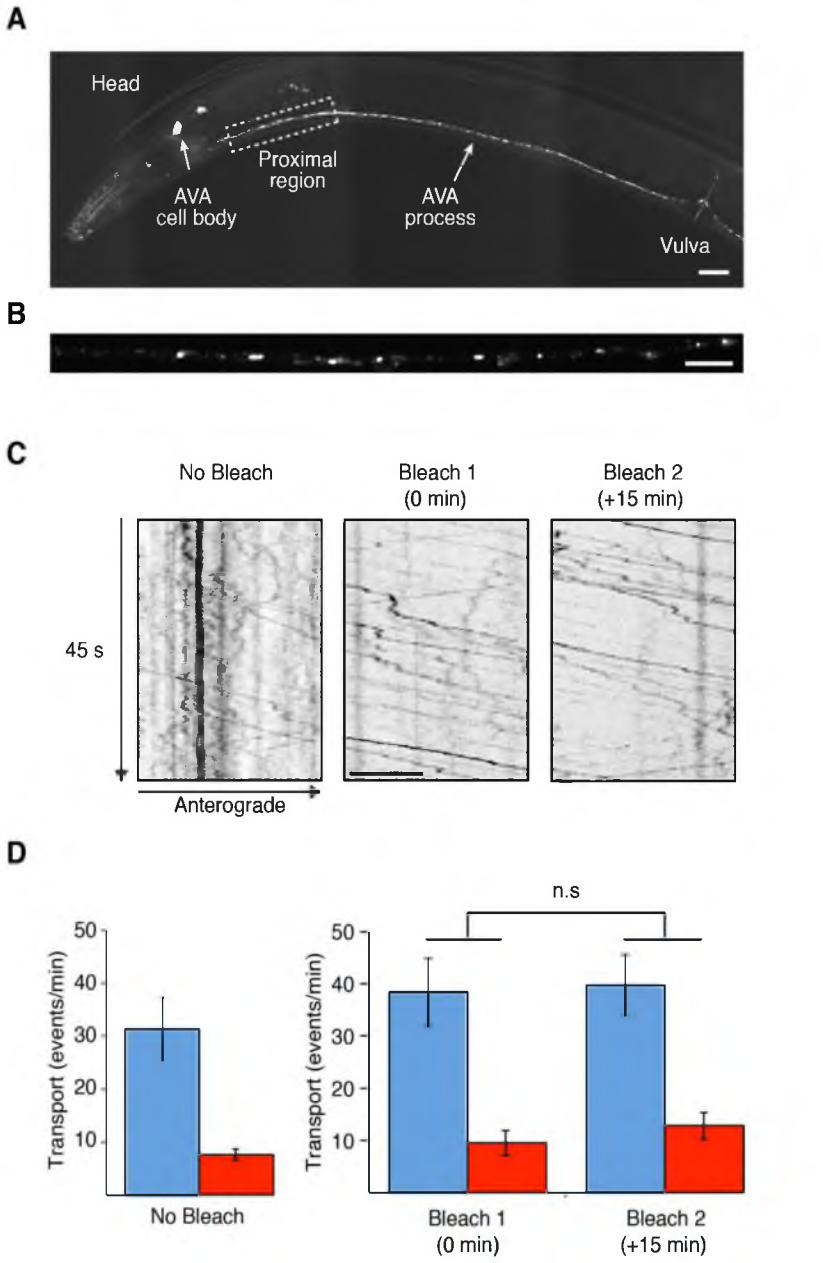


**Figure S1.** GLR-1::GFP is expressed in a punctate pattern along the length of the AVA processes. Supplemental data associated with Figure 1.

Supplemental text and figures: Hoerndli et al.

(A and B) Images of GLR-1::GFP in the AVA interneurons of transgenic wild-type worms. (A) Low resolution confocal image. Scale bar represents 10 μm. (B) High resolution confocal image of the boxed region in (A). Scale bar represents 5 μm. (C) Kymographs of GLR-1::GFP in AVA without photobleaching (left), after a single photobleach (middle) and after an additional photobleach of the same region following 15 minutes of recovery from the first photobleach (right). (D) Quantification of the number of GLR-1::GFP transport events. n=4 worms for the no photobleaching condition and n=6 for the multiple photobleaching condition. Scale bar represents 5 μm. Error bars indicate SEM.

Supplemental text and figures: Hoerndli et al.

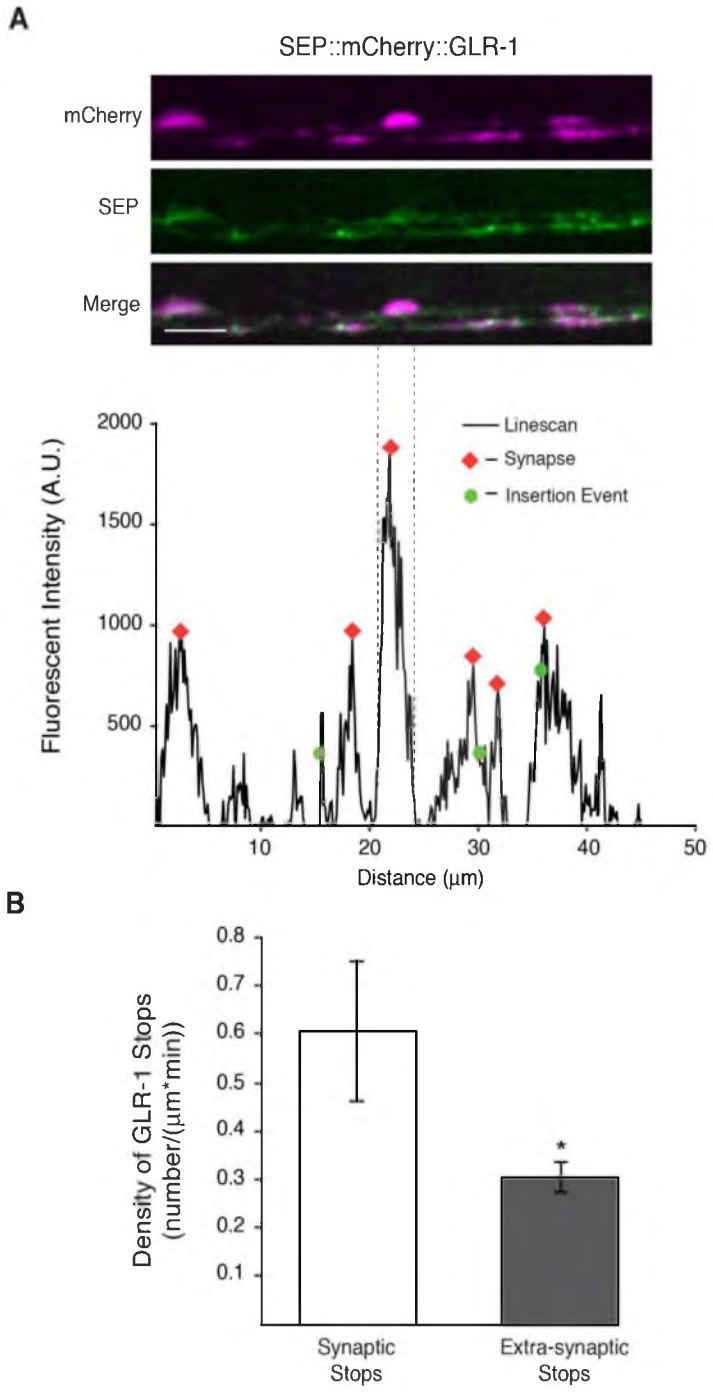

Supplemental text and figures: Hoerndli et al.

**Figure S2.** GLR-1 insertion events occur near existing synapses. Supplemental data associated with Figure 2.

(A) Single plane images from a simultaneous two-color streaming confocal movie of SEP::mCherry::GLR-1 before photobleaching (top). Corresponding linescan of the fluorescence intensity (bottom) of the mCherry channel from the above image. Red diamonds mark the peak fluorescence of synaptic puncta and green dots mark the relative position of all SEP::mCherry::GLR-1 insertion events over a 3.5 minute period. Scale bar represents 5 μm. (B) Quantification of SEP::mCherry::GLR-1 vesicle stops in synaptic and extrasynaptic regions. n=6 worms;*$p<0.05$, significantly different from Synaptic Stops.

Error bars indicate SEM.

Supplemental text and figures: Hoerndli et al.

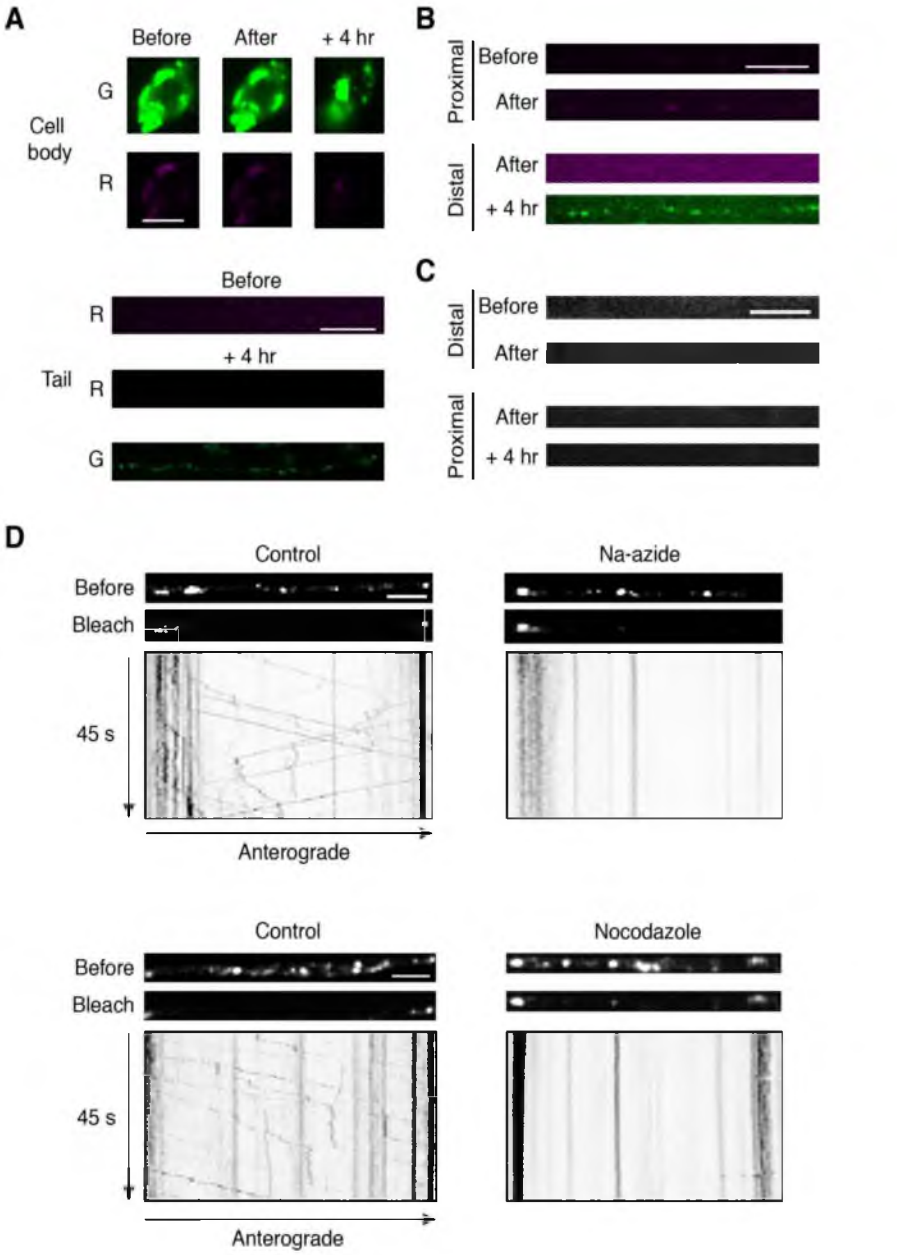


**Figure S3.** GLR-1 transport is dependent on ATP and microtubules. Supplemental data associated with Figures 3 and 4.

Supplemental text and figures: Hoerndli et al.

(A–C) Sham photoconversion or photoactivation of GLR-1::Dendra2 and GLR-1::PAGFP, respectively. All confocal images were taken before, immediately after, and 4 hr after sham conversion or photoactivation. (A) Images of GLR-1::Dendra2 in the cell body (top) and in the distal processes (bottom). Both green (G) and red (R) fluorescence are shown. (B) Images of GLR-1::Dendra2 after sham conversion in the proximal processes (only the red signal is shown); and at distal synapses (red and green signal shown) immediately after and 4 hr after sham conversion. (C) Images of GLR-1::PAGFP before and after sham photoactivation at proximal synapses. (D) Images of GLR-1::GFP in the AVA proximal processes before and after photobleaching and the corresponding kymographs of GLR-1::GFP in the photobleached region either with or without Na-azide (top) or nocodazole (bottom).

Scale bars represent 5 μm.

Supplemental text and figures: Hoerndli et al.

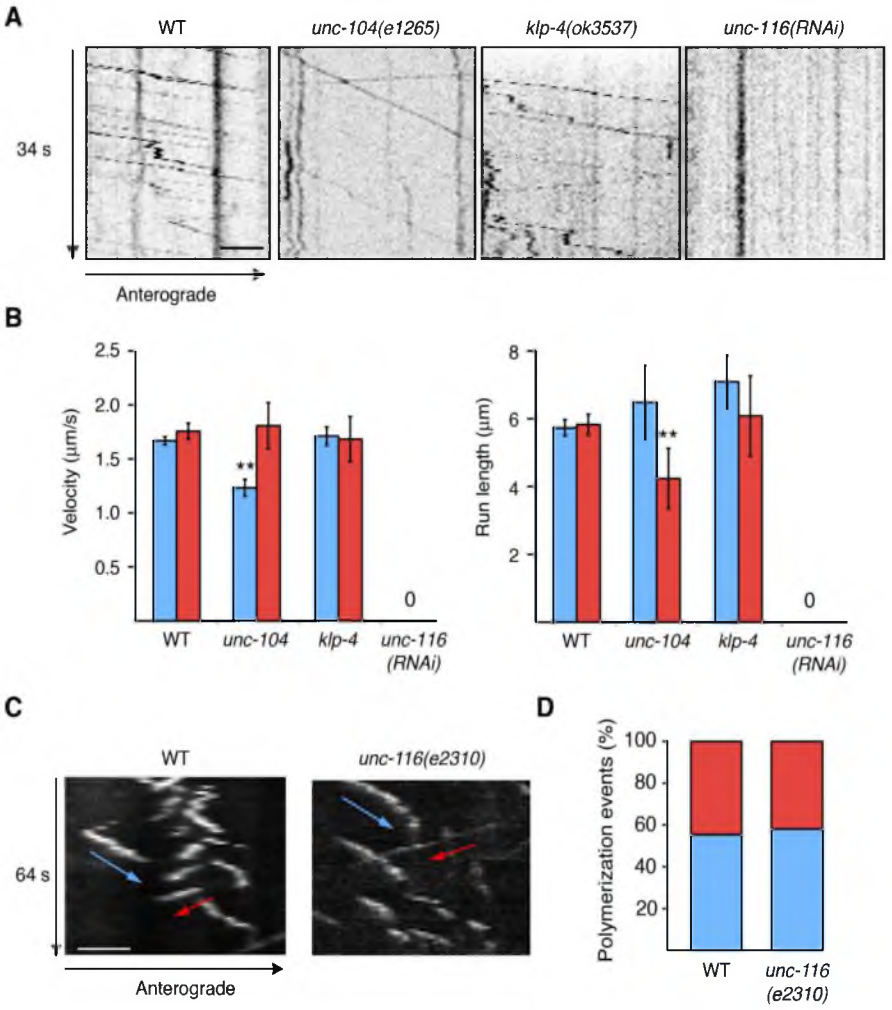


**Figure S4.** GLR-1 transport is normal in *klp-4* mutants and only minor defects were observed in *unc-104* mutants. Supplemental data associated with Figure 4.

(A) Kymographs of GLR-1::GFP transport in the AVA processes in wild-type worms, *unc-104*, *klp-4* and *unc-116(RNAi)* mutants. Scale bar represents 2 µm. (B) Quantification of GLR-1::GFP vesicle velocity and run length, n=10. ** $p \leq 0.01$, significantly different from wild type. Error bars indicate SEM. (C) Kymograph showing

Supplemental text and figures: Hoerndli et al.

anterograde (blue arrow) and retrograde (red arrow) movement of EBP-2::GFP in the proximal AVA processes in wild-type worms and *unc-116(e2310)* mutants. Scale bar represents 1 μm. (D) The relative number of anterograde (blue) and retrograde (red) EBP-2::GFP polymerization events, n=5 worms.

Supplemental text and figures: Hoerndli et al.

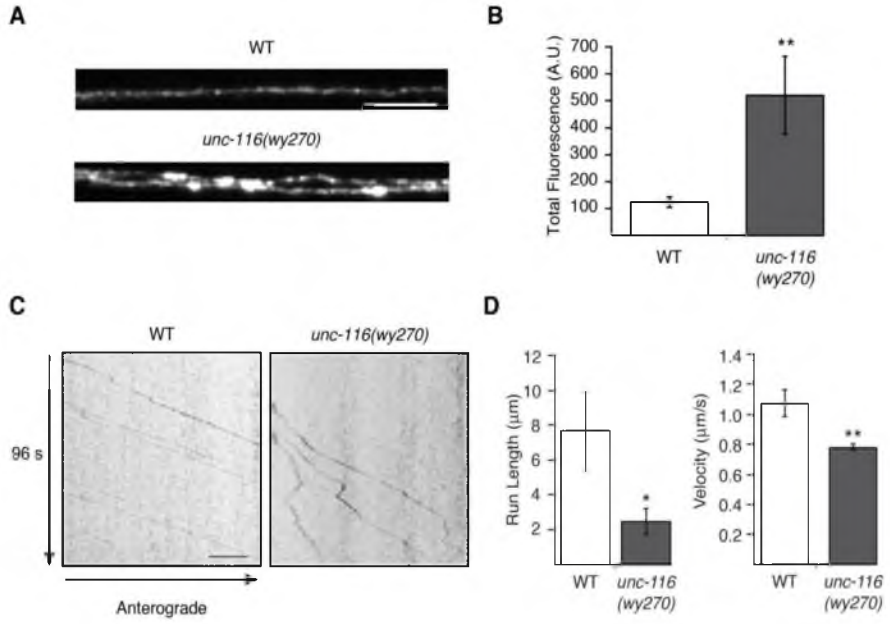


**Figure S5.** Synaptic localization and transport of the vertebrate GluA1 AMPAR subunit depends on UNC-116/KIF5. Supplemental data associated with Figures 4 and 5.

(A and B) Confocal images of GluA1::GFP (A) and quantification of the average GluA1::GFP fluorescence (B) in the AVA interneurons of transgenic wild-type worms and *unc-116(wy270)* mutants, n>10. (C) Kymograph of GluA1::GFP transport in wild-type worms and *unc-116(wy270)* mutants. (D) Quantification of run length and velocity of GluA1::GFP transport events, n>6.

Scale bars represent 5 µm. * p≤0.05, ** p≤0.01 significantly different from wild type. Error bars indicate SEM.

Supplemental text and figures: Hoerndli et al.

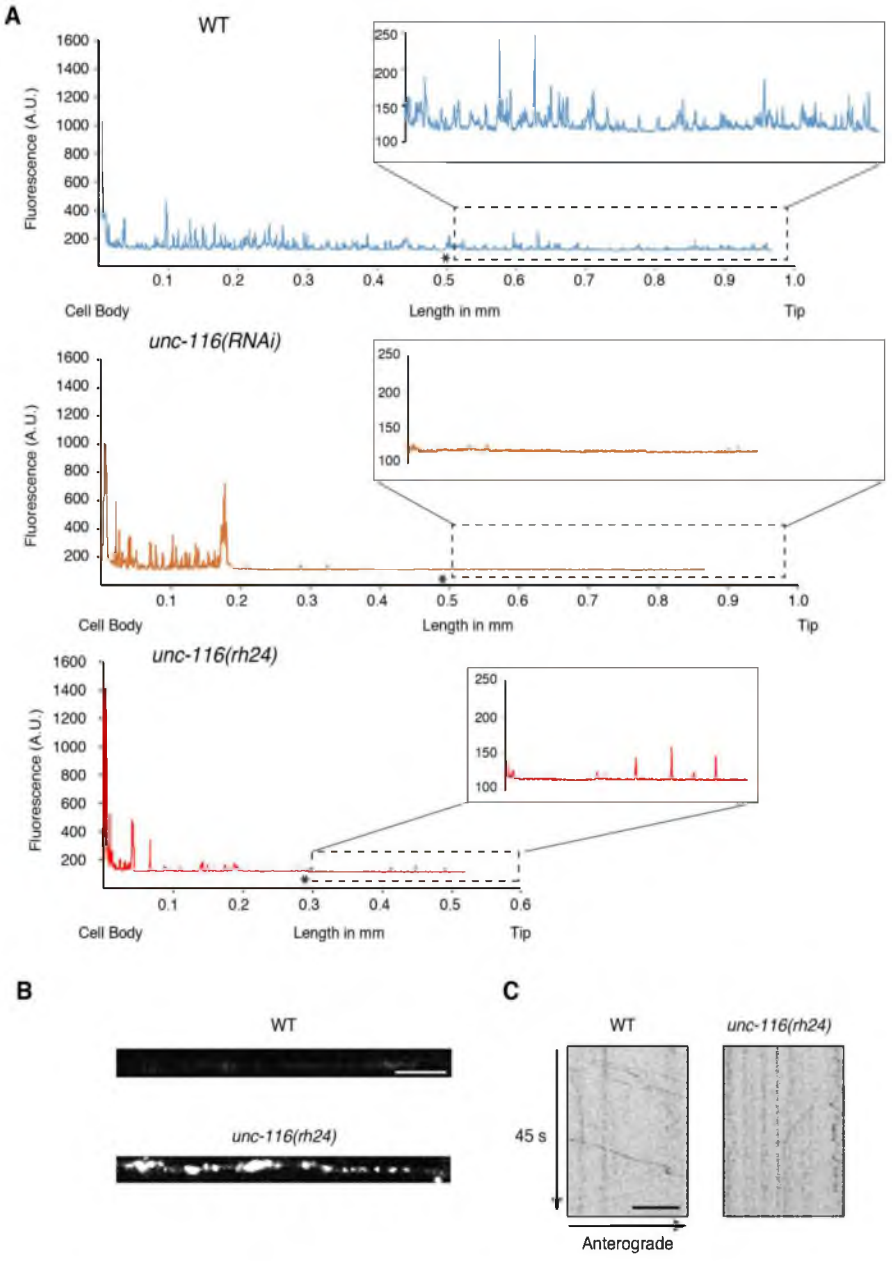


**Figure S6.** The distribution of GLR-1 in AVA is consistent with diffusion-mediated transport in *unc-116* mutants. Supplemental data associated with Figure 5.

Supplemental text and figures: Hoerndli et al.

(A) Representative linescans of GLR-1::GFP fluorescence in AVA from confocal images of transgenic WT, *unc-116(RNAi)* and *unc-116(rh24)* worms. Insets show an expanded view of the posterior region of AVA. * Indicates the position of the vulva. (B and C) Single plane confocal images (B) and kymographs (C) of GLR-1::GFP in WT and *unc-116(rh24)* at the L2 larval stage.

Scale bars represent 5μm.

Supplemental text and figures: Hoerndli et al.

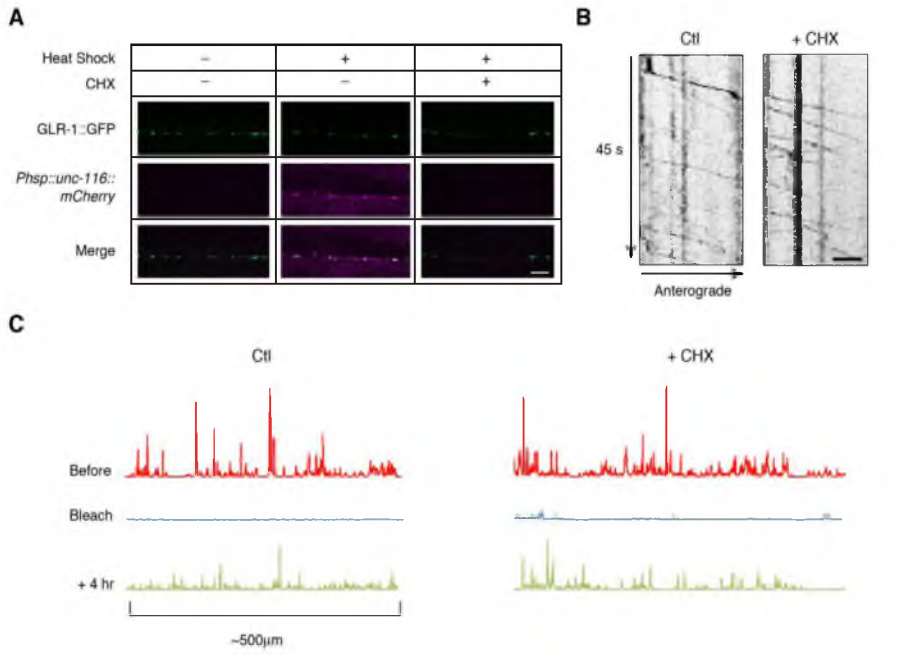


**Figure S7.** Local protein synthesis does not contribute to fast delivery of synaptic AMPARs. Supplemental data associated with Figure 5.

(A) Confocal images of GLR-1::GFP and UNC-116::mCherry in the AVA processes of worms with (+) or without (–) heat-shock treatment or treatment with cycloheximide (CHX). Scale bar represents 5 µm. (B) Kymographs of GLR-1::GFP movement in the AVA processes of adult worms with (+ CHX) and without (Ctl) cycloheximide treatment. Scale bar represents 2 µm. (C) Linescan of GLR-1::GFP fluorescence intensity in the distal region of AVA before and after photobleaching in wild-type worms with (+ CHX) or without (Ctl) cycloheximide treatment.

Supplemental text and figures: Hoerndli et al.

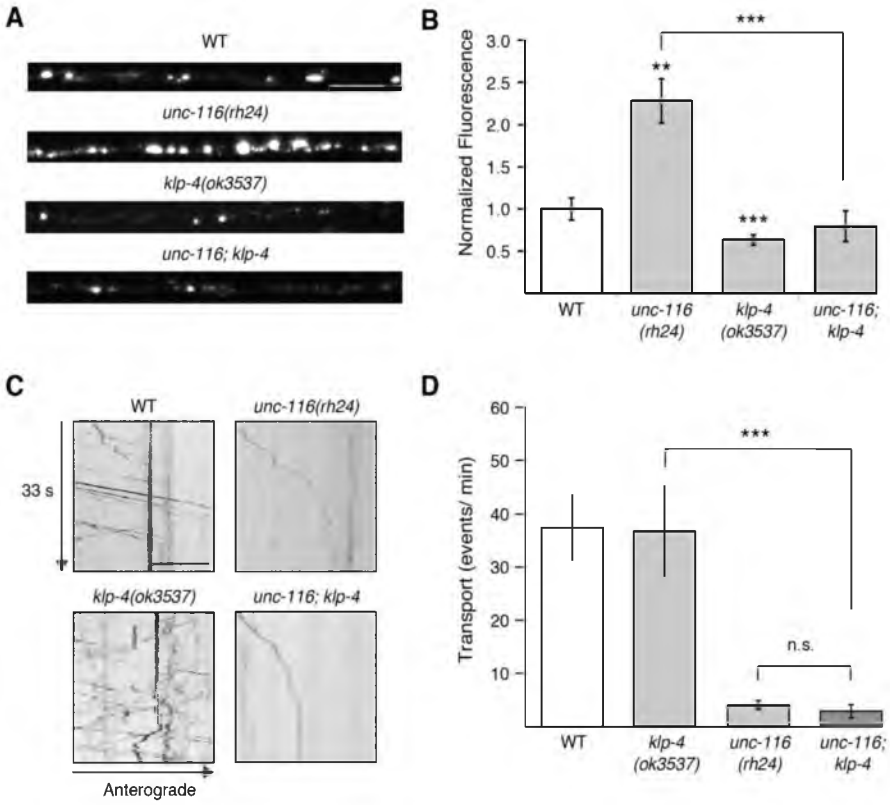


**Figure S8.** *klp-4* is epistatic to *unc-116* in the regulation of GLR-1 transport.

Supplemental data associated with Figure 5.

(A and B) Confocal images of GLR-1::GFP in AVA (A) and quantification of fluorescence intensity of synaptic puncta (B), n=10. (C and D) Kymographs of GLR-1::GFP transport (C) and quantification of the number of transport events (D), n > 8. Scale bars represent 5μm. ** p<0.01, *** p<0.001. Error bars indicate SEM.

Supplemental text and figures: Hoerndli et al.

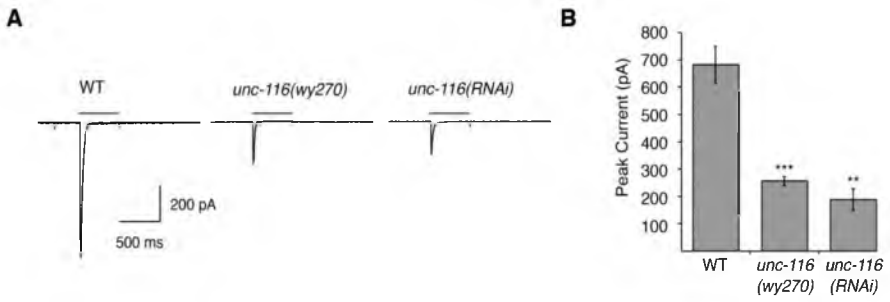


**Figure S9.** Glutamate gated currents are reduced in *unc-116* mutants. Supplemental data associated with Figure 7.

(A) Representative traces of glutamate-gated currents in AVA of wild-type worms and *unc-116* mutants without the GLR-1::GFP transgene. (B) Quantification of glutamate-gated currents, n=6 for WT and *unc-116(RNAi)*, n=3 for *unc-116(wy270)*. ** $p<0.01$, *** $p<0.001$, significantly different from wild type. For all recordings, cells were held at –60 mV. Bars indicate 3 mM glutamate application. Error bars indicate SEM.

Supplemental text and figures: Hoerndli et al.

**Table S1.** Description of *unc-116* alleles

| Allele | Mutation | Reference |
|---|---|---|
| *e2310* | Tc5 insertion:<br>ORF: 2576-77bp | Patel et al, 1993, PNAS |
| *wy270* | L129P | Yan et al., 2013 |
| *rh24* | E338K and I304M | Patel et al., 1993, PNAS and E. Jorgensen personal communication |

Supplemental data associated with Figure 4.

Supplemental text and figures: Hoerndli et al.

**Supplemental Experimental Procedures**

**Plasmids.** The following plasmids were used to generate transgenic animals: pJM23, *lin-15(+)*; pPB1, *Pnmr-1::GFP*; pDM1437, *Prig-3::HA::glr-1::gfp*; pDM1556, *Prig-3::HA::glr-1::mCherry*; pDM1633, *Pflp-18::unc-116::gfp*; pFH3-3, *Prig-3::unc-116::mCherry;* pDM1501, *Prig-3::ebp-2::gfp*; pDM1494, *Prig-3::mCherry*; pDM1442, *Prig-3::sep::glr-1*; pDM1586, *Pglr-1::unc-116::gfp*; pDM1550, *Prig-3::HA::glr-1::dendra2*; pDM1782, *Phsp16-2::unc-116::mCherry*; pDM1475, *Peat-4::ChR2::mCherry*; pDM1899, *Prig-3::HA::glr-1(4KR)::gfp*; pDM1439, *Prig-3::HA::glr-1::pagfp;* pDM1196, *Pnmr-1::mCherry;* pDM1983, *Prig-3::sep::mCherry::glr-1;* pDM2071, *Prig-3::sep::mCherry:glr-1(4KR);* pDM1973, *Pflp-18::gfp::glr-2;* pDM1788, *Pflp-18::gfp::sol-1;* pWR38, *Prig-3::sol-2::mCherry;* pDM1457, *Prig-3::stg-2(minigene)::gfp,* pCT61, *Pegl-20::nls::dsRed;* pDM1941, *Prig-3::stg-2(minigene)::TagRFP-T;* pDAM15, *Prig-3::yfp::sol-1;* pWR37,*Prig-3::sol-2::gfp;* pDM2101,*Pflp-18::γ-2::mCherry;* pDM2100, *Prig-3::gfp::GluA1(flip);* pDM1748, *Pflp-16::unc-116(E164A)::mCherry. Prig-3* was constructed using sequence published in (Feinberg et al., 2008). The UNC-116 knockdown construct, *unc-116(RNAi),* was generated using a published protocol (Esposito et al., 2007). Primer sequences are available upon request.

**Transgenic arrays**. In most cases, transgenic worms were generated by germline transformation of *lin-15(n765ts)* mutants by microinjecting the *lin-15*(+) rescuing plasmid (pJM23). In cases where *lin-15* mutants were not used, transgenic worms were identified by expression of soluble GFP, YFP or dsRed under the regulation of a cell

specific promoter encoded by the coinjected plasmid. Integrated and extra-chromosomal arrays were: *akIs1, Pnmr-1::GFP; akIs141, Prig-3::HA::glr-1::gfp*; *akIs143, Prig-3::HA::glr-1::gfp, akIs154, Prig-3::HA::glr-1::dendra2*; *akIs172, Prig-3::sep::glr-1 + Peat-4::ChR2::mCherry; akEx1182, Pflp-18::unc-116 RNAi*; *akEx2078, Prig-3::unc-116::mCherry*; *akEx1057, Prig-3::ebp-2::gfp + Prig-3::mCherry*; *akEx1268, Prig-2::ebp-2::gfp*; *akEx1912, Prig-3::HA::glr-1::mCherry + Pflp-18::unc-116::gfp*; *akEx1183, Pglr-1::unc-116::gfp*; *akEx2681, Prig-3::HA::glr-1(4KR)::gfp; akEx2942, Prig-3::sep::mCherry::glr-1*; *akEx1001, Prig-3::HA::glr-1::pagfp + Pnmr-1::mCherry*; *akEx2020, Pflp-18::unc-116(E160A)+Pegl-20:yfp; akEx3221, Prig-3::sep::mCherry::glr-1(4KR)*; *akEx3073, Pflp-18::gfp::glr-2 + Pflp-18::gfp::sol-1+ Prig-3::sol-2::mCherry + Prig-3::stg-2::gfp + Pegl-20::nls::dsRed; akEx3089, Prig-3::stg-2::Tag-RFP; akSi33, single copy MoSCI insert Prig-3::yfp::sol-1; akEx3267, Pflp-18::gfp::glr-2 + Prig-3::glr-1::mCherry + Pegl-20::nls::dsRed; akEx3330, Prig-3::gfp::GluA1(flip) + Pflp-18::γ-2::mCherry + Pegl-20::nls::dsRed; akEx2207, Phsp-16-2::unc-116::mCherry + Pegl-20::dsRed; akEx1395, Prig-3::sol-2::gfp+ Pflp-18::HA::glr-1::mCherry*, *akEx3301, Phsp-16-2::unc-116::mCherry + Pegl-20::dsRed.*

**Mutant alleles.** The mutant alleles used in this study were *glr-1(ky176)* (Maricq et al., 1995), *sol-1(ak63)* (Zheng et al., 2004), *sol-2(ak205)* (Wang et al., 2011), *stg-2(ak134)* (Wang et al., 2008), *lin-15(n765ts)* (Ferguson and Horvitz, 1985), *unc-116(e2310) (Patel et al., 1993), unc-116(wy270) (Yan et al., 2013), unc-116(rh24) (Patel et al., 1993), unc-104(e1265)* (Hall and Hedgecock, 1991*), klp-4(ok3537), klc-1(ok2609) (Sakamoto et al., 2005),* and *klc-2(km11)* (Byrd et al., 2001; Sakamoto et al., 2005). *nuIs145, vps-4(DN)*

Supplemental text and figures: Hoerndli et al.

(Chun et al., 2008) was a kind gift from J. Kaplan.

**Confocal Microscopy.** All confocal images were acquired using a Nikon Eclipse Ti microscope with a CSU-10 Yokagawa spinning disc confocal head with 491 and 561 excitation lasers (Cobalt), merge module provided by Solamere technologies, a Photometrics Cascade II 1024 EMCCD camera, and a Nikon 100x 1.49 NA TIRF objective. Two-color streaming movies were acquired using a WaveFX-X1 spinning disk confocal system (Quorum Technologies) with 491 and 561 excitation lasers (Coherent) and captured using two matched Cascade II 1024 EMCCD cameras (Photometrics) with 300 ms exposure times on a Nikon Eclipse Ti with a Nikon 100x 1.49 NA TIRF objective. Image acquisition and device control were enabled by Metamorph 7.7.7 (Molecular Devices).

**Image Analysis.** The comparison of immobile and mobile puncta was based on region measurements using ImageJ. Immobile puncta were defined initially identified as vertical streaks on the unbleached kymograph. Fluorescence values correspond to the average intensity in a region of interest (ROI) subtracted for fluorescence background intensity.

For GLR-1::Dendra2 photoconversion experiments, the fluorescence signal was quantified by drawing a ROI on the maximal projection images of confocal stacks, corrected for background and expressed as a percentage of the signal immediately after photoconversion.

Posterior AVA FRAP experiments were quantified by linescan analysis performed on maximum intensity projections of stitched confocal stacks of the entire posterior segment

of the worm using a journal kindly provided by Vincent Pelletier (Quorum Technologies).

For redistribution experiments using GLR-1::Dendra2 or GLR-1::PAGFP (*akIs154* and *akEx1001*, respectively), the average fluorescence was quantified in AVA using maximal intensity projections of confocal stacks in ImageJ. Single channel images were set to the same dynamic range and the fluorescence in AVA was then measured in both channels using an identical ROI. Background noise was subtracted from the signal measured in AVA.

For cell body and proximal AVA process redistribution, the fluorescence in the RFP channels was expressed as a percentage of the total fluorescence present in the distal region. For GLR-1::PAGFP, the signal after 4 hr was expressed as a percent of the signal immediately after photoactivation.

For quantification of fluorescence in the AVA processes, we used ImageJ to measure the average fluorescence in a ROI of a maximally projected stack with corrections for background fluorescence.

To determine the percentage of surface expressed SEP::mCherry::GLR-1, we summed the total fluorescence of synaptic puncta in each channel (See Synaptic Puncta Quantification) for each worm individually. The total SEP fluorescence (surface pool) was divided by the total mCherry fluorescence (total pool) for each worm to get the percentage of surface expressed receptors.

**Synaptic Puncta Quantification.** We used linescan analysis of fluorescence intensity in the ventral cord to identify synaptic puncta, using a criterion of 4 standard deviations

above the inter-punctal fluorescence. The region of the puncta was fit using a polynomial function to the natural logarithm of the intensity and the total fluorescence of a synaptic puncta calculated from the area under the curve of the fitted polynomial. We distinguished synaptic puncta from the smaller mobile puncta based on user-defined input of the mobile events.

**Kymograph Tracking.** Kymograph tracking was preformed using a modified version of the MATLAB code from (Mukherjee et al., 2011). Output files from this program were then loaded into a custom MATLAB script to extract parameters outlined in **Experimental Procedures**. GLR-1 transport vesicles were considered "stopped" if their instantaneous velocity dropped below 350 nm/s. These stop events were then separated into pauses and long stops based on a user-defined input of stop duration. Measurement of the relative distance of long stops and insertion events from the nearest synapse was performed by mapping the stops/insertions onto the linescan of the pre-bleached image. Synapses were identified using the **Synaptic Puncta Quantification** algorithm. The "synaptic region" was defined as the average width of the base of a synaptic puncta (750 nm) centered on the peak of each identified puncta. Thus, the length of each linescan was divided into two fractions: $F_s$, the fraction of the linescan that corresponds to sum of all synaptic regions, and $(1 - F_s)$, the fraction that is extrasynaptic. The density of stops/insertions was then computed by assignment of the stop/insertion event to the synaptic region or extrasynaptic region, then dividing by the total distance of the region as determined from the linescan.

Supplemental text and figures: Hoerndli et al.

**Cycloheximide and heatshock treatment.** Young adult worms were transferred to NGM plates with OP50 and either with or without CHX (2mg/ml) for 2 hrs. Worms were then imaged either for GLR-1::GFP transport or for GLR-1:GFP puncta as described in **Experimental Procedures**. For FRAP of the posterior region of AVA, worms were treated with or without CHX for 2 hrs prior to imaging. Worms were then mounted on 10% agarose pads, imaged before and after photobleaching, rescued from the pad and returned to their plates, respectively. Four hours later, worms were imaged again for fluorescence recovery. To control for CHX treatment, worms expressing GLR-1::GFP and *Phsp::unc-116::mCherry* were transferred to plates either with and without (2mg/ml) CHX for 2 hrs, then submitted to 1 hr heat-shock at 33°C and imaged 4 hrs after heat-shock treatment. Control worms were first transferred to OP50 plates with CHX (2mg/ml) for 2 hrs and imaged 4hrs later without heat-shock.

**Supplemental References**

Esposito, G., Di Schiavi, E., Bergamasco, C., and Bazzicalupo, P. (2007). Efficient and cell specific knock-down of gene function in targeted C. elegans neurons. Gene *395*, 170-176.

Ferguson, E.L., and Horvitz, H.R. (1985). Identification and characterization of 22 genes that affect the vulval cell lineages of the nematode Caenorhabditis elegans. Genetics *110*, 17-72.

Hall, D.H., and Hedgecock, E.M. (1991). Kinesin-related gene unc-104 is required for axonal transport of synaptic vesicles in C. elegans. Cell *65*, 837-847.

Mukherjee, A., Jenkins, B., Fang, C., Radke, R.J., Banker, G., and Roysam, B. (2011). Automated kymograph analysis for profiling axonal transport of secretory granules. Medical image analysis *15*, 354-367.

Patel, N., Thierry-Mieg, D., and Mancillas, J.R. (1993). Cloning by insertional mutagenesis of a cDNA encoding Caenorhabditis elegans kinesin heavy chain. Proceedings of the National Academy of Sciences of the United States of America *90*, 9181-9185.

Supplemental text and figures: Hoerndli et al.

Yan, J., Chao, D.L., Toba, S., Koyasako, K., Yasunaga, T., Hirotsune, S., and Shen, K. (2013). Kinesin-1 regulates dendrite microtubule polarity in Caenorhabditis elegans. eLife *2*, e00133.

# CHAPTER 3

# SUMMARY AND CONCLUSIONS

## Introduction

The proper trafficking and function of the AMPAR-type glutamate receptors (AMPARs) is essential for neuronal transmission in the brain. Indeed, disruption of AMPAR function results in defects in learning and memory (Anggono and Huganir, 2012; Kessels and Malinow, 2009) as well as a wide range of pathological conditions (Kwak and Weiss, 2006; Zhang and Abdullah, 2013). Therefore, elucidating the cellular mechanisms that regulate the trafficking of AMPARs to synapses will provide new insights into the pathophysiology of neuronal disorders associated with deficiencies in glutamatergic neurotransmission.

Over the last two decades, a plethora of studies in both vertebrate and invertebrate systems have elegantly shown the molecular pathways involved in the local trafficking of AMPARs at synapses. Briefly, endocytosis and exocytosis control the number of surface expressed AMPARs, while lateral diffusion and synaptic trapping via PDZ-domain proteins regulate the number of AMPARs at a synapse under basal conditions (Opazo and Choquet, 2011). These various processes are altered during synaptic activity, with LTP protocols increasing the rates of exocytosis and synaptic trapping, and LTD protocols leading to global receptor endocytosis (Hanley, 2010; Malinow and Malenka, 2002; Shepherd and Huganir, 2007). Furthermore, auxiliary proteins play a major role in the localization and function of AMPARs at the synapse (Nicoll et al., 2006; Straub and Tomita, 2012). Despite our profound knowledge of local AMPAR movements at the synapse, our understanding of the mechanisms regulating the

long-range AMPAR transport to synapses is severely deficient. To address this fundamental question, we have elected to study long-range AMPAR transport in the simple nervous system of *C. elegans*. Using a combination of genetics, cell biology, electrophysiology and live cell imaging, we have identified the molecular mechanisms regulating the transport of the AMPAR subunit GLR-1 to synapses *in vivo.*

## Transport of GLR-1 *In Vivo*

To determine the pathway(s) regulating the transport of GLR-1 to the synapse, we first generated transgenic animals expressing GLR-1::GFP under a promoter which limited transgene expression in the VNC to the AVA processes. Visualization by confocal microscopy showed that GLR-1::GFP was distributed in a punctate pattern along the length of the AVA processes. These puncta have been previously shown to mark postsynaptic sites (Burbea et al., 2002; Rongo et al., 1998). In vertebrate systems, AMPARs have been shown to be trafficked to synapses by at least three mechanisms: motor-driven transport (Kim and Lisman, 2001; Setou et al., 2002), lateral diffusion in the plasma membrane (Adesnik et al., 2005) and local synthesis of AMPARs at the synapse (Ho et al., 2011; Ju et al., 2004). To differentiate between these models, we looked at real-time streaming movies of GLR-1::GFP after photobleaching the synaptic puncta fluorescence. These movies revealed a population of highly mobile transport events, displaying speed and processivity consistent with transport by molecular motors.

## GLR-1 Is Transported by UNC-116/KIF5

To determine the identity of the molecular motor(s) responsible for the transport of GLR-1 in AVA, we monitored GLR-1::GFP trafficking in candidate motor protein mutants. We discovered that mutations in the kinesin-1, *unc-116,* severely disrupted both anterograde and retrograde transport of GLR-1. As MTs in AVA have a mixed polarity, these results suggest that a single molecular motor can mediate the bidirectional transport of cargo. In concurrence with this model, we observed colocalization of GLR-1::mCherry and UNC-116::GFP in a subset of transport events, including both anterograde and retrograde transport events.

Kinesin motors are a hetero-tetrameric complex consisting of two heavy-chain subunits (UNC-116/KIF5) and two light-chain subunits. The *C. elegans* genome encodes two kinesin light chain subunits, *klc-1* and *klc-2* (Koushika and Nonet, 2000; Sakamoto et al., 2005). To determine if these light-chain subunits regulate GLR-1 movement, we looked at GLR-1::GFP transport in light-chain mutants. Mutations in *klc-2*, but not *klc-1*, severely disrupted GLR-1::GFP transport, suggesting that a specific kinesin complex regulates the transport of GLR-1 in AVA.

Interestingly, this same UNC-116/KLC-2 motor complex has also been shown to regulate the transport of the *C. elegans* presynaptic vesicle protein, *snb-1,* in motor neurons (Byrd et al., 2001; Sakamoto et al., 2005). This begs the question: what other proteins might be involved in the association of GLR-1 with UNC-116/KIF5? Studies in multiple systems have shown that molecular motors use a complex arrangement of adaptor proteins to regulate motor function and

cargo specificity (reviewed in Franker and Hoogenraad, 2013). In particular, Setou et al. (2002) showed that the kinesin-1 KIF5 is directed towards different neuronal compartments by binding to different adaptor proteins. By interacting with Jun-interacting protein 3 (JIP3), KIF5 is preferentially steered towards the axon (Setou et al., 2002). Conversely, if KIF5 associates with the AMPAR binding protein GRIP1, this complex is targeted to dendrites (Setou et al., 2002). Consistent with these results, the *C. elegans* adaptor proteins UNC-16, the homologue of JIP3, and UNC-14, a RUN-domain protein, interact with UNC-116/KIF5 to regulate the transport of *snb-1* (Byrd et al., 2001; Sakamoto et al., 2005). Interestingly, mutations in *unc-16* and *unc-14* also affect the transport of GLR-1. These results suggest the possibility of an unknown adaptor protein, which can regulate the attachment of either SNB-1 or GLR-1 to the UNC-116/KIF5 motor complex (Figure 3.1A). Alternatively, GLR-1 transport vesicles might associate directly with the UNC-116/KLC-2 complex (Figure 3.1B). Experiments are currently underway to differentiate between these models.

## Transport Events Deliver GLR-1 to Synapses

Analysis of streaming confocal movies showed GLR-1::GFP transport events preferentially stopped at existing GLR-1 synapses, suggesting that molecular motor-based transport delivers new receptors to synapses. To determine if these new receptors were delivered to an intracellular pool or directly to the cell membrane, we observed the trafficking of GLR-1 tagged with a pH-sensitive variant of GFP, superecliptic pHlourin (SEP), and an mCherry

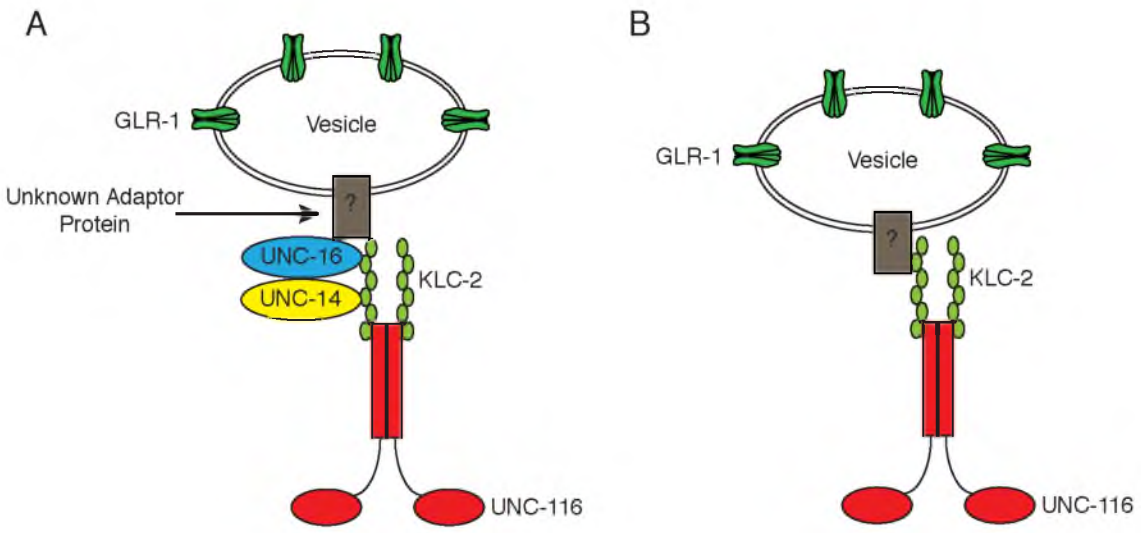


**Figure 3.1.** A hypothetical UNC-116 motor complex. A and B) The kinesin motor consists of two kinesin heavy chain subunits (UNC-116) and two kinesin light chain subunits (KLC-2). A) GLR-1 may be loaded for transport by attaching to the adaptor proteins UNC-16 or UNC-14 by some unknown adaptor protein. B) GLR-1 vesicles may attach directly to the motor complex.

fluorophore (SEP::mCherry::GLR-1); this allowed us to simultaneously visualize both the total population (red) and the surface-expressed population (green) of GLR-1. If GLR-1 is delivered directly to an intracellular pool, then when an SEP::mCherry::GLR-1 trafficking event stops, we will only see red signal. Conversely, if stopping correlates with the delivery of GLR-1 to the plasma membrane, we would expect to see both red and green signals. Two-color simultaneous streaming movies revealed that GLR-1 is first delivered to an intracellular pool, then, after a variable delay, GLR-1 can be inserted into the plasma membrane. Interestingly, GLR-1 insertion events preferentially occurred near existing synapses, though extrasynaptic insertion events were also observed. This marks the first time AMPAR insertion events have been observed *in vivo*, clarifying the current discrepancy in the literature regarding the location of AMPAR exocytosis in *in vitro* studies (Gerges et al., 2006; Jaskolski et al., 2009; Patterson et al., 2010; Yudowski et al., 2007).

## GLR-1 Is Redistributed Between Synapses

In addition to delivery to synapses, we also observed motor-driven vesicles of AMPARs leaving synapses. Where do AMPARs leaving synaptic puncta go? To address this, we performed a series of experiments using the photoconvertible fluorophore Dendra2 tagged to GLR-1 (GLR-1::Dendra2). Following the photoconversion of all GLR-1::Dendra2 fluorescence in the proximal half of the VNC, we observed photoconverted signal at distal synapses 4 hours later. Similarly, 4 hours after photoconverting all the GLR-1::PAGFP

fluorescence in the distal half of the VNC, we observed photoconverted GLR-1 at synapses in the proximal half of the worm. These experiments conclusively show that GLR-1 is not destine for a single synapse, but can be actively redistributed between distant synapses. Although AMPARs have been observed diffusing between synapses *in vitro* (Ehlers et al., 2007), redistribution between distant synapses has not been previously observed. Our calculations suggest that redistribution over these distances and time scales could not have been mediated by lateral diffusion of GLR-1 in the membrane, and could only have occurred by motor-driven transport.

## GLR-1 Delivery and Removal Are Reduced in *unc-116* Mutants

Given that mutations in *unc-116* disrupt the transport of GLR-1::GFP in AVA, we hypothesized that the levels of GLR-1 at synapses in *unc-116* mutants should be reduced. Contrary to our prediction, we observed an accumulation of GLR-1::GFP at synapses proximal to the AVA cell body. One plausible model to explain this observation is that UNC-116/KIF5 is required for the removal of GLR-1 from synapses. In agreement with this hypothesis, experiments examining the removal of GLR-1::Dendra2 from synapses after photoconversion revealed that the rate of GLR-1 removal is slower in *unc-116* mutants compared to wild-type worms. Thus, the accumulations of GLR-1 at proximal synapses are due to a reduced rate of motor-dependent removal of receptors.

In contrast to the accumulations observed at proximal synapses, in *unc-116* mutants the fluorescent intensity of GLR-1::GFP at distal synapses was

markedly decreased compared to wild-type. These data suggest that *unc-116* may also be involved in the long-range delivery of GLR-1 to synapses. To test this prediction, we performed photobleaching studies to look at the recovery of GLR-1::GFP fluorescent signal in the distal tip of AVA. If UNC-116/KIF5 also mediates the delivery of GLR-1 to distal synapses, then mutations in *unc-116* should eliminate the fluorescent recovery. However, if GLR-1 delivery occurs via a different pathway, then recovery of the fluorescent signal should occur at a rate similar to wild-type. As predicted, fluorescent recovery of GLR-1::GFP in the distal part of AVA required UNC-116/KIF5 function. In the absence of transport, essentially no recovery of GLR-1::GFP was observed, suggesting that lateral diffusion and local translation do not mediate the long-range transport of GLR-1 over the timescale of 4 hours. Moreover, direct evaluation of local synthesis of AMPARs by preforming FRAP experiments after treatment with CHX showed similar recovery rates as control worms, suggesting that local synthesis of AMPARs does not contribute to recovery of GLR-1::GFP on this timescale.

These results are consistent with a model where motor-dependent transport is the major mode of AMPAR trafficking *in vivo*. Although lateral diffusion and local translation may occur, these processes do not significantly contribute to long-range GLR-1 trafficking on the timescale of these experiments. Thus, active transport of GLR-1 by UNC-116/KIF5 mediates the rapid delivery, and surprisingly, the removal of GLR-1 from the synapse.

## Surface Expression of GLR-1 Is Increased *unc-116* Mutants

Given the accumulations of GLR-1 at proximal synapses in *unc-116* mutants, we wanted to determine if these receptors were located on the cell surface or in intracellular compartments. To determine this, we performed confocal imaging of SEP::GLR-1 in AVA. Compared to wild-type, *unc-116* mutants showed higher levels of surface-expressed GLR-1 at proximal synapses. Since this increase in surface expression could be due to the observed accumulations of GLR-1 at proximal synapses in *unc-116* mutants, we looked at the ratio of surface-expressed receptors using SEP::mCherry::GLR-1. In *unc-116* mutants, the ratio of surface receptors at the synapse was significantly higher than in wild-type animals, suggesting that almost all GLR-1 is at the cell surface in *unc-116* mutants. Furthermore, GLR-1 insertion events, which are clearly visible in wild-type animals, were surprisingly absent in *unc-116* mutants. Together, these data suggest a model where in the absence of motor transport, GLR-1 is inserted at the AVA cell body and is subsequently trafficked to synapses via lateral diffusion in the plasma membrane. In concurrence with this model, GLR-1 in *unc-116* mutants is mostly surface expressed and shows an exponential-like distribution in AVA, analogous to results obtained from mathematical simulations of AMPAR transport by lateral diffusion (Earnshaw and Bressloff, 2008). Alternatively, the increase in the total number and ratio of surface-expressed GLR-1 at the synapse in *unc-116* mutants could be explained by the lack of proper endocytic machinery in the absence of motor transport. Thus in this model, receptors at the synapse cannot be internalized leading to an

increase in surface expression and lack of insertion events. Although we favor the first model because we found the distribution of GLR-1 to be consistent with a diffusion-mediated process in *unc-116* mutants, discrimination of these two models will require a systematic characterization of the GLR-1 endocytosis and exocytosis pathways.

## Glutamate-gated Currents Are Decreased in *unc-116* Mutants

Due to the increased surface expression of GLR-1 in *unc-116* mutants, we predicted that glutamate-gated currents in AVA should also be correspondingly increased. Paradoxically, we found that *unc-116* mutants have smaller glutamate-gated currents than wild-type worms. How can *unc-116* mutants have smaller currents yet higher GLR-1 surface expression? One possibility is that the GLR-1 signaling complex is nonfunctional due to reduced delivery of a key postsynaptic component in the absence of motor function. To test this model, we generated a transgenic worm expressing GLR-1::GFP in combination with a second transgenic array containing all the known components of the GLR-1 signaling complex: SOL-1, SOL-2, GLR-2 and STG-2 (Brockie et al., 2001a; Mellem et al., 2002; Walker et al., 2006b; Wang et al., 2008, 2012; Zheng et al., 2004, 2006). Expression of this second array in *unc-116* mutants not only rescues glutamate-gated currents, but also massively increases currents compared to wild-type controls. These results raise three extremely interesting points. First, by overexpressing all the known GLR-1 auxiliary proteins, we can rescue glutamate-gated currents in *unc-116* mutants, suggesting that the

transport and delivery of at least one of the proteins in this second array is critically dependent on motor function. Secondly, we can modify the stoichiometry of the receptor-signaling complex at the synapse such that non-functional surface-expressed GLR-1 complexes in *unc-116* mutants become functional again upon overexpression of the GLR-1 signaling complex. Finally, transport by molecular motors regulates the number of functional GLR-1 receptor complexes at a particular synapse. In wild-type worms, overexpression of the signaling complex array does not appreciably change glutamate-gated currents. This suggests that synapses can signal to molecular motors to regulate the number and composition of surface-expressed AMPAR signaling complexes, possibly through the removal and redistribution of AMPARs.

## Trafficking of GLR-2 Is Critically Dependent on UNC-116/KIF5

What are the missing component(s) required for GLR-1 signaling in *unc-116* mutants? To determine this, we looked at the localization of each component of the GLR-1 signaling complex by confocal microscopy. In *unc-116* mutants, SOL-1, SOL-2 and STG-2 all exhibited synaptic accumulations in the proximal process of AVA, similar to that observed with GLR-1. However, confocal imaging of the AMPAR subunit GLR-2 showed that GFP::GLR-2 was surprisingly absent from synaptic puncta in *unc-116* mutants, yet clearly visible in wild-type worms. Given this result, we postulated that UNC-116/KIF5 mediates the transport of GLR-2 out of the cell body; thus, in *unc-116* mutants, we should see an increase in the amount of GFP::GLR-2 fluorescence in the AVA cell body.

Although GFP::GLR-2 fluorescence was clearly evident in wild-type worms, in *unc-116* mutants, GLR-2::GFP levels in the cell body were almost undetectable. This observation led us to wonder if GLR-2 is being degraded in the absence of transport. To test this, we generated a double mutant between *unc-116* and a dominant negative variant of VPS-4 (VPS-4(DN)). VPS-4 is a critical protein in the multivesicular body trafficking pathway involved in endosomal recycling and protein degradation; thus, VPS-4(DN) cannot properly traffic cargo to the lysosome for degradation. Looking at GFP::GLR-2 levels in *unc-116; vps-4(DN)* double mutants, we observed an increase in the amount of fluorescence in the cell body, confirming our hypothesis that GLR-2 is degraded in the absence of molecular motor transport. These results suggest that by regulating the amount of GLR-1/GLR-2 heteromers trafficked by UNC-116/KIF5; the neuron can regulate the magnitude of glutamate-gated currents in AVA (Figure 3.2).

## Ongoing Role of Motor Transport in the Adult Nervous System

In AVA, UNC-116/KIF5 regulates synaptic strength through the delivery, removal and redistribution of AMPARs. However, *unc-116* may also be required during development for proper synapse formation. To test this hypothesis, we drove expression of *unc-116* using a heat-shock-inducible promoter (HSP) in adult transgenic worms. Under normal growth conditions, the HSP is quiescent; however, when transgenic worms are exposed to temperatures of 30° C or more, the HSP becomes active and drives expression of a particular gene of interest in many tissue types – including neurons and muscle. We generated transgenic

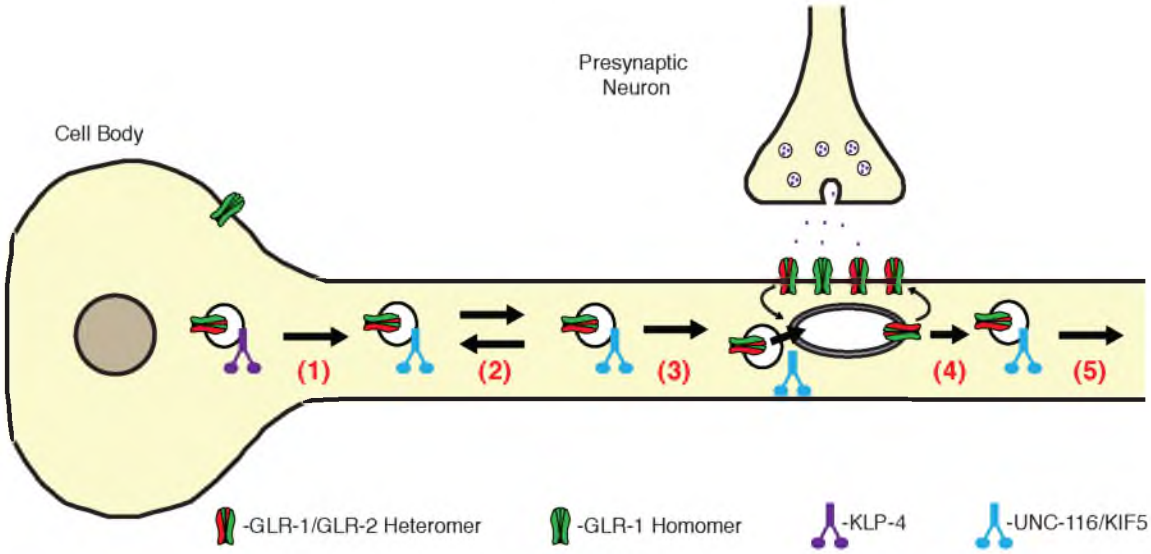


**Figure 3.2.** A model of long-range transport of GLR-1 by UNC-116/KIF5. (1) At the cell body, GLR-1 is transferred from KLP-4 to UNC-116/KIF5. (2) In the process, UNC-116/KIF5 mediates the fast, bidirectional transport of GLR-1, delivery to synapses (3), removal from subsynaptic compartments (4) and redistribution of GLR-1 between synapses (5).

*unc-116* mutant worms expressing *unc-116* driven by the HSP (HSP::UNC-116). Interestingly, we found heat shock of adult *unc-116* transgenic worms expressing HSP::UNC-116 rescued defects in GLR-1 transport and synaptic puncta compared to controls. Additionally, heat shock alone did not rescue GLR-1 puncta or transport in nontransgenic *unc-116* mutants. In agreement with the normalization of GLR-1 synaptic puncta, we also observed an increase in glutamate-gated currents in heat-shocked adult *unc-116* transgenic worms compared to controls. These data show that transport of GLR-1 is ongoing and suggest a model where transport of GLR-1 by UNC-116/KIF5 regulates synaptic strength in the adult nervous system.

## Transport of AMPARs Is Evolutionarily Conserved

Our results clearly show molecular motor transport is essential for AMPAR localization and synaptic function in the invertebrate *C. elegans.* How do our results translate to the molecular mechanisms employed by vertebrate systems to regulate the long-range transport of AMPARs? To address this, we generated transgenic animals expressing the vertebrate AMPAR subunit GluA1::GFP in AVA. GluA1::GFP is functional and localizes to synaptic puncta in the AVA processes (Brockie et al., 2013). We hypothesized that if the molecular mechanisms of AMPAR transport are conserved between vertebrates and invertebrates, then the vertebrate GluA1 should be transported via the same pathway as the *C. elegans* AMPAR GLR-1. Indeed, streaming confocal movies revealed the rapid, bidirectional transport of GluA1::GFP in transgenic animals.

Consistent with our hypothesis, mutations in *unc-116* resulted in disruption of GluA1 transport and in accumulations of GluA1 at synaptic puncta. These data suggests that the underlying molecular mechanisms regulating the localization and trafficking of AMPARs are conserved between vertebrates and invertebrates.

## Regulation of GLR-1 Transport

We have demonstrated that the kinesin-1, UNC-116/KIF5, mediates the delivery, removal and redistribution of the *C. elegans* AMPAR GLR-1. In *unc-116* mutants, we show that although homomeric GLR-1 receptors can diffuse out of the cell body and accumulate at proximal synapses, glutamatergic signaling is impaired due to the lack of GLR-2-containing AMPARs (Figure 3.3). Even after prolonged loss of motor function, defects in synaptic transmission could be rectified by transient expression of functional kinesin-1 motors in adult mutant animals. Thereby, motor-dependent transport of GLR-1 is ongoing in the adult nervous system and is essential for proper synaptic function *in vivo*. Although this study has yielded new mechanistic insights into the long-range transport of AMPARs, it also raises several important questions.

A surprising result from our study is the regulation of GLR-1 transport by at least two molecular motors. In contrast to the phenotype observed in *unc-116*, mutations in the kinesin-like protein, *klp-4*, show a decrease in the levels of GLR-1::GFP in the VNC. Analysis of GLR-1::GFP localization in *klp-4;unc-116* double mutants indicates that *klp-4* is epistatic to *unc-116*, suggesting that KLP-4 functions upstream of UNC-116. As no defects in GLR-1 transport in the AVA

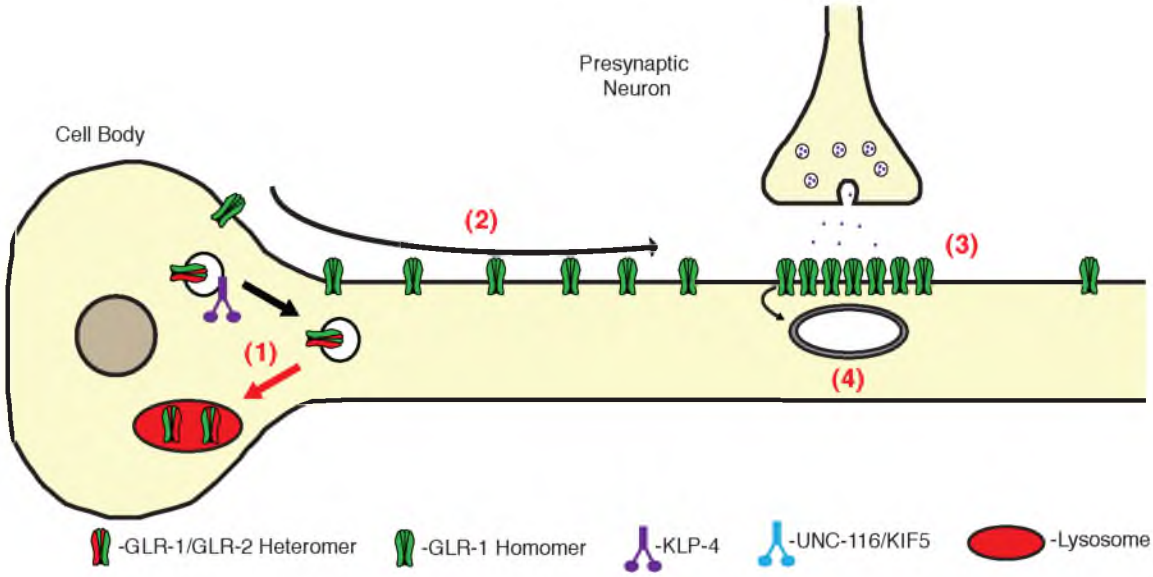


**Figure 3.3.** A model of GLR-1 transport in *unc-116* mutants. (1) GLR-1/GLR-2 heteromeric receptors are preferentially degraded in *unc-116* mutants. (2) GLR-1 homomeric receptors can traffic to the synapse by lateral diffusion where they accumulate at proximal synapses (3), secondary to defective removal in the absence of *unc-116.* (4) Subcellular trafficking of GLR-1 is disrupted in *unc-116* mutants.

processes were observed in *klp-4* mutants, these data suggest that KLP-4 functions to regulate the anterograde transport of GLR-1 out of the cell body. How and where GLR-1 is transferred between KLP-4 and UNC-116 warrants further investigation.

Our study clearly demonstrates that UNC-116/KIF5 mediates the bidirectional transport of GLR-1 in the AVA neurite; however, there is the formal possibility that other molecular motors could contribute to this process. Studies have shown that transport vesicles can contain multiple classes of molecular motors on the same vesicle (Kural et al., 2005; Leidel et al., 2012). Additionally, transport parameters such as processivity and stopping depend on the number and type of motors on the vesicle (Bhat and Gopalakrishnan, 2013; Klumpp and Lipowsky, 2005; Müller et al., 2008). Whether other molecular motors play a role in GLR-1 transport in the VNC will be examined in future studies.

Once cargo is being transported, how does the synapse signal to molecular motors to stop and deliver their cargo? Is motor stopping dependent on synaptic activity, or is there a fixed probability of motor stopping? A recent study from the Hirokawa laboratory looking at the trafficking of NMDARs by KIF17 showed that $Ca^{2+}$ signaling through CaMKII is critical for NMDAR delivery to the synapse (Yin et al., 2012). During synaptic activity, CaMKII-dependent phosphorylation of KIF17 at S1029 causes the release of NMDARs at synapses and facilitates their insertion into the membrane (Guillaud et al., 2008; Yin et al., 2012). As $Ca^{2+}$ signaling regulates a wide variety of processes, one can imagine that similar signaling mechanisms could be involved in the delivery of GLR-1 to

synapses by UNC-116/KIF5. Alternatively, delivery of AMPARs could occur via local modification of microtubules causing motors to become detached, hand-off of the cargo to myosin-class motors at the synapse or local depletion of ATP levels around the synapse, causing the stalling of motors (Kapitein et al., 2013; Maas et al., 2009; Newby and Bressloff, 2010, 2009). In order to gain insight into the mechanism of stopping, we looked at two-color simultaneous streaming movies of fluorescently tagged GLR-1::mCherry and UNC-116::GFP. Preliminary studies observing cotransported events show that both the UNC-116/KIF5 and GLR-1 stop together. As UNC-116/KIF5 is also localized at synapses, this suggests an attractive model where each synapse contains a local pool of molecular motors to mediate the removal and redistribution of AMPARs to other synapses. Future studies in *C. elegans* will help to differentiate between the mechanisms for motor-driven delivery and removal of AMPARs to the synapse.

## Trafficking of Auxiliary Proteins

Confocal imaging of fluorescently tagged auxiliary proteins showed that the localization of SOL-1, SOL-2 and STG-2 were dependent on UNC-116/KIF5 function. This result begs the question: is the GLR-1 signaling complex transported as a unit, or is the transport of these proteins individually regulated? Preliminary data looking at simultaneous two-color streaming videos of SOL-1::GFP and GLR-1::mCherry has shown that both SOL-1 and GLR-1 are actively transported by UNC-116/KIF5; yet, the transport of these proteins occurs in separate populations of vesicles. An attractive model, based on these

preliminary results, is that the components of the GLR-1 signaling complex are all individually trafficked, allowing for single synapse, subunit-specific delivery of components to regulate the magnitude of AMPAR-mediated synaptic transmission. Future experiments will determine if other auxiliary proteins are co-transported with GLR-1 and how this signaling complex is regulated once at the synapse. Given the evolutionary conservation of AMPAR trafficking pathways and regulatory proteins, results from these experiments could have a significant impact on studies of synaptic scaling in higher organisms.

## Molecular Motors And Synaptic Plasticity

How experience-dependent neural activity changes the strength of synaptic communication between neurons is still an open question. During LTP, the synapse undergoes molecular changes resulting in an increase in the strength of synaptic communication through the addition of AMPARs. Our experiments suggest that the underlying mechanism for synaptic strengthening is an increase in the rate of AMPAR delivery to the synapse by molecular motors. In this model, each synapse is only seconds away from a molecular motor complex transporting AMPARs, allowing for rapid changes in synaptic strength, as long as transport is not impaired. Although synaptic plasticity of AMPAR-containing synapses has yet to be discovered in *C. elegans*, recent work with the $\alpha$-7 acetylcholine receptor, ACR-16, has demonstrated that the underlying machinery necessary for activity-dependent changes in synaptic strength exists in *C. elegans* (Jensen et al., 2012). We are currently assessing the role, if any,

that synaptic activity has on modifying motor-dependent delivery and removal of GLR-1.

## Concluding Remarks

Regulating the function of the nervous system is a fascinating and complex question. Only recently have we been able to gain insight into the cellular and molecular mechanisms that underlie processes such as learning and memory. This research describing the regulatory mechanisms of AMPAR transport in *C. elegans* has revealed how molecular motors function to control changes in synaptic strength through delivery, removal and redistribution of AMPARs. Because many of the signaling mechanisms that regulate synaptic function are conserved from invertebrates to vertebrates, we hypothesize that our results will have direct relevance to ongoing studies in the vertebrate nervous system, and will ultimately lead to new therapeutic modalities for neuronal disorders associated with defects in glutamatergic neurotransmission.

## References

Adesnik, H., Nicoll, R.A., and England, P.M. (2005). Photoinactivation of native AMPA receptors reveals their real-time trafficking. Neuron *48*, 977–985.

Anggono, V., and Huganir, R.L. (2012). Regulation of AMPA receptor trafficking and synaptic plasticity. Curr. Opin. Neurobiol. *22*, 461–469.

Bhat, D., and Gopalakrishnan, M. (2013). Memory, bias, and correlations in bidirectional transport of molecular-motor-driven cargoes. Phys. Rev. E Stat. Nonlin. Soft Matter Phys. *88*, 042702.

Brockie, P.J., Mellem, J.E., Hills, T., Madsen, D.M., and Maricq, A.V. (2001). The C. elegans glutamate receptor subunit NMR-1 is required for slow NMDA-activated currents that regulate reversal frequency during locomotion. Neuron *31*, 617–630.

Brockie, P.J., Jensen, M., Mellem, J.E., Jensen, E., Yamasaki, T., Wang, R., Maxfield, D., Thacker, C., Hoerndli, F., Dunn, P.J., et al. (2013). Cornichons control ER export of AMPA receptors to regulate synaptic excitability. Neuron *80*, 129–142.

Burbea, M., Dreier, L., Dittman, J.S., Grunwald, M.E., and Kaplan, J.M. (2002). Ubiquitin and AP180 regulate the abundance of GLR-1 glutamate receptors at postsynaptic elements in C. elegans. Neuron *35*, 107–120.

Byrd, D.T., Kawasaki, M., Walcoff, M., Hisamoto, N., Matsumoto, K., and Jin, Y. (2001). UNC-16, a JNK-signaling scaffold protein, regulates vesicle transport in C. elegans. Neuron *32*, 787–800.

Ehlers, M.D., Heine, M., Groc, L., Lee, M.-C., and Choquet, D. (2007). Diffusional trapping of GluR1 AMPA receptors by input-specific synaptic activity. Neuron *54*, 447–460.

Franker, M.A.M., and Hoogenraad, C.C. (2013). Microtubule-based transport – basic mechanisms, traffic rules and role in neurological pathogenesis. J. Cell Sci. *126*, 2319–2329.

Gerges, N.Z., Backos, D.S., Rupasinghe, C.N., Spaller, M.R., and Esteban, J.A. (2006). Dual role of the exocyst in AMPA receptor targeting and insertion into the postsynaptic membrane. EMBO J. *25*, 1623–1634.

Guillaud, L., Wong, R., and Hirokawa, N. (2008). Disruption of KIF17-Mint1 interaction by CaMKII-dependent phosphorylation: a molecular model of kinesin-cargo release. Nat. Cell Biol. *10*, 19–29.

Hanley, J.G. (2010). Endosomal sorting of AMPA receptors in hippocampal neurons. Biochem. Soc. Trans. *38*, 460–465.

Ho, V.M., Lee, J.-A., and Martin, K.C. (2011). The cell biology of synaptic plasticity. Science *334*, 623–628.

Jaskolski, F., Mayo-Martin, B., Jane, D., and Henley, J.M. (2009). Dynamin-dependent membrane drift recruits AMPA receptors to dendritic spines. J. Biol. Chem. *284*, 12491–12503.

Jensen, M., Hoerndli, F.J., Brockie, P.J., Wang, R., Johnson, E., Maxfield, D., Francis, M.M., Madsen, D.M., and Maricq, A.V. (2012). Wnt signaling regulates acetylcholine receptor translocation and synaptic plasticity in the adult nervous system. Cell *149*, 173–187.

Ju, W., Morishita, W., Tsui, J., Gaietta, G., Deerinck, T.J., Adams, S.R., Garner, C.C., Tsien, R.Y., Ellisman, M.H., and Malenka, R.C. (2004). Activity-dependent regulation of dendritic synthesis and trafficking of AMPA receptors. Nat. Neurosci. *7*, 244–253.

Kapitein, L.C., van Bergeijk, P., Lipka, J., Keijzer, N., Wulf, P.S., Katrukha, E.A., Akhmanova, A., and Hoogenraad, C.C. (2013). Myosin-V opposes microtubule-based cargo transport and drives directional motility on cortical actin. Curr. Biol. CB *23*, 828–834.

Kessels, H.W., and Malinow, R. (2009). Synaptic AMPA receptor plasticity and behavior. Neuron *61*, 340–350.

Kim, C.H., and Lisman, J.E. (2001). A labile component of AMPA receptor-mediated synaptic transmission is dependent on microtubule motors, actin, and N-ethylmaleimide-sensitive factor. J. Neurosci. Off. J. Soc. Neurosci. *21*, 4188–4194.

Klumpp, S., and Lipowsky, R. (2005). Cooperative cargo transport by several molecular motors. Proc. Natl. Acad. Sci. U. S. A. *102*, 17284–17289.

Koushika, S.P., and Nonet, M.L. (2000). Sorting and transport in C. elegans: a model system with a sequenced genome. Curr. Opin. Cell Biol. *12*, 517–523.

Kural, C., Kim, H., Syed, S., Goshima, G., Gelfand, V.I., and Selvin, P.R. (2005). Kinesin and dynein move a peroxisome in vivo: a tug-of-war or coordinated movement? Science *308*, 1469–1472.

Kwak, S., and Weiss, J.H. (2006). Calcium-permeable AMPA channels in neurodegenerative disease and ischemia. Curr. Opin. Neurobiol. *16*, 281–287.

Leidel, C., Longoria, R.A., Gutierrez, F.M., and Shubeita, G.T. (2012). Measuring molecular motor forces in vivo: implications for tug-of-war models of bidirectional transport. Biophys. J. *103*, 492–500.

Maas, C., Belgardt, D., Lee, H.K., Heisler, F.F., Lappe-Siefke, C., Magiera, M.M., van Dijk, J., Hausrat, T.J., Janke, C., and Kneussel, M. (2009). Synaptic activation modifies microtubules underlying transport of postsynaptic cargo. Proc. Natl. Acad. Sci. U.S.A. *106*, 8731–8736.

Malinow, R., and Malenka, R.C. (2002). AMPA receptor trafficking and synaptic plasticity. Annu. Rev. Neurosci. *25*, 103–126.

Mellem, J.E., Brockie, P.J., Zheng, Y., Madsen, D.M., and Maricq, A.V. (2002). Decoding of polymodal sensory stimuli by postsynaptic glutamate receptors in C. elegans. Neuron *36*, 933–944.

Müller, M.J.I., Klumpp, S., and Lipowsky, R. (2008). Tug-of-war as a cooperative mechanism for bidirectional cargo transport by molecular motors. Proc. Natl. Acad. Sci. U.S.A. *105*, 4609–4614.

Newby, J., and Bressloff, P.C. (2010). Local synaptic signaling enhances the stochastic transport of motor-driven cargo in neurons. Phys. Biol. *7*, 036004.

Newby, J.M., and Bressloff, P.C. (2009). Directed intermittent search for a hidden target on a dendritic tree. Phys. Rev. E Stat. Nonlin. Soft Matter Phys. *80*, 021913.

Nicoll, R.A., Tomita, S., and Bredt, D.S. (2006). Auxiliary subunits assist AMPA-type glutamate receptors. Science *311*, 1253–1256.

Opazo, P., and Choquet, D. (2011). A three-step model for the synaptic recruitment of AMPA receptors. Mol. Cell. Neurosci. *46*, 1–8.

Patterson, M.A., Szatmari, E.M., and Yasuda, R. (2010). AMPA receptors are exocytosed in stimulated spines and adjacent dendrites in a Ras-ERK-dependent manner during long-term potentiation. Proc. Natl. Acad. Sci. U.S.A. *107*, 15951–15956.

Rongo, C., Whitfield, C.W., Rodal, A., Kim, S.K., and Kaplan, J.M. (1998). LIN-10 is a shared component of the polarized protein localization pathways in neurons and epithelia. Cell *94*, 751–759.

Sakamoto, R., Byrd, D.T., Brown, H.M., Hisamoto, N., Matsumoto, K., and Jin, Y. (2005). The Caenorhabditis elegans UNC-14 RUN domain protein binds to the kinesin-1 and UNC-16 complex and regulates synaptic vesicle localization. Mol. Biol. Cell *16*, 483–496.

Setou, M., Seog, D.-H., Tanaka, Y., Kanai, Y., Takei, Y., Kawagishi, M., and Hirokawa, N. (2002). Glutamate-receptor-interacting protein GRIP1 directly steers kinesin to dendrites. Nature *417*, 83–87.

Shepherd, J.D., and Huganir, R.L. (2007). The cell biology of synaptic plasticity: AMPA receptor trafficking. Annu. Rev. Cell Dev. Biol. *23*, 613–643.

Straub, C., and Tomita, S. (2012). The regulation of glutamate receptor trafficking and function by TARPs and other transmembrane auxiliary subunits. Curr. Opin. Neurobiol. *22*, 488–495.

Walker, C.S., Brockie, P.J., Madsen, D.M., Francis, M.M., Zheng, Y., Koduri, S., Mellem, J.E., Strutz-Seebohm, N., and Maricq, A.V. (2006). Reconstitution of invertebrate glutamate receptor function depends on stargazin-like proteins. Proc. Natl. Acad. Sci. U.S.A. *103*, 10781–10786.

Wang, R., Walker, C.S., Brockie, P.J., Francis, M.M., Mellem, J.E., Madsen, D.M., and Maricq, A.V. (2008). Evolutionary conserved role for TARPs in the gating of glutamate receptors and tuning of synaptic function. Neuron *59*, 997–1008.

Wang, R., Mellem, J.E., Jensen, M., Brockie, P.J., Walker, C.S., Hoerndli, F.J., Hauth, L., Madsen, D.M., and Maricq, A.V. (2012). The SOL-2/Neto auxiliary protein modulates the function of AMPA-subtype ionotropic glutamate receptors. Neuron *75*, 838–850.

Yin, X., Feng, X., Takei, Y., and Hirokawa, N. (2012). Regulation of NMDA receptor transport: a KIF17–cargo binding/releasing underlies synaptic plasticity and memory in vivo. J. Neurosci. *32*, 5486–5499.

Yudowski, G.A., Puthenveedu, M.A., Leonoudakis, D., Panicker, S., Thorn, K.S., Beattie, E.C., and von Zastrow, M. (2007). Real-time imaging of discrete exocytic events mediating surface delivery of AMPA receptors. J. Neurosci. Off. J. Soc. Neurosci. *27*, 11112–11121.

Zhang, J., and Abdullah, J.M. (2013). The role of GluA1 in central nervous system disorders. Rev. Neurosci. *24*, 499–505.

Zheng, Y., Mellem, J.E., Brockie, P.J., Madsen, D.M., and Maricq, A.V. (2004). SOL-1 is a CUB-domain protein required for GLR-1 glutamate receptor function in C. elegans. Nature *427*, 451–457.

Zheng, Y., Brockie, P.J., Mellem, J.E., Madsen, D.M., Walker, C.S., Francis, M.M., and Maricq, A.V. (2006). SOL-1 is an auxiliary subunit that modulates the gating of GLR-1 glutamate receptors in Caenorhabditis elegans. Proc. Natl. Acad. Sci. U.S.A. *103*, 1100–110

# APPENDIX

# CORNICHONS CONTROL ER EXPORT OF AMPA RECEPTORS TO REGULATE SYNAPTIC EXCITABILITY

Reprinted from Neuron, 80 (1), Brockie, P.J., Jensen, M., Mellem, J.E., Jensen, E., Yamasaki, T., Wang, R., Maxfield, D. A., Thacker, C., Hoerndli, F., Dunn, P.J., Tomita, S., Madsen, D. M. and Maricq, A.V., Cornichons Control ER Export of AMPA Receptors to Regulate Synaptic Excitability, 129-142, Copyright (2013) with permission from Elsevier.

My contribution to this work includes the following:

1) Assisted in microscopy experiments
2) Developed kymograph analysis of GLR-1::GFP movement
3) Developed and performed analysis of GLR-1::GFP puncta

Neuron
Article

# Cornichons Control ER Export of AMPA Receptors to Regulate Synaptic Excitability

Penelope J. Brockie,[1,3] Michael Jensen,[1,3] Jerry E. Mellem,[1] Erica Jensen,[1] Tokiwa Yamasaki,[2] Rui Wang,[1] Dane Maxfield,[1] Colin Thacker,[1] Frédéric Hoerndli,[1] Patrick J. Dunn,[2] Susumu Tomita,[2] David M. Madsen,[1] and Andres V. Maricq[1,*]

[1]Department of Biology, University of Utah, Salt Lake City, UT 84112-0840, USA
[2]CNNR, Department of Cellular and Molecular Physiology, Yale University School of Medicine, New Haven, CT 06510, USA
[3]These authors contributed equally to this work
*Correspondence: maricq@biology.utah.edu
http://dx.doi.org/10.1016/j.neuron.2013.07.028

## SUMMARY

The strength of synaptic communication at central synapses depends on the number of ionotropic glutamate receptors, particularly the class gated by the agonist AMPA (AMPARs). Cornichon proteins, evolutionarily conserved endoplasmic reticulum cargo adaptors, modify the properties of vertebrate AMPARs when coexpressed in heterologous cells. However, the contribution of cornichons to behavior and in vivo nervous system function has yet to be determined. Here, we take a genetic approach to these questions by studying CNI-1—the sole cornichon homolog in *C. elegans*. *cni-1* mutants hyperreverse, a phenotype associated with increased glutamatergic synaptic transmission. Consistent with this behavior, we find larger glutamate-gated currents in *cni-1* mutants with a corresponding increase in AMPAR number. Furthermore, we observe opposite phenotypes in transgenic worms that overexpress CNI-1 or vertebrate homologs. In reconstitution studies, we provide support for an evolutionarily conserved role for cornichons in regulating the export of vertebrate and invertebrate AMPARs.

## INTRODUCTION

Rapid, excitatory synaptic communication that occurs in vertebrate brains, as well as in most other nervous systems, is primarily mediated by the neurotransmitter glutamate. The strength of this communication is dependent on the number of AMPA class ionotropic glutamate receptors, as well as on their functional properties. Synaptic strength is plastic, and nervous system activity can change the number and properties of AMPA receptors (AMPARs) (Anggono and Huganir, 2012; Kerchner and Nicoll, 2008; Kessels and Malinow, 2009).

While the properties of AMPARs can be modified by RNA editing (Wright and Vissel, 2012) and posttranslational modification of receptors (Lu and Roche, 2012), more recent genetic studies have demonstrated that AMPAR trafficking and function are critically dependent on auxiliary proteins, most prominently the TARP and SOL classes of transmembrane proteins (Jackson and Nicoll, 2011; Wang et al., 2008, 2012; Yan and Tomita, 2012; Zheng et al., 2004). Furthermore, proteomic studies have identified a host of new candidate auxiliary proteins (Schwenk et al. 2009, 2012; Shanks et al., 2012; von Engelhardt et al., 2010), including the vertebrate cornichon (CNIH) proteins CNIH-2 and CNIH-3 (Schwenk et al., 2009).

Cornichon was first identified in *Drosophila*, where the Cni protein binds to the EGF-like ligand Gurken, thus acting as a cargo receptor for recruitment of Gurken into COPII vesicles. In the absence of Cni, export from the endoplasmic reticulum (ER) and secretion of ligand are disrupted (Bökel et al., 2006; Roth et al., 1995). More recently, affinity purification of native AMPARs from rat brain followed by mass spectroscopy analysis identified CNIH-2 and CNIH-3 as AMPAR-interacting proteins. When coexpressed with AMPAR subunits in heterologous cells, these proteins slowed the kinetics of receptor desensitization and deactivation and increased surface expression (Coombs et al., 2012; Kato et al., 2010; Schwenk et al., 2009; Shi et al., 2010).

Subsequent studies have revealed additional complexities. While CNIH-2 was found at the cell surface of hippocampal neurons, it did not reach the surface of cerebellar Purkinje neurons in stargazer mice, which lack the γ-2 TARP (Gill et al., 2011). Studies in HeLa cells found that overexpression of CNIH-2 altered the glycosylation pattern of the GluA2 AMPAR subunit, suggesting that CNIH-2 regulates AMPAR maturation in the ER, which may affect AMPAR function at synapses (Harmel et al., 2012). While studies in various heterologous cells have provided important insights into CNIH-2 function, these cells might express different proteins and use different trafficking pathways than those present in neurons. Consequently, studies to date have not fully resolved whether CNIHs primarily have a forward trafficking role in neurons, whether they are also recruited away from the ER-Golgi early secretory pathway to function at synapses, or whether they function as auxiliary proteins at synapses to modify the functional properties of AMPARs. Clearly, a deeper understanding of the contribution of CNIHs to nervous system function and behavior would benefit from in vivo studies. Genetic-based studies of cornichon function in neurons are a challenge in vertebrates, which express four cornichon homologs with possible redundant functions. In contrast, only one cornichon homolog is found in the *C. elegans* genome.

The study of synaptic signaling in the simple, well-defined nervous system of *C. elegans* has provided new insights into

AMPAR function and behaviors regulated by glutamatergic signaling (de Bono and Maricq, 2005). In *C. elegans*, the GLR-1 AMPAR subunit is required for fast glutamate-gated current in specialized command interneurons that control the switch between forward and backward movement; thus, reversal frequency is disrupted in *glr-1* loss-of-function or gain-of-function mutants (Hart et al., 1995; Maricq et al., 1995; Zheng et al., 1999). Genetic screens for modifiers of this behavior have led to the identification of three classes of auxiliary proteins that associate with GLR-1 and modify the kinetics of glutamate-gated current. These include the evolutionarily and functionally conserved TARP proteins, STG-1 and STG-2 (Walker et al., 2006a; Wang et al., 2008), and two classes of CUB-domain transmembrane proteins, SOL-1 and SOL-2 (Walker et al., 2006a, 2006b; Wang et al., 2012; Zheng et al., 2004, 2006).

Sequence analysis of the *C. elegans* genome revealed the presence of a single cornichon homolog (*cni-1*). We found that *cni-1* mutants exhibited a hyperreversal phenotype in contrast to the hyporeversal phenotype observed in strains with loss-of-function mutations in either the GLR-1 subunit or in the auxiliary proteins (Brockie et al., 2001b; Mellem et al., 2002; Zheng et al., 2004). Cornichon's well-characterized role in the export of specific proteins from the ER (Bökel et al., 2006; Castro et al., 2007; Herzig et al., 2012; Roth et al., 1995) prompted us to examine the in vivo trafficking of GLR-1. Compared to wild-type, we found increased anterograde transport of GLR-1 in *cni-1* mutants, with corresponding increases in synaptic GLR-1 expression and GLR-1-mediated currents. In contrast, trafficking and current were reduced with overexpression of CNI-1, the yeast homolog (Evr14p), or vertebrate CNIH-2. Reconstitution experiments revealed that cornichon proteins have evolutionarily conserved roles in limiting the export of AMPARs and modifying receptor function, thus contributing to the regulation of neuronal excitability.

## RESULTS

### CNI-1 Is the Sole Cornichon Homolog in *C. elegans*

Analysis of the *C. elegans* genome for genes that encode proteins with significant identity to members of the vertebrate cornichon family identified only one candidate homolog (T09E8.3; http://www.wormbase.org), which had significant identity to vertebrate and invertebrate corichon proteins as well as to the yeast protein Erv14p (Figures S1A and S1C available online). Analysis of the primary amino acid sequence predicted three transmembrane domains (TMDs), as well as the topological arrangement of intra- and extracellular regions found in previously described cornichon proteins (Figure S1C). Invertebrate cornichon proteins as well as vertebrate CNIH-1 and CNIH-4 lack the signature 16 amino acid region found in the first extracellular domain of vertebrate CNIH-2 and CNIH-3. The T09E8.3 gene was originally named *cnih-2* (Zhang et al., 2012); but because the protein lacks the signature region, a consensus decision was made to rename the gene *cni-1* (C. Rongo, personal communication). An available deletion mutation in *cni-1* removes over half of the coding region and disrupts the 3′ UTR signal required for polyadenylation (Figure S1B).

### Reversal Frequency Is Increased in *cni-1* Mutants

*C. elegans* regulates the frequency of turning and reversals to mediate avoidance and attraction behaviors and to aid in the exploration of their environs by restricting or expanding the search area (Hills et al., 2004). The neural circuitry that controls these reversals has been identified and includes the command interneurons that express the GLR-1 AMPAR (Brockie et al., 2001a; Chalfie et al., 1985; de Bono and Maricq, 2005; Piggott et al., 2011). Mutations in genes that disrupt glutamate release (*eat-4*) or the function of postsynaptic glutamate receptors (*glr-1*, *sol-1*, and *stg-2*) decrease reversal frequency (Figure 1A) (Brockie et al., 2001b; Mellem et al., 2002; Walker et al., 2006a; Wang et al., 2008, 2012; Zheng et al., 2004). In contrast, transgenic "lurcher" worms that express a gain-of-function mutation in GLR-1 have an increased reversal frequency (Zheng et al., 1999). Thus, reversal frequency provides a behavioral readout of the strength of AMPAR-mediated synaptic signaling.

We found that the average forward time in *cni-1* mutants was considerably shorter than in wild-type, with a corresponding increase in the frequency of reversals (Figure 1A). This increase suggested that the strength of AMPAR-mediated signaling was increased in *cni-1* mutants. In contrast, we did not observe phenotypes associated with loss of GLR-1-mediated signaling, such as altered avoidance responses to tactile or osmotic stimuli (Figure S2), nor did the *cni-1* mutation suppress the behavioral defects of *glr-1* mutants (Figure 1A and Figure S2A).

To further address whether the increased reversal frequency observed in *cni-1* mutants was dependent on glutamatergic signaling, we examined relevant single and double mutants (Figure 1A). Double mutants with *cni-1* and *eat-4*, which encodes the vesicular glutamate transporter, were indistinguishable from *eat-4* mutants alone, indicating that the hyperreversal behavior in *cni-1* mutants was dependent on glutamatergic neurotransmission. We next asked whether the hyperreversal behavior was dependent on the GLR-1 AMPAR. Compared to wild-type, reversal frequency was decreased in *glr-1* mutants (Brockie et al., 2001b), and the *glr-1* mutation suppressed the hyperreversal phenotype of *cni-1* mutants (Figure 1A). These results indicate that the effects of *cni-1* on reversal behavior primarily depend on AMPAR-mediated synaptic signaling. In support of this hypothesis, we found that the *cni-1* reversal phenotype was also dependent on AMPAR auxiliary proteins. Thus, reversals were suppressed in the double mutants *sol-1; cni-1* and *stg-2; cni-1* (Figure 1A).

### The Amplitude of Glutamate-Gated Currents Is Increased in *cni-1* Mutants

To evaluate the contributions of CNI-1 to AMPAR-mediated currents, we turned to in vivo patch-clamp electrophysiological analysis. Compared to wild-type, the amplitude of the glutamate-gated and GLR-1-dependent current in the AVA command interneurons was significantly increased in *cni-1* mutants (Figures 1B and 1C). We found the same relative increase when we used the partial agonist kainate and there was no apparent difference in the efficacy of the two agonists (Figure S3A). In contrast, overexpression of CNI-1 in AVA dramatically reduced the amplitude of the glutamate-gated current. In these transgenic worms, the amount of CNI-1 expressed

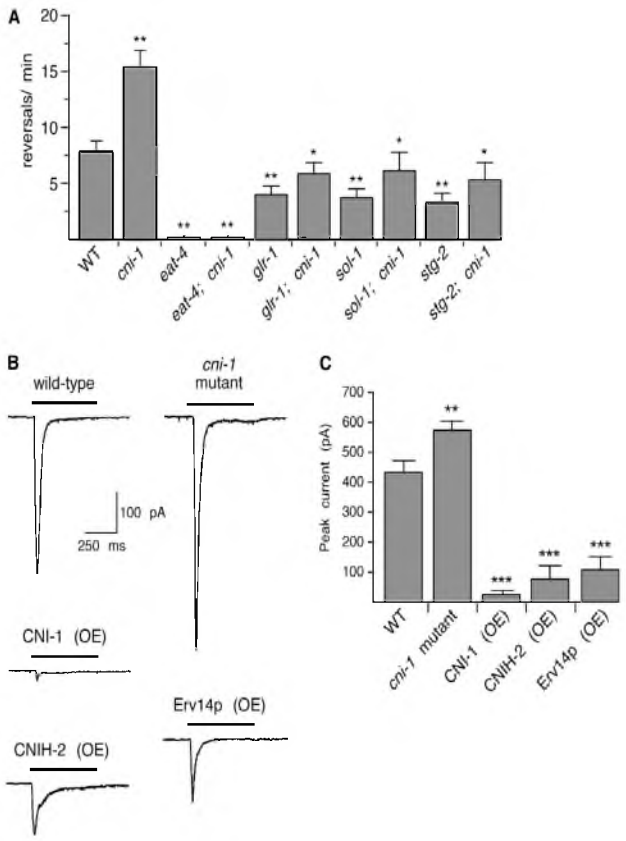


**Figure 1. Reversal Frequency and Glutamate-Gated Currents Are Increased in *cni-1* Mutants**

(A) Reversal frequency in wild-type worms and various single and double mutants. For wild-type and *cni-1* mutants, n = 8; for *glr-1*, *sol-1*, and *stg-2* single and double mutants, n = 7; and for *eat-4* single and double mutants, n = 5. Significantly different from both wild-type and *cni-1* mutants (**p < 0.01). Significantly different from *cni-1* mutants (*p < 0.05).

(B) Currents measured in AVA neurons in response to pressure application of 3 mM glutamate. Cells were voltage clamped at –60 mV.

(C) Average peak glutamate-gated current in wild-type worms (n = 11), *cni-1* mutants (n = 11), and transgenic mutants that overexpressed (OE) CNI-1 (n = 6), CNIH-2 (n = 8), or Erv14p (n = 7). Significantly different from wild-type (**p < 0.01 and ***p < 0.001).

Error bars indicate SEM. See also Figures S1, S2, and S3.

from the multicopy transgene is predicted to be much greater than that from the endogenous *cni-1* gene. We next asked whether currents were also modified in transgenic *cni-1* mutants that overexpressed the related vertebrate CNIH-2 or yeast Erv14p cornichon proteins. We found dramatically reduced currents in these transgenic worms, consistent with an evolutionarily conserved role for cornichon proteins (Figures 1B and 1C).

We also evaluated whether NMDA receptors (NMDARs) were dependent on CNI-1. Peak NMDA-gated currents were increased in *cni-1* mutants and reduced with overexpression of either CNI-1 or CNIH-2 (Figures S3B and S3C). In contrast to what we observed for AMPARs, overexpression of CNI-1 or CNIH-2 caused much smaller changes in NMDA-gated current. These effects are not likely secondary to changes in GLR-1 given that NMDAR-mediated currents in *glr-1* mutants are indistinguishable from those in wild-type worms (Brockie et al., 2001b; Mellem et al., 2002; Zheng et al., 2004). These results, together with our behavioral data, demonstrate that CNI-1's most prominent role in AVA appears to be the regulation of AMPARs. Our findings are consistent with an earlier study in yeast demonstrating that Erv14p regulates multiple classes of proteins (Herzig et al., 2012).

## The Number of Synaptic GLR-1 AMPARs Is Increased in *cni-1* Mutants

The increased current that we observed in *cni-1* mutants might be secondary to an increase in the number of synaptic AMPARs. To evaluate whether the number of receptors at synapses is modified in *cni-1* mutants, we used confocal microscopy to image transgenic strains that expressed a functional GLR-1::GFP fusion protein. Consistent with our earlier behavioral and electrophysiological data, we found that the fluorescence intensity of GLR-1::GFP was greater in transgenic *cni-1* mutants and reduced with overexpression of CNI-1, CNIH-2, or Erv14p (Figures 2A and 2B). We obtained similar results with overexpression of CNI-1 in transgenic wild-type worms (Figure S4A). To address whether the surface expression of GLR-1 was modified by the mutation in *cni-1*, we tagged GLR-1 with the pH-sensitive reporter superecliptic phluorin (SEP). The fluorescence of SEP is quenched by the relatively acidic pH of intracellular vesicles but exhibits greatly enhanced fluorescence at extracellular pH, thus distinguishing intracellular proteins from those at the surface (Miesenböck et al., 1998; Wang et al., 2012). We also found that the surface expression of GLR-1 was increased in *cni-1* mutants (Figure S4B), which is again consistent with the observed increase in GLR-1-mediated current (Figures 1B and 1C).

We did not find any apparent changes in AVA morphology in *cni-1* mutants or in transgenic worms that overexpressed CNI-1. In addition, changing the expression of CNI-1 did not affect all components of the GLR-1 signaling complex. Thus, in *cni-1* mutants or transgenic mutants that overexpressed

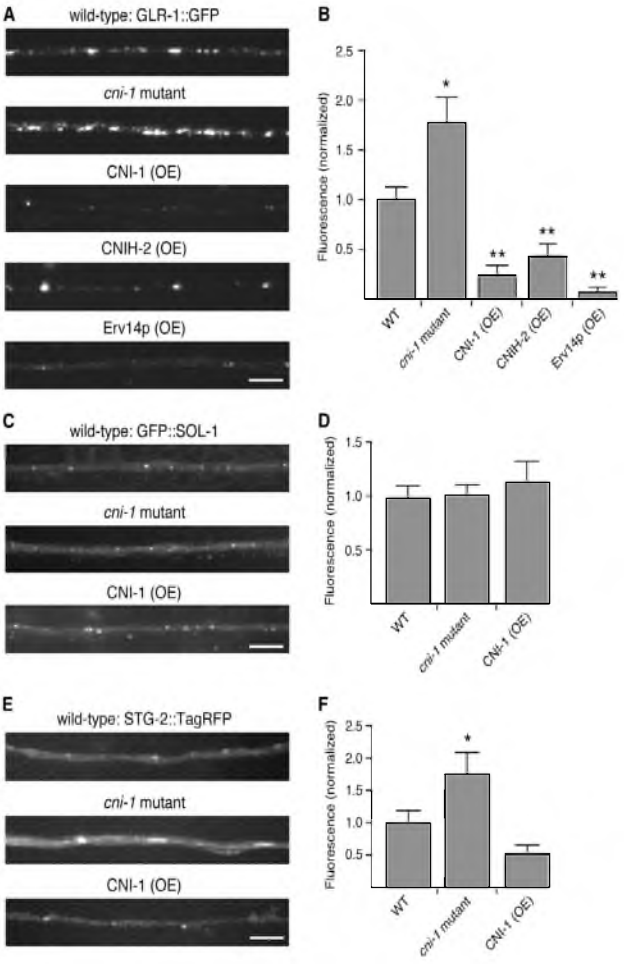


**Figure 2. Synaptic Levels of GLR-1::GFP Are Increased in *cni-1* Mutants and Decreased by Overexpression of Cornichon Proteins**

(A and B) Confocal images of GLR-1::GFP (A) and the total GFP fluorescence (B) in the AVA processes of wild-type worms (n = 11), *cni-1* mutants (n = 11), and transgenic mutants that overexpressed CNI-1 (n = 10), CNIH-2 (n = 9), or Erv14p (n = 7).

(C and E) Confocal images of either GFP::SOL-1 (C) or STG-2::TagRFP (E) in the AVA neurons of transgenic worms.

(D and F) GFP (D) or TagRFP (F) fluorescence in transgenic wild-type worms (GFP, n = 12; TagRFP, n = 15), *cni-1* mutants (GFP, n = 11; TagRFP, n = 10), and transgenic mutants that overexpressed CNI-1 (GFP, n = 5; TagRFP, n = 8).

Significantly different from wild-type (*$p < 0.05$ and **$p < 0.01$). Scale bars represent 5 μm. Error bars represent SEM. See also Figure S4.

CNI-1, the intensity of GFP::SOL-1 was relatively unaffected compared to the pronounced changes in GLR-1 (Figures 2C and 2D). We also generated transgenic worms that coexpressed GLR-1::GFP and STG-2::TagRFP. Interestingly, we observed a significant increase in STG-2::TagRFP in *cni-1* mutants and a decrease with CNI-1 overexpression (Figures 2E and 2F). However, these changes might be secondary to changes in GLR-1 given that when CNI-1 overexpression dramatically reduced GLR-1::GFP fluorescence in the ventral cord, STG-2::TagRFP shifted from punctate to a more diffuse distribution (Figure S4C).

## Transport of GLR-1 AMPARs Is Increased in *cni-1* Mutants

The increase in synaptic GLR-1 in *cni-1* mutants might be caused by changes in either the anterograde or retrograde transport of GLR-1. To address these possibilities, we obtained streaming confocal images of GLR-1::GFP (Figure 3A). In *cni-1* mutants, the frequency of anterograde transport events in the AVA process was significantly increased compared to wild-type (Figure 3B), whereas these events were dramatically decreased in transgenic worms that overexpressed CNI-1 or CNIH-2. Interestingly, the *cni-1* mutation had less effect on retrograde transport (Figure 3C). However, retrograde events were significantly reduced by overexpression of either CNI-1 or CNIH-2, which we suggest was most likely consequent to the dramatic reduction in anterograde transport of AMPARs (Figure 3). Thus, the behavioral and electrophysiological changes in *cni-1* mutants appear secondary to the increased export of AMPARs from the cell body.

## CNI-1 Is Expressed in AMPAR-Expressing Neurons and Localizes to the ER

To determine the cellular distribution of CNI-1, we used confocal microscopy to examine transgenic strains in which the *cni-1* promoter drove expression of GFP (Figure S5A). We found expression in many tissues, including widespread distribution in the nervous system (Figure 4A and Figure S5B). To address whether CNI-1 is expressed in the same neurons as GLR-1, we coexpressed CNI-1::GFP and mCherry driven by the *glr-1* promoter and found that CNI-1 was expressed in all GLR-1-expressing neurons (Figure S5B). In independent experiments, we confirmed that CNI-1 is expressed in the AVA interneurons using the *flp-18* promoter to identify AVA (Feinberg et al., 2008)

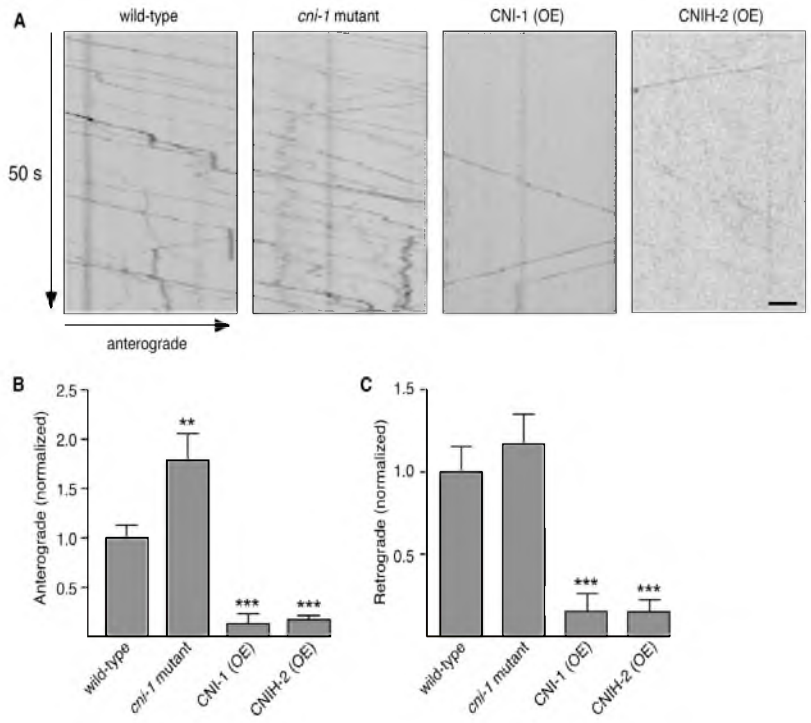


**Figure 3. The Frequency of GLR-1 Anterograde Transport Is Increased in *cni-1* Mutants**

(A) Kymographs showing the movement of GLR-1::GFP in the AVA interneurons. Scale bar represents 2 μm.

(B and C) Quantification of the number of anterograde (B) and retrograde (C) transport events in wild-type worms (n = 13), *cni-1* mutants (n = 9), and *cni-1* transgenic mutants that overexpressed either CNI-1 (n = 10) or CNIH-2 (n = 10). Significantly different from wild-type (**p < 0.01 and ***p < 0.001). Error bars represent SEM.

(Figure S5C). In neuronal cell bodies, CNI-1::GFP appeared punctate and distinctively clustered at perinuclear sites, suggestive of localization to the ER (Figure 4A).

To better examine the subcellular localization of CNI-1, we coexpressed CNI-1 with either TRAM-1, a marker of rough ER, or PISY-1, a general ER marker that also labels Golgi structures (Leber et al., 1995; Löfke et al., 2008; Rolls et al., 2002). While the distribution of PISY-1 (Figure 4B) was more localized compared to the diffuse reticular distribution of TRAM-1 (Figure 4C), we found that CNI-1 colocalized with both markers and that CNI-1 and GLR-1 colocalized (Figure 4D). To address whether accumulations of CNI-1 and GLR-1 were near ER exit sites (ERESs), we coexpressed either CNI-1::GFP or GLR-1::GFP with the COPII protein, SEC-24 (F12F6.6), tagged with mCherry. In the cell body, both CNI-1::GFP and GLR-1::GFP were found localized adjacent to mCherry::SEC-24 puncta (Figures 4E and 4F) in a pattern similar to that described previously for localization of nicotinic acetylcholine receptors to ERESs (Srinivasan et al., 2011). These data show that CNI-1 is expressed in discrete regions of the ER/Golgi where it colocalized with GLR-1.

The colocalization of CNI-1 and GLR-1 also suggests that the two proteins might interact with each other. To test this possibility, we coexpressed HA::GLR-1 and CNI-1::GFP in *Xenopus* oocytes and found an association between the proteins using an immunoprecipitation strategy (Figure 4G). Together, the biochemical and cell biological data indicate a close association between CNI-1 and GLR-1, a finding that is also consistent with studies that demonstrate an association between CNIH-2 and the vertebrate GluA1 AMPAR subunit (Kato et al., 2010; Schwenk et al., 2009; Shi et al., 2010).

## CNI-1 Colocalizes with Surface GLR-1 in the Processes of AVA

In *C. elegans*, ER extends into neural processes (Rolls et al., 2002). We found that CNI-1 was also expressed in the processes of AVA, where it was distributed in a punctate pattern that colocalized with the ER/Golgi marker, PISY-1 (Figure 5A). When we examined the localization of CNI-1::GFP and GLR-1::mCherry in the AVA neural processes, we noted a prominent punctate distribution of both proteins where a subset of GLR-1 puncta colocalized with CNI-1 puncta (Figure 5B). While these experiments suggested that the majority of CNI-1 was intracellular and associated with organelles, they did not distinguish between intracellular and cell-surface localization of CNI-1. Therefore, we

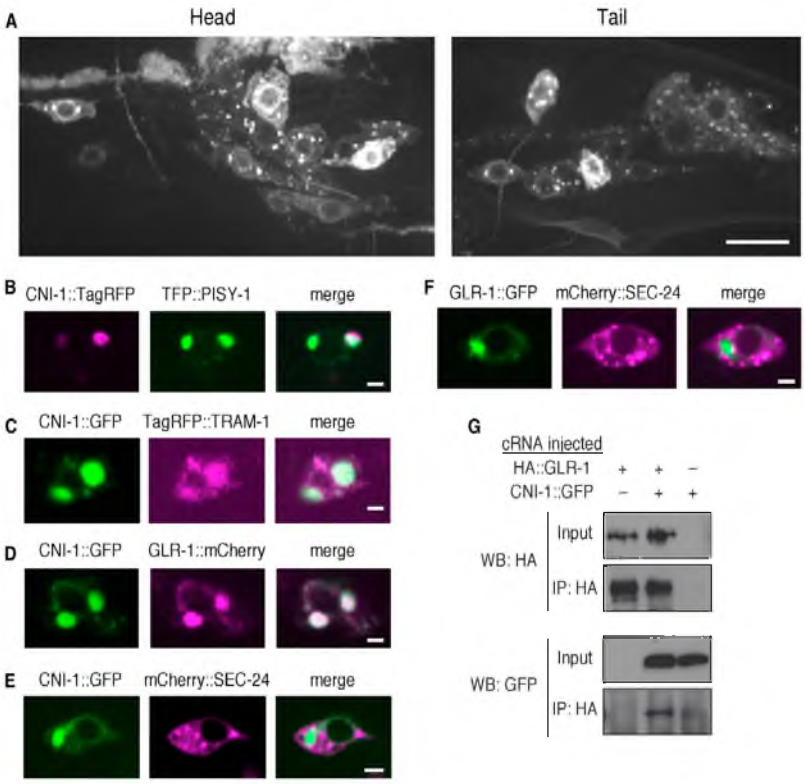


**Figure 4. CNI-1 Is Widely Expressed in the Nervous System where It Colocalizes with GLR-1 in the ER**

(A) Confocal images of the head and tail region of a transgenic worm that expressed the CNI-1::GFP reporter shown in Figure S5A. Scale bar represents 10 μm.

(B–F) Single plane, confocal images of the AVA cell bodies in transgenic worms that expressed various combinations of fluorescently labeled proteins. Scale bars represent 2 μm.

(G) Immunoprecipitation of HA::GLR-1 and CNI-1::GFP coexpressed in *Xenopus* oocytes.

See also Figure S5.

also tagged CNI-1 with SEP and GLR-1 with pHTomato, a red-shifted pH-sensitive reporter (Li and Tsien, 2012), and coexpressed these tagged proteins in AVA (Figure 5C). Because of reduced intracellular fluorescence using these pH-sensitive fluorophores, we were able to observe extensive colocalization of CNI-1 and GLR-1 with approximately 40%–80% of the GLR-1 puncta colocalizing with CNI-1 puncta. Although less dramatic than the colocalization of GLR-1 with STG-2 (Figure 5D) (Wang et al., 2008), the punctate colocalization of GLR-1 with CNI-1 suggests that CNI-1 might also function at synapses. Surface expression of CNI-1 was also supported by in vivo antibody labeling experiments (Figure S6). These results indicate that CNI-1 is not restricted to the cell body or intracellular organelles and that CNI-1 is present at synapses.

### CNI-1 Limits ER Export of GLR-1

Our data are consistent with a model in which CNI-1 functions to limit export of GLR-1 to synapses. However, in transgenic worms that overexpressed CNI-1, we also found that the fluorescence intensity of GLR-1::GFP was considerably reduced in cell bodies (Figures 6A and 6B). We reasoned that overexpression of CNI-1 might lead to the shunting of retained GLR-1 to the endoplasmic-reticulum-associated protein degradation (ERAD) pathway and ultimately the proteasome. To test this hypothesis, we treated worms with the proteasome inhibitor MG-132, a drug that is commonly used to evaluate ERAD-mediated degradation of transmembrane proteins (Altier et al., 2011). In transgenic worms that overexpressed CNI-1, incubation with MG-132 markedly increased GLR-1 fluorescence. In contrast, we did not observe an increase in fluorescence in wild-type controls or *cni-1* mutants (Figures 6A and 6B). These results are consistent with the hypothesis that CNI-1 overexpression blocks export of GLR-1, leading to subsequent degradation by the proteasome.

If CNI-1 has a role in ER export, then the glycoslylation of GLR-1 might be altered in *cni-1* mutants. The glycosylation state

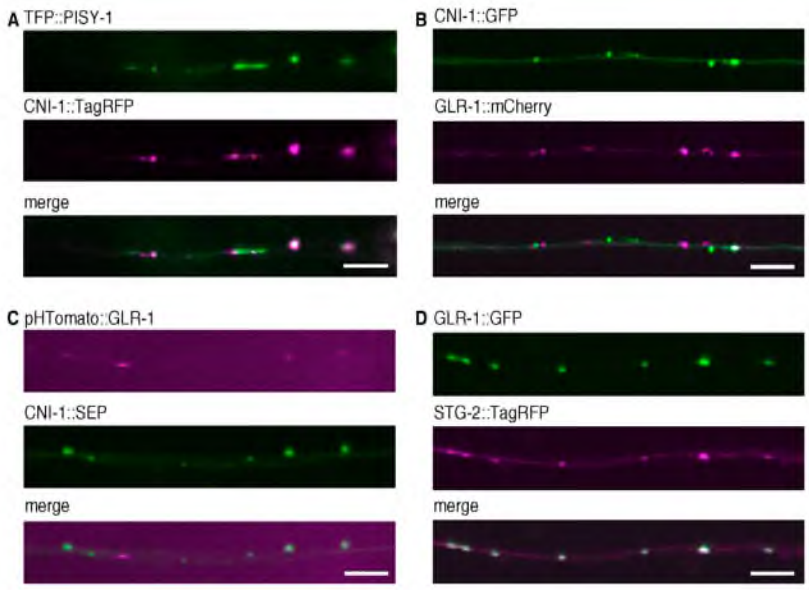


**Figure 5. Surface Expressed CNI-1 Colocalizes with Synaptic GLR-1**

(A–D) Confocal images of the AVA processes in transgenic worms that coexpressed either TFP::PISY-1 and CNI-1::TagRFP (A), GLR-1::mCherry and CNI-1::GFP (B), pHTomato::GLR-1 and CNI-1::SEP (C), or GLR-1::GFP and STG-2::TagRFP (D). Scale bars represent 5 μm.

See also Figure S6.

of proteins in the ER is distinct from those in the Golgi and can be distinguished by differential sensitivity to the enzyme Endoglycosidase H (Endo H) (Chun et al., 2008). We found that the relative amount of GLR-1 that was resistant to Endo H was increased in *cni-1* mutants compared to wild-type worms (Figures 6C and 6D). This result is consistent with the increased GLR-1 anterograde trafficking observed in *cni-1* mutants (Figure 3).

## Reconstitution Experiments Support a Conserved Role for Cornichons in Limiting AMPAR Export from the ER

In *C. elegans*, muscle cells do not express glutamate receptor subunits or known auxiliary proteins for iGluRs, thus providing an ideal system for genetic-based reconstitution experiments. We recorded glutamate-gated currents from muscle cells in transgenic worms that ectopically expressed GLR-1, SOL-1, and STG-1 and compared them to currents from muscle cells that expressed these three proteins along with either CNI-1 or CNIH-2. Similar to what we observed with overexpression studies in the AVA neurons, the amplitude of glutamate-gated current in muscle was significantly decreased with overexpression of either CNI-1 or CNIH-2 (Figures 7A and 7B). We next asked whether CNI-1 modified glutamate-gated currents mediated by vertebrate AMPARs expressed in *C. elegans* muscle and found that CNI-1 also reduced the amplitude of currents mediated by GluA1 (Figure S7A) and reduced SEP::GluA1 fluorescence (Figure S7B).

Our evaluation of surface AMPARs in transgenic worms relied on measurements of fluorescence intensity. To more directly compare surface expression and receptor-mediated currents, we turned to reconstitution studies in *Xenopus* oocytes. Overexpression of CNI-1 or CNIH-2 reduced GLR-1-mediated currents as well as surface expression of GLR-1 (Figures 7C and 7D). Similarly, overexpression of CNI-1 reduced GluA1-mediated currents and surface expression of GluA1 (Figures S7C and S7D). While coexpression of CNIH-2 with GluA1, GluA2, and the γ-8 TARP auxiliary subunit reduced AMPAR surface expression, it increased the peak glutamate-gated current, suggesting an additional effect of cornichon proteins on AMPAR function (Figures 7E and 7F). In contrast, coexpression of the Neto2 CUB-domain protein had no effect on either AMPAR-mediated current or surface expression (Figures 7E and 7F).

We next extended our reconstitution studies to address whether invertebrate and vertebrate cornichons have conserved roles in limiting the export of vertebrate AMPARs in neurons. Therefore, we coexpressed GFP-tagged GluA1 and γ-8 either with or without a cornichon protein in the AVA neurons. We found that overexpression of CNI-1, or vertebrate CNIH-2 or CNIH-1, dramatically reduced the fluorescence intensity of GFP::GluA1 in transgenic worms (Figures 8A and 8B). Electrophysiological analysis showed a reduction in peak glutamate- or kainate-gated current with overexpression of cornichon proteins (Figures 8C and 8D, black traces).

The reduced currents that we observed in transgenic worms that overexpressed either CNI-1 or CNIH-2 are consistent with cornichon's putative role in the export of GLR-1 from the ER.

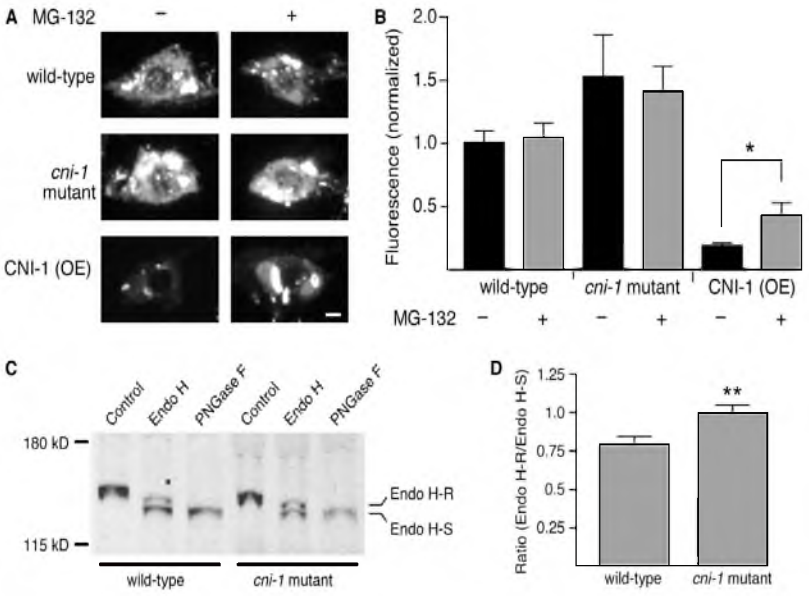


**Figure 6. Overexpression of CNI-1 Results in GLR-1::GFP Accumulation in Neuronal Cell Bodies and Its Subsequent Degradation**

(A) Confocal images of GLR-1::GFP in AVA cell bodies in worms either with or without MG-132 treatment. Scale bar represents 2 μm.

(B) Average GFP fluorescence intensity in worms either with (wild-type, n = 20; *cni-1* mutant, n = 12; CNI-1 [OE], n = 15) or without (wild-type, n = 22; *cni-1* mutant, n = 13; CNI-1 [OE], n = 16) MG-132 treatment. *p < 0.05.

(C) Western blot showing the relative amounts of Endo H-sensitive (Endo H-S) and -resistant (Endo H-R) GLR-1::GFP isolated from transgenic wild-type worms and *cni-1* mutants.

(D) The ratio of Endo H-R to Endo H-S GLR-1::GFP in wild-type (n = 11) and *cni-1* mutants (n = 10). **p < 0.01.

Error bars represent SEM.

However, these reconstitution experiments did not address whether cornichon proteins might have additional effects on receptor function. To address this question, we determined the relative efficacy of cyclothiazide (CTZ), a drug that blocks the desensitization of vertebrate AMPARs, thereby causing potentiation of the peak current in response to the relatively slow speed of pressure application of agonist (Partin et al., 1993). In preliminary studies, we found that CTZ strongly potentiated glutamate- and kainate-gated currents in transgenic worms that overexpressed vertebrate GluA1 and γ-8 in the AVA neurons. However, we observed far less potentiation in strains that coexpressed either worm CNI-1 or vertebrate CNIH-2 (Figures 8C and 8D). One interpretation of these data is that coexpression of cornichons slowed AMPAR desensitization or otherwise modified AMPAR properties (Gill et al., 2011, 2012; Schwenk et al., 2009), thus reducing the potentiation by CTZ.

The results from our genetic studies together with our reconstitution experiments in *C. elegans* neurons and muscle cells and *Xenopus* oocytes demonstrate an evolutionarily conserved role for cornichon proteins in regulating the ER export of AMPARs. Furthermore, cornichon proteins colocalized with AMPARs at synapses and, when overexpressed, modified receptor function either directly or indirectly.

## DISCUSSION

### CNI-1 Regulates ER Export of AMPARs in *C. elegans*

The number of functional AMPARs at central excitatory synapses is a critical determinant of synaptic strength, and the strength of synaptic transmission is determined in part by the balance between delivery and removal of synaptic AMPARs. Our study has demonstrated that invertebrate and vertebrate cornichon proteins have conserved roles in the control of AMPAR export from the ER. In *cni-1* mutants, the export of AMPARs is unregulated, causing increased transport of receptors, larger synaptic currents, neuronal hyperexcitability, and disrupted foraging behavior secondary to an increased reversal frequency. While CNI-1 might affect many proteins (Bökel et al., 2006; Castro et al., 2007; Herzig et al., 2012; Roth et al., 1995), the hyperreversal phenotype observed in *cni-1* mutants is primarily dependent on synaptic AMPARs, as demonstrated by the strong suppression of the *cni-1* mutant phenotype by mutations in *glr-1*, *sol-1*, or *stg-2*.

In support of our hypothesis that CNI-1 regulates GLR-1 export from the ER, we found that CNI-1 colocalized with ER markers in the AVA neuronal cell bodies. Of particular interest was the colocalization of CNI-1 with GLR-1 and with the ER/Golgi marker PISY-1. We also found that CNI-1 and GLR-1

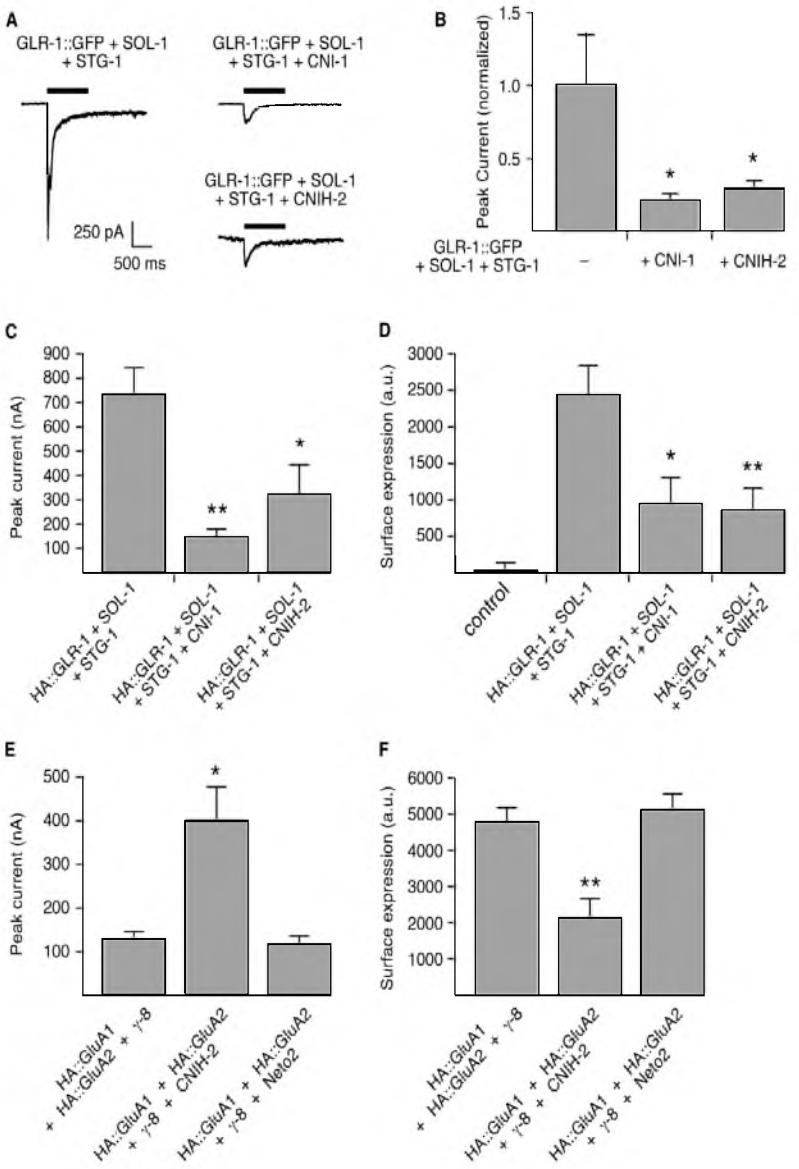


**Figure 7. Overexpressing CNI-1 or CNIH-2 Modifies Glutamate-Gated Current and AMPAR Surface Expression**

(A) Glutamate-gated current in transgenic muscle cells in response to pressure application of 3 mM glutamate. Cells were voltage clamped at −60 mV.

(B) Average peak glutamate-gated current in muscle cells that expressed GLR-1::GFP, SOL-1, and STG-1 (n = 6); GLR-1::GFP, SOL-1, STG-1, and CNI-1 (n = 5); or GLR-1::GFP, SOL-1, STG-1, and CNIH-2 (n = 11). Significantly different from GLR-1::GFP + SOL-1 + STG-1 (*$p < 0.05$).

(C and D) Glutamate-gated current in *Xenopus* oocytes (C) and GLR-1 surface expression (D) in noninjected control oocytes or in oocytes that expressed HA::GLR-1, SOL-1, and STG-1 either with or without coexpression of CNI-1 or CNIH-2 (n = 6 for all conditions). Significantly different from HA::GLR-1 + SOL-1 + STG-1 (*$p < 0.05$ and **$p < 0.01$).

(E and F) Glutamate-gated current (E) and AMPAR surface expression (F) in *Xenopus* oocytes (n = 6 for all conditions). Significantly different from HA::GluA1 + HA::GluA2 + γ-8 (*$p < 0.05$ and **$p < 0.01$).

Error bars represent SEM. See also Figure S7.

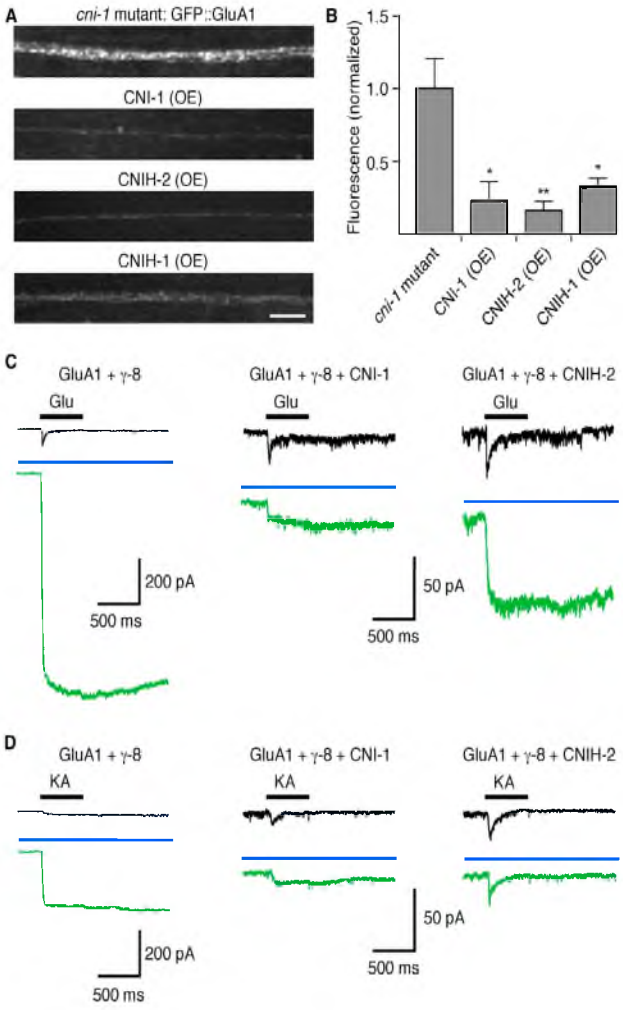


**Figure 8. Cornichon Proteins Decrease GluA1-Mediated Current and Synaptic GluA1 Levels when Coexpressed in *C. elegans* AVA Neurons**

(A and B) Confocal images (A) and quantification (B) of GFP::GluA1 fluorescence in the AVA neurons of transgenic *cni-1* mutants (n = 9) or transgenic mutants that also overexpressed CNI-1 (n = 4), CNIH-2 (n = 5), or CNIH-1 (n = 5). Scale bar represents 5 μm; error bars represent SEM. Significantly different from *cni-1* mutants (*p < 0.05, **p < 0.01).

(C and D) GluA1-mediated glutamate- (C) and kainate- (D) gated current in the AVA neurons of various transgenic worms both before (black) and after (green) treatment with 100 μM cyclothiazide. The blue bar indicates the presence of cyclothiazide.

were in close apposition to SEC-24/COPII puncta, which mark putative ER export sites (Srinivasan et al., 2011). These data suggest that CNI-1 might have a spatially restricted role and act to control the export of GLR-1 at the ER-Golgi interface. In support of this hypothesis, we found a larger percentage of Endo H-resistant GLR-1 in *cni-1* mutants, suggesting ER export was increased in the mutants compared to wild-type. These data are consistent with reconstitution experiments in HeLa cells that demonstrated a CNIH-2-dependent increase in immature-glycosylated GluA2 receptors (Harmel et al., 2012).

## Cornichon Proteins Have a Conserved Role in Limiting the ER Export of AMPARs

To address whether vertebrate cornichons had conserved roles in limiting the export of vertebrate AMPARs, we reconstituted GluA1 function in *C. elegans* neurons. We generated transgenic *glr-1; cni-1; stg-2* triple mutants that coexpressed the vertebrate GluA1 AMPAR and the vertebrate γ-8 auxiliary protein. *glr-1* and *stg-2* mutants lack fast glutamate-gated currents in AVA (Brockie and Maricq, 2006; Zheng et al., 2004), thereby facilitating the interpretation of our reconstitution studies. Interestingly, we found punctate expression of GluA1 in neuronal processes and we could record glutamate-gated current, indicating that the vertebrate receptors were transported to the surface and were functional. In these transgenic worms, coexpression of vertebrate CNIH-2 or CNIH-1 or worm CNI-1 dramatically reduced GFP::GluA1 fluorescence in neuronal processes. Furthermore, CNIH-2 and CNI-1 reduced glutamate- and kainate-gated currents, indicating that an evolutionarily conserved role of cornichon proteins is to limit the export of AMPARs.

While our manuscript was in revision, a study was published that evaluated the contribution of CNIH-2 and CNIH-3 to AMPAR-mediated synaptic transmission in CA1 neurons of the vertebrate hippocampus (Herring et al., 2013). In this study, the authors found that genetic perturbation of CNIH-2 and CNIH-3, a subset of the four cornichon proteins expressed in the brain that appear predominant in the hippocampus, was associated with reduced numbers of GluA1-containing AMPARs along with a corresponding decrease in peak glutamate-gated currents. Given the results from our reconstitution studies of vertebrate GluA1 in *C. elegans* neurons, the finding of reduced current in the conditional knockout mice suggests that vertebrate CA1 neurons might express additional quality control machinery. For example, GluA1 receptors not associated with a cornichon protein might be more susceptible to degradation in vertebrate neurons.

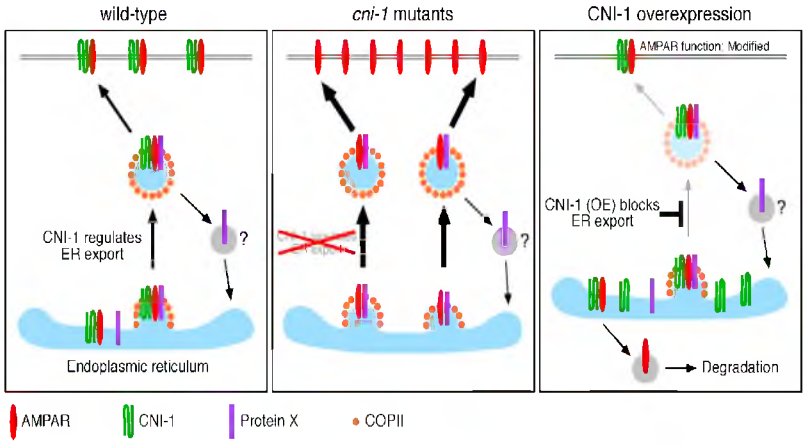


**Figure 9. CNI-1 Modifies Neuron Excitability by Regulating the Export of AMPARs from the ER**

In this model, GLR-1 binds to CNI-1, which masks an ER export signal and prevents export. Association of a putative Protein X modifies the complex such that the ER export signal is exposed and the AMPAR can exit the ER. Thus, in *cni-1* mutants AMPARs more readily exit the ER. In contrast, AMPAR exit from the ER is slowed by overexpression of CNI-1. Furthermore, the function of AMPARs that do reach synapses is modified.

## CNI-1 Differentially Regulates the Components of the GLR-1 Signaling Complex

Auxiliary proteins are known to contribute to AMPAR function (Jackson and Nicoll, 2011; Yan and Tomita, 2012). In *C. elegans*, the auxiliary proteins SOL-1, SOL-2, and STG-2 co-localize with GLR-1 at synapses (Wang et al., 2008, 2012; Zheng et al., 2004). These transmembrane proteins did not show the same dependence on cornichon as that observed for GLR-1. Thus, the levels of SOL-1 were not appreciably altered in the processes of AVA in *cni-1* mutants or with overexpression of CNI-1. Although we did find an increase in STG-2 in *cni-1* mutants and a minor decrease when CNI-1 was overexpressed, we suspect that these effects were secondary to changes in GLR-1.

Recent analysis of the yeast cornichon homolog Erv14p provides a possible mechanism for cornichon's cargo specificity (Herzig et al., 2012). Erv14p associates with many transmembrane proteins and target specificity appears to be associated with the length of the transmembrane domain(s). However, other mechanisms also contribute to ER export and cargo can be made independent of Erv14p by the addition of different trafficking domains (Herzig et al., 2012).

## CNI-1 Modifies Neuronal Excitability by Regulating the Number of Synaptic AMPARs

The study of *cni-1* mutants along with transgenic rescue and AMPAR reconstitution experiments demonstrate that an ancient evolutionarily conserved role for cornichon proteins is to regulate the ER export of AMPARs. We envision two possible mechanisms. In the first model, CNI-1 binds to AMPAR subunits and blocks export from the ER—perhaps by masking an ER export signal. Binding of a putative Protein X exposes the export signal, thereby allowing the complex to exit the ER (Figure 9). In *cni-1* mutants, AMPARs more readily exit the ER, resulting in greater delivery of receptors to the cell surface and synapses. This model is similar to one postulated for the regulation of TGF-$\alpha$ from the ER (Castro et al., 2007). Here, cornichon binds to TGF-$\alpha$, thus limiting ER export until it associates with the transmembrane protein Star.

In the second model, AMPARs directly bind to COPII proteins for export. Overexpression of CNI-1 limits export of AMPARs by competing for COPII binding sites. Conversely, in the absence of *cni-1* more COPII sites are available for GLR-1 binding, resulting in increased ER export. In both models, ER-retained receptors are susceptible to subsequent degradation. Although we favor the first model because we found that AMPARs and their auxiliary proteins do not have the same dependence on CNI-1, discrimination of the two models will require a systematic study of the molecular requirements for ER export of AMPARs.

## CNI-1 and CNIH-2 Overexpression Modifies Export and Function of Vertebrate AMPARs

Importantly, we showed in reconstitution studies in transgenic worms that vertebrate and *C. elegans* cornichon proteins similarly decreased the ER export of vertebrate AMPARs and decreased glutamate-gated currents. These data provide further evidence for the conservation of cornichon function. Our results also highlight the utility of reconstituting vertebrate receptors in *C. elegans*. This strategy not only reveals conserved functions but also points out significant differences. For example, the interesting difference between our results and those of Herring et al. (2013) suggests that additional machinery contributes to the regulation of AMPAR signaling complexes in vertebrates.

Our data showing that CTZ efficacy was decreased by overexpression of cornichon proteins suggests that cornichons might also function as classical auxiliary proteins to modify either the kinetics of AMPAR desensitization or receptor sensitivity to

CTZ. Alternatively, cornichon might modify AMPAR function by interacting with associated auxiliary proteins or exert indirect effects by modifying the maturation of synaptic receptors, e.g., the glycosylation state or stoichiometry of the receptor complex. In preliminary studies, we did not find an obvious difference in GLR-1 kinetics in wild-type and *cni-1* mutants (data not shown), suggesting that the effects of wild-type CNI-1 on AMPAR function might be subtle compared to those observed with overexpression of cornichon proteins. Unfortunately, we were not able to determine the relative effects of CTZ on GLR-1-mediated currents given that *C. elegans* AMPARs are insensitive to CTZ treatment (data not shown). A third possibility is raised by a recent proteomic study that identified many potential auxiliary proteins (Schwenk et al., 2012). Perhaps cornichon proteins help recruit or assemble these or yet to be identified proteins to the receptor complex.

## CNI-1 Colocalizes with GLR-1 in Neural Processes

We also found substantial CNI-1 in neuronal processes. Much of CNI-1 appeared to be intracellular and associated with organelles marked by PISY-1. However, more refined analysis revealed that CNI-1 was also at the surface of neuronal processes and colocalized with surface GLR-1, similar to what we have observed for STG-2, SOL-1, and SOL-2 auxiliary subunits (Wang et al., 2008, 2012; Zheng et al., 2004). Although the changes in peak glutamate-gated current in *cni-1* mutants, and with overexpression of cornichon proteins, can be explained by changes in surface expression, the presence of CNI-1 at synapses is intriguing. Our reconstitution studies demonstrating changes in CTZ sensitivity are consistent with a possible auxiliary role for CNI-1 at synapses. Alternatively, CNI-1 might regulate local trafficking of AMPARs between endosomal compartments and synapses—a possible role that might be analogous to its function as a regulator of GLR-1 export from the ER.

Our results help provide a mechanistic view of the global regulation of receptor numbers at the postsynaptic membrane. Neurons rely on compensatory homeostatic mechanisms that regulate synaptic strength and optimize neuronal excitability (Davis, 2006; Goold and Nicoll, 2010; Turrigiano, 2008). In *cni-1* mutants, the neural circuit that regulates reversals used for avoidance and foraging behaviors is hyperexcitable secondary to an increase in the number of synaptic AMPARs. We propose that CNI-1 regulates the export of AMPARs in response to external or internal cues, thus contributing to homeostatic processes such as global regulation of neuronal excitability.

## EXPERIMENTAL PROCEDURES

### General Methods, Genetics, and Plasmids

All *C. elegans* strains were raised at 20°C under standard laboratory conditions. Transgenic strains carrying multicopy transgene arrays were generated using microinjection into the gonad of adult hermaphrodite *lin-15(n765ts)* mutants, wild-type worms, or relevant mutant worms. Transgenic worms were selected by rescue of the *lin-15(n765ts)* mutant phenotype or by expression of a coinjected fluorescent marker. Single-copy transgenic strains were generated following an established protocol (Frøkjaer-Jensen et al., 2008). Fluorescently labeled CNI-1 was found to be functional in transgenic experiments that showed the fusion protein had a similar effect on the localization of fluorescently tagged GLR-1 as that of untagged CNI-1. Function of fluorescently labeled STG-2 was confirmed by rescue of *stg-2(ak134)* suppression of the lurcher worm hyperreversal phenotype. Plasmids, transgenes, and mutant strains are described in Supplemental Experimental Procedures.

### Confocal Microscopy

Confocal images were acquired using a Nikon Ti-eclipse equipped with a WaveFX-X1 spinning-disc confocal system (Quorum Technologies) and captured by a Cascade 1024B EMCCD camera (Photometrics). Streaming movies (100 ms exposure) of GLR-1::GFP transport were acquired in a single focal plane in the AVA processes. Image acquisition and kymographs were generated using MetaMorph 7.7.10 (Molecular Devices). Anterograde and retrograde events were quantified by counting the number of trajectories in each direction with the experimenter blind to the genotype.

### Electrophysiological Studies

Electrophysiological recordings from AVA interneurons and muscle cells from dissected transgenic worms were performed as described (Jensen et al., 2012; Mellem et al., 2002).

### Behavioral Analysis

Reversal frequency, nose touch response, and osmotic avoidance assays were performed as previously described (Brockie et al., 2001b; Mellem et al., 2002). A reversal was defined as a switch from forward to backward or from backward to forward movement. All behavioral assays were performed blind. Statistical significance was determined by using the standard Student's t test.

### MG-132 Treatment

Proteasome inhibition assays were performed as described (Orsborn et al., 2007). Briefly, adult worms were placed in liquid medium containing 1 μM MG-132 for 3 hr. Controls were incubated in liquid medium without MG-132. Immediately following incubation, GLR-1::GFP in the AVA cell bodies was imaged by confocal microscopy.

### Quantification of Fluorescence

Total fluorescence in neuronal processes was measured using a linescan measurement in MetaMorph 7.7.10 (Molecular Devices) and analyzed with a custom-written MATLAB script (based on http://terpconnect.umd.edu/~toh/spectrum/PeakFindingandMeasurement.htm). A detailed description of the quantification of fluorescence signals can be found in Supplemental Experimental Procedures.

### Electrophysiology, Surface Labeling, and Coimmunoprecipitation Studies in *Xenopus* Laevis Oocytes

Two-electrode voltage-clamp recordings and surface labeling using HA::GLR-1, HA::GluA1, and anti-HA antibodies were performed as described (Morimoto-Tomita et al., 2009). For coimmunoprecipitations, oocyte membranes were suspended in lysis buffer containing TED (25 mM Tris-Cl pH 7.4, 2 mM EDTA, and 1 mM DTT), 1% Triton X-100, Halt protease inhibitors (Pierce) and centrifuged at 100,000 × *g* for 30 min (Morimoto-Tomita et al., 2009). The supernatants were then incubated with 5 μg anti-HA antibody and 30 μl protein G sepharose beads. The beads were then washed five times with 1% Triton in TEEN (25 mM Tris-Cl pH 7.4, 1 mM EDTA, 1 mM EGTA, and 150 mM NaCl). Bound proteins were eluted by heating the resin in 40 μl 1 × SDS-PAGE sample buffer and analyzed by SDS-PAGE.

### Antibody Staining in Transgenic Worms

Transgenic worms that expressed CNI-1::GFP in the AVA neurons were immunolabeled as previously described (Gottschalk and Schafer, 2006; Zheng et al., 2004). Briefly, anti-GFP polyclonal sera (Molecular Probes) was diluted (1:1,000) in injection buffer and injected into the pseudocoelome of transgenic worms. Worms were allowed to recover for 2 hr before imaging.

### Endo H Digestion and Western Blots

Mixed-stage worms were washed off plates with M9 buffer. After an additional wash in M9, excess buffer was removed and worms were resuspended in two volumes of protein sample buffer and frozen in liquid nitrogen. Samples were heated at 95°C for 10 min and the resulting lysates were diluted in reaction

Neuron
CNI-1 Regulates AMPAR Export and Neurotransmission

buffer for either Endo H or PNGase F (as per protocol, New England BioLabs) and digested with 250 units for 30 min at 37°C. Products were run on 7% TGX precast gels (Bio-Rad) and transferred to nitrocellulose membranes. Blots were incubated with monoclonal anti-GFP antibodies (Santa Cruz Biotechnology) in Odyssey Blocking Buffer (LI-COR). Bands were detected with IRDye 800CW on the Odyssey Imager (LI-COR). Endo H sensitivity was quantified in ImageJ.

### Statistical Analysis

The results were analyzed using an unpaired Student's t test.

## SUPPLEMENTAL INFORMATION

Supplemental Information includes Supplemental Experimental Procedures and seven figures and can be found with this article online at http://dx.doi.org/10.1016/j.neuron.2013.07.028.

## ACKNOWLEDGMENTS

We thank members of the Maricq laboratory and Marcus Babst for comments on the manuscript, Craig Walker for the preliminary analysis of *cni-1* mutants and Aleksander Maricq for assistance writing the MATLAB script. Some strains were provided by the *Caenorhabditis* Genetics Center (CGC), which is funded by NIH Office of Research Infrastructure Programs (P40 OD010440). This research was made possible by support from NIH Grants NS35812 (A.V.M.) and MH077939 (S.T.). T.Y. is supported by the Program for Young Researcher Overseas Visits, Graduate School of Pharmaceutical Science, The University of Tokyo.

Accepted: July 16, 2013
Published: October 2, 2013

## REFERENCES

Altier, C., Garcia-Caballero, A., Simms, B., You, H., Chen, L., Walcher, J., Tedford, H.W., Hermosilla, T., and Zamponi, G.W. (2011). The Cavβ subunit prevents RFP2-mediated ubiquitination and proteasomal degradation of L-type channels. Nat. Neurosci. *14*, 173–180.

Anggono, V., and Huganir, R.L. (2012). Regulation of AMPA receptor trafficking and synaptic plasticity. Curr. Opin. Neurobiol. *22*, 461–469.

Bökel, C., Dass, S., Wilsch-Bräuninger, M., and Roth, S. (2006). Drosophila Cornichon acts as cargo receptor for ER export of the TGFalpha-like growth factor Gurken. Development *133*, 459–470.

Brockie, P.J., Madsen, D.M., Zheng, Y., Mellem, J., and Maricq, A.V. (2001a). Differential expression of glutamate receptor subunits in the nervous system of Caenorhabditis elegans and their regulation by the homeodomain protein UNC-42. J. Neurosci. *21*, 1510–1522.

Brockie, P.J., and Maricq, A.V. (2006). Building a synapse: genetic analysis of glutamatergic neurotransmission. Biochem. Soc. Trans. *34*, 64–67.

Brockie, P.J., Mellem, J.E., Hills, T., Madsen, D.M., and Maricq, A.V. (2001b). The C. elegans glutamate receptor subunit NMR-1 is required for slow NMDA-activated currents that regulate reversal frequency during locomotion. Neuron *31*, 617–630.

Castro, C.P., Piscopo, D., Nakagawa, T., and Derynck, R. (2007). Cornichon regulates transport and secretion of TGFalpha-related proteins in metazoan cells. J. Cell Sci. *120*, 2454–2466.

Chalfie, M., Sulston, J.E., White, J.G., Southgate, E., Thomson, J.N., and Brenner, S. (1985). The neural circuit for touch sensitivity in Caenorhabditis elegans. J. Neurosci. *5*, 956–964.

Chun, D.K., McEwen, J.M., Burbea, M., and Kaplan, J.M. (2008). UNC-108/Rab2 regulates postendocytic trafficking in Caenorhabditis elegans. Mol. Biol. Cell *19*, 2682–2695.

Coombs, I.D., Soto, D., Zonouzi, M., Renzi, M., Shelley, C., Farrant, M., and Cull-Candy, S.G. (2012). Cornichons modify channel properties of recombinant and glial AMPA receptors. J. Neurosci. *32*, 9796–9804.

Davis, G.W. (2006). Homeostatic control of neural activity: from phenomenology to molecular design. Annu. Rev. Neurosci. *29*, 307–323.

de Bono, M., and Maricq, A.V. (2005). Neuronal substrates of complex behaviors in C. elegans. Annu. Rev. Neurosci. *28*, 451–501.

Feinberg, E.H., Vanhoven, M.K., Bendesky, A., Wang, G., Fetter, R.D., Shen, K., and Bargmann, C.I. (2008). GFP Reconstitution Across Synaptic Partners (GRASP) defines cell contacts and synapses in living nervous systems. Neuron *57*, 353–363.

Frøkjaer-Jensen, C., Davis, M.W., Hopkins, C.E., Newman, B.J., Thummel, J.M., Olesen, S.P., Grunnet, M., and Jorgensen, E.M. (2008). Single-copy insertion of transgenes in Caenorhabditis elegans. Nat. Genet. *40*, 1375–1383.

Gill, M.B., Kato, A.S., Roberts, M.F., Yu, H., Wang, H., Tomita, S., and Bredt, D.S. (2011). Cornichon-2 modulates AMPA receptor-transmembrane AMPA receptor regulatory protein assembly to dictate gating and pharmacology. J. Neurosci. *31*, 6928–6938.

Gill, M.B., Kato, A.S., Wang, H., and Bredt, D.S. (2012). AMPA receptor modulation by cornichon-2 dictated by transmembrane AMPA receptor regulatory protein isoform. Eur. J. Neurosci. *35*, 182–194.

Goold, C.P., and Nicoll, R.A. (2010). Single-cell optogenetic excitation drives homeostatic synaptic depression. Neuron *68*, 512–528.

Gottschalk, A., and Schafer, W.R. (2006). Visualization of integral and peripheral cell surface proteins in live Caenorhabditis elegans. J. Neurosci. Methods *154*, 68–79.

Harmel, N., Cokic, B., Zolles, G., Berkefeld, H., Mauric, V., Fakler, B., Stein, V., and Klöcker, N. (2012). AMPA receptors commandeer an ancient cargo exporter for use as an auxiliary subunit for signaling. PLoS ONE *7*, e30681.

Hart, A.C., Sims, S., and Kaplan, J.M. (1995). Synaptic code for sensory modalities revealed by C. elegans GLR-1 glutamate receptor. Nature *378*, 82–85.

Herring, B.E., Shi, Y., Suh, Y.H., Zheng, C.Y., Blankenship, S.M., Roche, K.W., and Nicoll, R.A. (2013). Cornichon proteins determine the subunit composition of synaptic AMPA receptors. Neuron *77*, 1083–1096.

Herzig, Y., Sharpe, H.J., Elbaz, Y., Munro, S., and Schuldiner, M. (2012). A systematic approach to pair secretory cargo receptors with their cargo suggests a mechanism for cargo selection by Erv14. PLoS Biol. *10*, e1001329.

Hills, T., Brockie, P.J., and Maricq, A.V. (2004). Dopamine and glutamate control area-restricted search behavior in Caenorhabditis elegans. J. Neurosci. *24*, 1217–1225.

Jackson, A.C., and Nicoll, R.A. (2011). The expanding social network of ionotropic glutamate receptors: TARPs and other transmembrane auxiliary subunits. Neuron *70*, 178–199.

Jensen, M., Hoerndli, F.J., Brockie, P.J., Wang, R., Johnson, E., Maxfield, D., Francis, M.M., Madsen, D.M., and Maricq, A.V. (2012). Wnt signaling regulates acetylcholine receptor translocation and synaptic plasticity in the adult nervous system. Cell *149*, 173–187.

Kato, A.S., Gill, M.B., Ho, M.T., Yu, H., Tu, Y., Siuda, E.R., Wang, H., Qian, Y.W., Nisenbaum, E.S., Tomita, S., and Bredt, D.S. (2010). Hippocampal AMPA receptor gating controlled by both TARP and cornichon proteins. Neuron *68*, 1082–1096.

Kerchner, G.A., and Nicoll, R.A. (2008). Silent synapses and the emergence of a postsynaptic mechanism for LTP. Nat. Rev. Neurosci. *9*, 813–825.

Kessels, H.W., and Malinow, R. (2009). Synaptic AMPA receptor plasticity and behavior. Neuron *61*, 340–350.

Leber, A., Hrastnik, C., and Daum, G. (1995). Phospholipid-synthesizing enzymes in Golgi membranes of the yeast, Saccharomyces cerevisiae. FEBS Lett. *377*, 271–274.

Li, Y., and Tsien, R.W. (2012). pHTomato, a red, genetically encoded indicator that enables multiplex interrogation of synaptic activity. Nat. Neurosci. *15*, 1047–1053.

Löfke, C., Ischebeck, T., König, S., Freitag, S., and Heilmann, I. (2008). Alternative metabolic fates of phosphatidylinositol produced by phosphatidylinositol synthase isoforms in Arabidopsis thaliana. Biochem. J. *413*, 115–124.

Lu, W., and Roche, K.W. (2012). Posttranslational regulation of AMPA receptor trafficking and function. Curr. Opin. Neurobiol. *22*, 470–479.

Maricq, A.V., Peckol, E., Driscoll, M., and Bargmann, C.I. (1995). Mechanosensory signalling in C. elegans mediated by the GLR-1 glutamate receptor. Nature *378*, 78–81.

Mellem, J.E., Brockie, P.J., Zheng, Y., Madsen, D.M., and Maricq, A.V. (2002). Decoding of polymodal sensory stimuli by postsynaptic glutamate receptors in C. elegans. Neuron *36*, 933–944.

Miesenböck, G., De Angelis, D.A., and Rothman, J.E. (1998). Visualizing secretion and synaptic transmission with pH-sensitive green fluorescent proteins. Nature *394*, 192–195.

Morimoto-Tomita, M., Zhang, W., Straub, C., Cho, C.H., Kim, K.S., Howe, J.R., and Tomita, S. (2009). Autoinactivation of neuronal AMPA receptors via glutamate-regulated TARP interaction. Neuron *61*, 101–112.

Orsborn, A.M., Li, W., McEwen, T.J., Mizuno, T., Kuzmin, E., Matsumoto, K., and Bennett, K.L. (2007). GLH-1, the C. elegans P granule protein, is controlled by the JNK KGB-1 and by the COP9 subunit CSN-5. Development *134*, 3383–3392.

Partin, K.M., Patneau, D.K., Winters, C.A., Mayer, M.L., and Buonanno, A. (1993). Selective modulation of desensitization at AMPA versus kainate receptors by cyclothiazide and concanavalin A. Neuron *11*, 1069–1082.

Piggott, B.J., Liu, J., Feng, Z., Wescott, S.A., and Xu, X.Z. (2011). The neural circuits and synaptic mechanisms underlying motor initiation in C. elegans. Cell *147*, 922–933.

Rolls, M.M., Hall, D.H., Victor, M., Stelzer, E.H., and Rapoport, T.A. (2002). Targeting of rough endoplasmic reticulum membrane proteins and ribosomes in invertebrate neurons. Mol. Biol. Cell *13*, 1778–1791.

Roth, S., Neuman-Silberberg, F.S., Barcelo, G., and Schüpbach, T. (1995). cornichon and the EGF receptor signaling process are necessary for both anterior-posterior and dorsal-ventral pattern formation in Drosophila. Cell *81*, 967–978.

Schwenk, J., Harmel, N., Brechet, A., Zolles, G., Berkefeld, H., Müller, C.S., Bildl, W., Baehrens, D., Hüber, B., Kulik, A., et al. (2012). High-resolution proteomics unravel architecture and molecular diversity of native AMPA receptor complexes. Neuron *74*, 621–633.

Schwenk, J., Harmel, N., Zolles, G., Bildl, W., Kulik, A., Heimrich, B., Chisaka, O., Jonas, P., Schulte, U., Fakler, B., and Klöcker, N. (2009). Functional proteomics identify cornichon proteins as auxiliary subunits of AMPA receptors. Science *323*, 1313–1319.

Shanks, N.F., Savas, J.N., Maruo, T., Cais, O., Hirao, A., Oe, S., Ghosh, A., Noda, Y., Greger, I.H., Yates, J.R., 3rd., et al. (2012). Differences in AMPA and kainate receptor interactomes facilitate identification of AMPA receptor auxiliary subunit GSG1L. Cell Rep. *1*, 590–598.

Shi, Y., Suh, Y.H., Milstein, A.D., Isozaki, K., Schmid, S.M., Roche, K.W., and Nicoll, R.A. (2010). Functional comparison of the effects of TARPs and cornichons on AMPA receptor trafficking and gating. Proc. Natl. Acad. Sci. USA *107*, 16315–16319.

Srinivasan, R., Pantoja, R., Moss, F.J., Mackey, E.D., Son, C.D., Miwa, J., and Lester, H.A. (2011). Nicotine up-regulates alpha4beta2 nicotinic receptors and ER exit sites via stoichiometry-dependent chaperoning. J. Gen. Physiol. *137*, 59–79.

Turrigiano, G.G. (2008). The self-tuning neuron: synaptic scaling of excitatory synapses. Cell *135*, 422–435.

von Engelhardt, J., Mack, V., Sprengel, R., Kavenstock, N., Li, K.W., Stern-Bach, Y., Smit, A.B., Seeburg, P.H., and Monyer, H. (2010). CKAMP44: a brain-specific protein attenuating short-term synaptic plasticity in the dentate gyrus. Science *327*, 1518–1522.

Walker, C.S., Brockie, P.J., Madsen, D.M., Francis, M.M., Zheng, Y., Koduri, S., Mellem, J.E., Strutz-Seebohm, N., and Maricq, A.V. (2006a). Reconstitution of invertebrate glutamate receptor function depends on stargazin-like proteins. Proc. Natl. Acad. Sci. USA *103*, 10781–10786.

Walker, C.S., Francis, M.M., Brockie, P.J., Madsen, D.M., Zheng, Y., and Maricq, A.V. (2006b). Conserved SOL-1 proteins regulate ionotropic glutamate receptor desensitization. Proc. Natl. Acad. Sci. USA *103*, 10787–10792.

Wang, R., Mellem, J.E., Jensen, M., Brockie, P.J., Walker, C.S., Hoerndli, F.J., Hauth, L., Madsen, D.M., and Maricq, A.V. (2012). The SOL-2/Neto auxiliary protein modulates the function of AMPA-subtype ionotropic glutamate receptors. Neuron *75*, 838–850.

Wang, R., Walker, C.S., Brockie, P.J., Francis, M.M., Mellem, J.E., Madsen, D.M., and Maricq, A.V. (2008). Evolutionary conserved role for TARPs in the gating of glutamate receptors and tuning of synaptic function. Neuron *59*, 997–1008.

Wright, A., and Vissel, B. (2012). The essential role of AMPA receptor GluR2 subunit RNA editing in the normal and diseased brain. Front. Mol. Neurosci. *5*, 34.

Yan, D., and Tomita, S. (2012). Defined criteria for auxiliary subunits of glutamate receptors. J. Physiol. *590*, 21–31.

Zhang, D., Isack, N.R., Glodowski, D.R., Liu, J., Chen, C.C., Xu, X.Z., Grant, B.D., and Rongo, C. (2012). RAB-6.2 and the retromer regulate glutamate receptor recycling through a retrograde pathway. J. Cell Biol. *196*, 85–101.

Zheng, Y., Brockie, P.J., Mellem, J.E., Madsen, D.M., and Maricq, A.V. (1999). Neuronal control of locomotion in *C. elegans* is modified by a dominant mutation in the GLR-1 ionotropic glutamate receptor. Neuron *24*, 347–361.

Zheng, Y., Brockie, P.J., Mellem, J.E., Madsen, D.M., Walker, C.S., Francis, M.M., and Maricq, A.V. (2006). SOL-1 is an auxiliary subunit that modulates the gating of GLR-1 glutamate receptors in Caenorhabditis elegans. Proc. Natl. Acad. Sci. USA *103*, 1100–1105.

Zheng, Y., Mellem, J.E., Brockie, P.J., Madsen, D.M., and Maricq, A.V. (2004). SOL-1 is a CUB-domain protein required for GLR-1 glutamate receptor function in C. elegans. Nature *427*, 451–457.

**Neuron, Volume *80***

## Supplemental Information

# Cornichons Control ER Export of AMPA Receptors to Regulate Synaptic Excitability

Penelope J. Brockie, Michael Jensen, Jerry E. Mellem, Erica Jensen, Tokiwa Yamasaki, Rui Wang, Dane Maxfield, Colin Thacker, Frédéric Hoerndli, Patrick J. Dunn, Susumu Tomita, David M. Madsen, and Andres V. Maricq

Supplemental text and figures: Brockie et al.

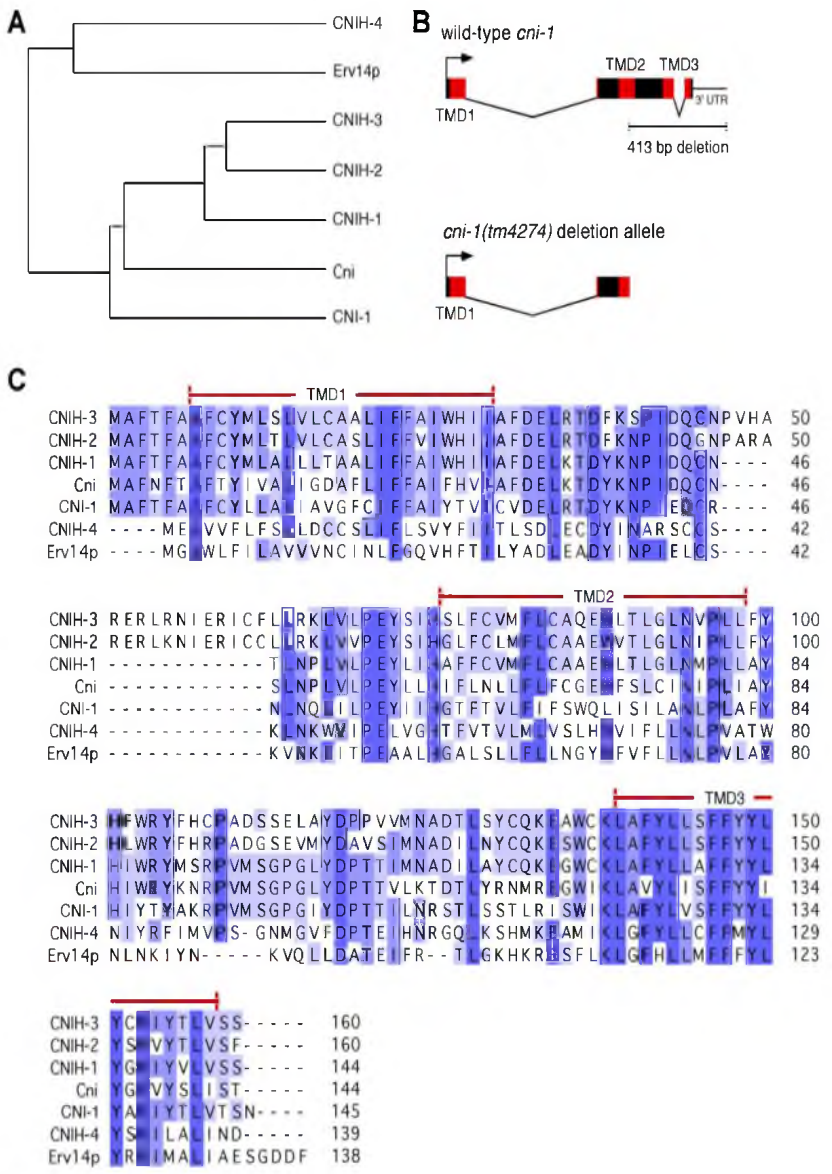

Supplemental text and figures: Brockie et al.

**Figure S1**. *C. elegans cni-1* encodes a member of the family of cornichon proteins. Supplemental data associated with Figure 1.

(A) Phylogenetic tree of *C. elegans* (CNI-1), *Drosophila* (Cni), rat (CNIH-1, 2, 3 and 4) and yeast (Erv14p) cornichon proteins. (B) Genomic organization of wild-type *cni-1* (top) and the *cni-1(tm4274)* 413 bp deletion allele (bottom). Boxes and lines represent exons and introns, respectively. The red boxes show the regions that encode the predicted transmembrane domains (TMDs). (C) Amino acid sequences of cornichon proteins. The red bars indicate the TMDs predicted for *Drosophila* Cni. *C. elegans* CNI-1 shares 57% identity with *Drosophila* Cni, 59% identity with rat CNIH-1, 50% identity with rat CNIH-2 and 33% identity with yeast Erv14p. Dark blue boxes represent identity >80% and light blue boxes represent between 60% and 80% identity.

Supplemental text and figures: Brockie et al.

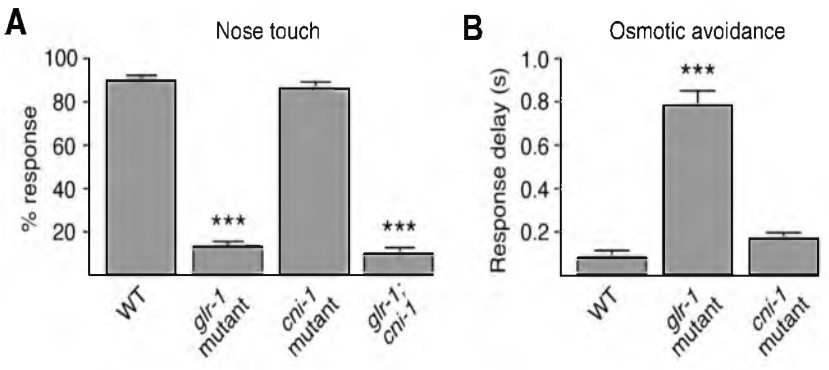


**Figure S2**. *cni-1* is not required for either the nose touch or osmotic avoidance response. Supplemental data associated with Figure 1.

(A) The percent response to 10 nose touch stimuli per worm in wild-type worms, *glr-1* and *cni-1* single mutants (n=14) and *glr-1; cni-1* double mutants (n=8). (B) The average time taken to respond to a hyper-osmotic stimulus in wild-type worms (n=11), *glr-1* mutants (n=5) and *cni-1* mutants (n=15).

*** Significantly different from wild type ($p<0.001$). Error bars represent SEM.

Supplemental text and figures: Brockie et al.

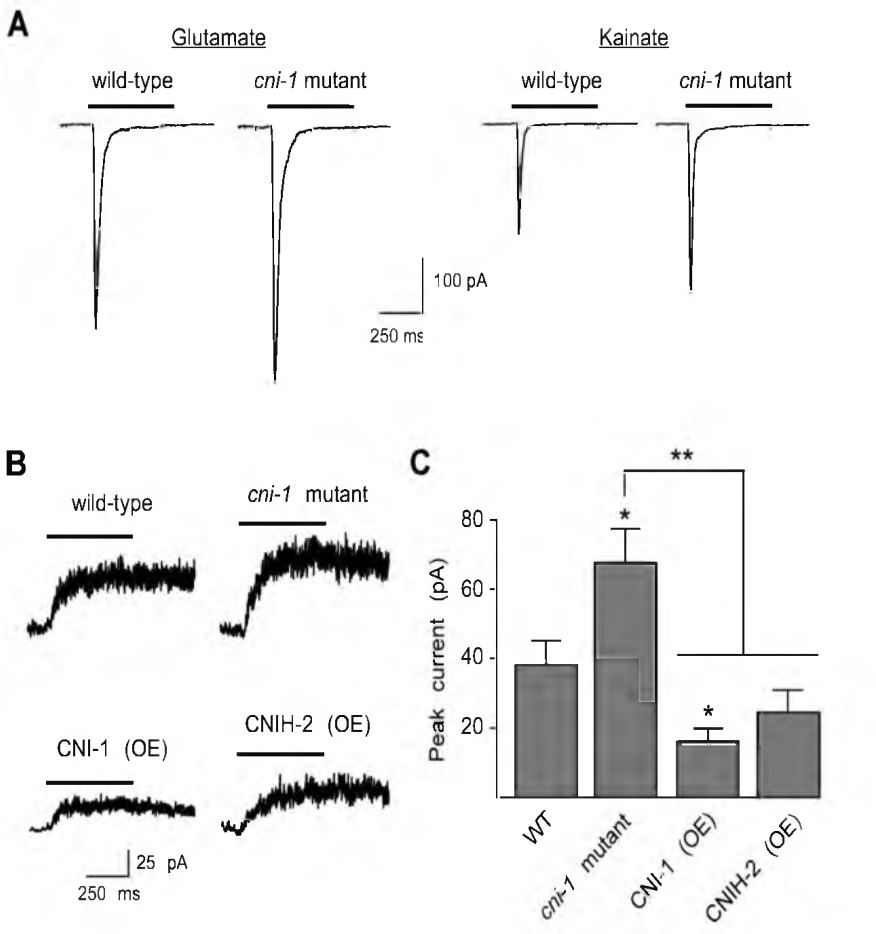


**Figure S3**. Kainate- and NMDA-gated currents are increased in *cni-1* mutants.

Supplemental data associated with Figure 1.

(A) Representative glutamate- and kainate-gated currents in the AVA neurons of wild-type worms and *cni-1* mutants. Cells were voltage-clamped at –60 mV. (B) Currents measured in AVA neurons in response to pressure application of 1 mM NMDA. Cells were voltage-clamped at +40 mV. (C) Average peak NMDA-gated current in wild-type worms (n=9), *cni-1* mutants (n=9) and transgenic mutants that overexpressed either CNI-

1 (n=6) or CNIH-2 (n=6). * Significantly different from wild-type ($p<0.05$). ** $p<0.01$.

Error bars represent SEM.

Supplemental text and figures: Brockie et al.

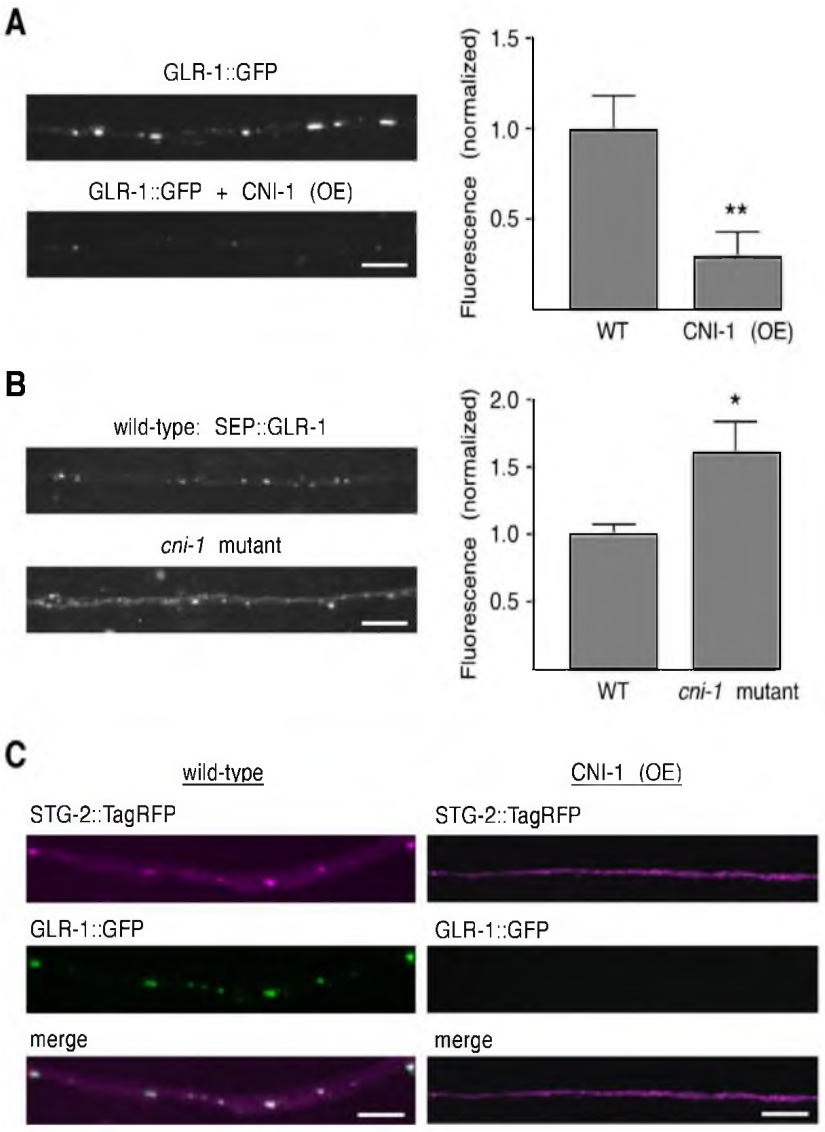


**Figure S4.** GLR-1 surface expression is increased in *cni-1* mutants. Supplemental data associated with Figure 2.

(A) Confocal images of GLR-1::GFP (left) and quantification of GFP fluorescence (right) in the AVA processes of transgenic wild-type worms either with (n=10) or without

(n=12) CNI-1 overexpression. (B) Confocal images of SEP::GLR-1 (left) and quantification of SEP fluorescence (right) in the AVA processes of transgenic wild-type worms (n=10) and *cni-1* mutants (n=9). (C) Confocal images of transgenic wild-type worms that coexpressed STG-2::TagRFP and GLR-1::GFP in AVA either with (right) or without (left) CNI-1 overexpression.

Scale bars represent 5 μm. Significantly different from wild type (* $p<0.05$; ** $p<0.01$). Error bars represent SEM.

Supplemental text and figures: Brockie et al.

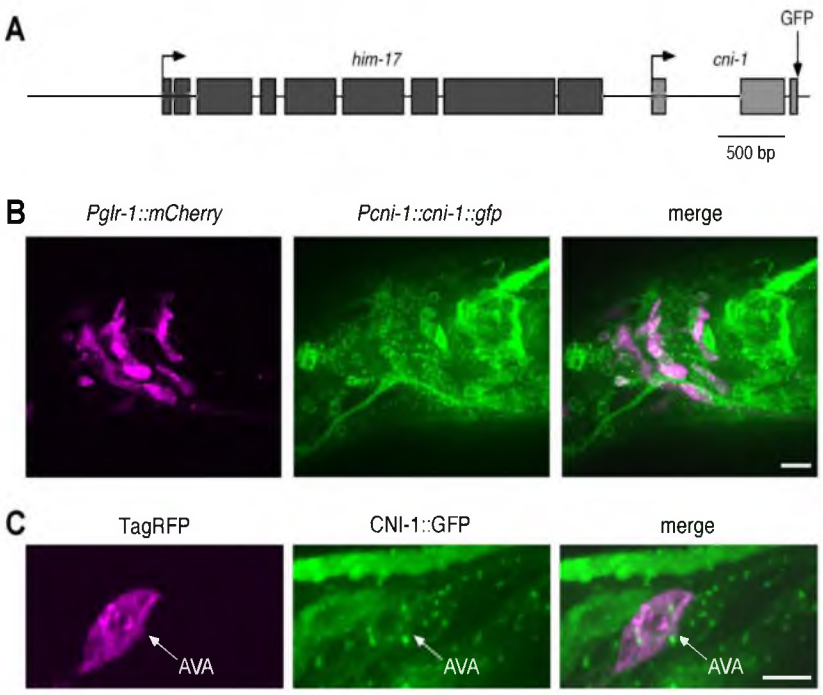


**Figure S5**. CNI-1 is coexpressed with GLR-1 in the nervous system. Supplemental data associated with Figure 4.

(A) Exon and intron organization of the *Pcni-1::cni-1::gfp* reporter construct. *cni-1* is in an operon with the gene *him-17*. A frame shift mutation resulting in an early stop codon was engineered into *him-17* to prevent its expression. (B) Confocal images of neuronal cell bodies in a transgenic worm that expressed *Pglr-1::mCherry* and the CNI-1::GFP reporter construct shown in A. Scale bar represents 10 μm. (C) Confocal images of the CNI-1::GFP reporter and TagRFP expressed in the AVA interneurons under the regulation of the *flp-18* promoter. Scale bar represents 5 μm.

Supplemental text and figures: Brockie et al.

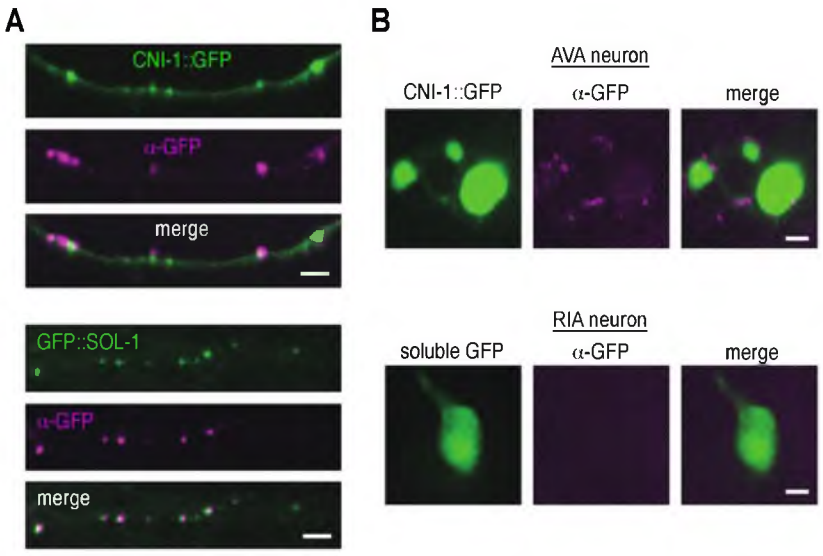


**Figure S6**. CNI-1 is expressed on the cell surface. Supplemental data associated with Figure 5.

(A) Confocal images of transgenic worms that expressed either CNI-1::GFP (top panels) or GFP::SOL-1 (bottom panels) and immunolabeled with an anti-GFP antibody. Scale bars represent 5 μm. (B) Anti-GFP antibody labeling of neuronal cell bodies in transgenic worms that expressed CNI-1::GFP in AVA and soluble GFP in the RIA neurons under regulation of the *glr-3* promoter (Brockie et al., 2001a). Scale bars represent 2 μm.

Supplemental text and figures: Brockie et al.

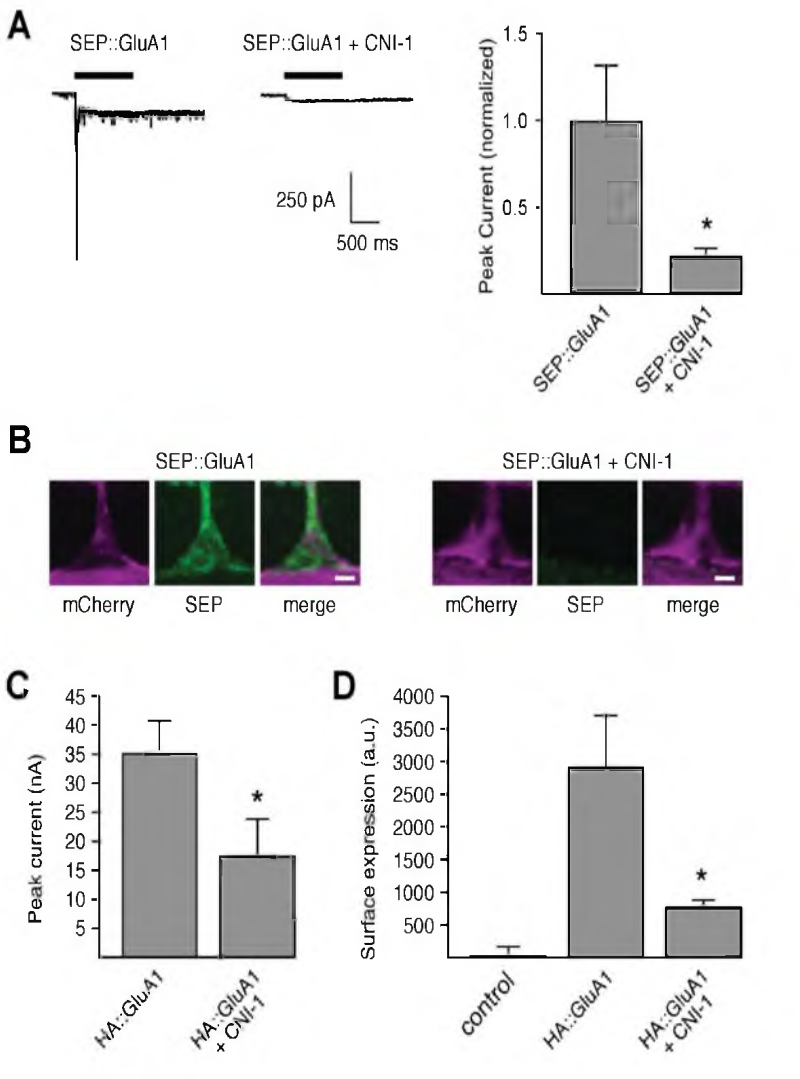


**Figure S7**. CNI-1 reduces glutamate-gated current and GluA1 surface expression.

Supplemental data associated with Figure 7.

(A) Glutamate-gated current in muscle cells of transgenic worms (left) and the average peak glutamate-gated current (right) in muscle cells that expressed SEP::GluA1 (n=8), or SEP::GluA1 and CNI-1 (n=5). Cells were voltage-clamped at –60 mV. * $p<0.05$. (B)

Supplemental text and figures: Brockie et al.

Confocal images of muscle arms in transgenic worms that expressed SEP::GluA1 either with or without CNI-1. Scale bars represent 2 μm. (C and D) Glutamate-gated current in *Xenopus* oocytes (C) and GluA1 surface expression (D) in non-injected control oocytes (n=9) or in oocytes that expressed HA::GluA1 either alone or coexpressed with CNI-1 (n=8). Significantly different from HA::GluA1 alone (* $p<0.05$).

Error bars represent SEM.

Supplemental text and figures: Brockie et al.

**Supplemental experimental procedures**

**Plasmids**. The following plasmids were used to generate transgenic worms: pPB1, *Pnmr-1::gfp*; pJM23, *lin-15(+)*; pDM1915, *Pflp-18::cni-1* (cDNA); pDM1196, *Pnmr-1::mCherry*; pDM1971, *Pflp-18::cnih-2* (cDNA); pDM2055, *Pflp-18::Erv14p* (cDNA); pDM1437, *Prig-3::HA::glr-1::gfp*; PEgl20RFP, *Pegl-20::rfp*; pDAM17, *Prig-3::gfp::sol-1*; pCT26, *Pflp-18::mTFP::pisy-1*; pDM1930, *Pflp-18::cni-1::TagRFP*; pDM1556, *Prig-3::glr-1::mCherry*; pDM1911, *Pflp-18::cni-1::gfp*; pCSW44-1, *Pglr-3::gfp*; pDM2060, *Pflp-18::mCherry::sec-24.1*; PEgl20YFP, *Pegl-20::yfp*; pDM1941, *Prig-3::stg-2::TagRFP*; pCT61, *Pegl-20::nls::dsRed*; pDM1965, *Pflp-18::cni-1::sep*; pDM1843, *Pcni-1::cni-1::gfp*; pYZ318, *Pmyo-3::HA::glr-1::gfp*; pYZ146, *Pmyo-3::sol-1*; pDM796, *Pmyo-3::stg-1*; pDM1893, *Pmyo-3::cni-1*; pDM1879, *Pmyo-3::cnih-2*; pCFJ104, *Pmyo-3::mCherry* (a gift from C. Frøkjær-Jensen); pDM1962, *Pmyo-3::sep::GluA1(flip)*; and pCT27, *Pflp-18::TagRFP::tram-1*; pDM1284, *Pglr-1::mCherry*; pDM1982, *Pflp-18::cnih-1*; pDM2100, *Prig-3::gfp::GluA1(flip)*; pDM2076, *Pflp-18::cnih-2::mCherry*; pDM2096, *Pflp-18::γ-8*; pDM2024, *Prig-3::pHTomato::glr-1*. The following plasmids were used in experiments with *Xenopus* oocytes: pDM2001, HA::GLR-1; pDM350, SOL-1; pDM654, STG-1; pCSW174, CNI-1; pDM2105, CNI-1::GFP; HA::GluA1(flip); HA::GluA2; Neto2 and CNIH-2.

**Transgenic arrays**. The transgenic arrays used were *akIs1*, *Pnmr-1::gfp + lin-15(+)*; *akEx2833*, *Pflp-18::cni-1 + Pnmr-1::mCherry*; *akEx3104*, *Pflp-18::cnih-2 + Pnmr-1::gfp*; *akEx3173*, *Pflp-18::Erv14p + Pnmr-1::mCherry*; *akEx3174*, *Pflp-18::Erv14p + Pnmr-1::mCherry*; *akIs141*, *Prig-3::HA::glr-1::gfp + lin-15(+)*; *akEx2740*, *Pflp-18::cni-*

*1 + Pegl-20::rfp*; *akEx2918*, *Pflp-18::cnih-2 + Pnmr-1::mCherry*; *akEx3172*, *Pflp-18::Erv14p + Pnmr-1::mCherry*; *akSi32*, *Prig-3::gfp::sol-1*; *akEx3117, Pnmr-1::mCherry + Pflp-18::cni-1*; *akSi18*, *Pflp-18::mTFP::pisy-1*; *akEx3160*, *Pflp-18::cni-1::TagRFP + Pegl-20::yfp*; *akEx1097*, *Prig-3::glr-1::mCherry + lin-15(+)*; *akEx2719*, *Pflp-18::cni-1::gfp + Pglr-3::gfp*; *akEx3159*, *Pflp-18::cni-1::gfp + Pflp-18::mCherry::sec-24 + Pegl-20::yfp*; *akEx3169*, *Pflp-18::mCherry::sec-24 + Pegl-20::yfp*; *akEx3089*, *Prig3::stg-2::TagRFP + Pegl-20::nls::dsRed*; *akEx3097*, *Pflp-18::cni-1::sep + Pegl-20::nls::dsRed*; *akEx3047*, *Pcni-1::cni-1::gfp + lin-15(+)*; *akEx3189*, *Pmyo-3::HA::glr-1::gfp + Pmyo-3::sol-1 + Pmyo-3::stg-1 + Pmyo-3::mCherry + lin-15(+)*; *akEx3205*, *Pmyo-3::HA::glr-1::gfp + Pmyo-3::sol-1 + Pmyo-3::stg-1 + Pmyo-3::cni-1 + Pmyo-3::mCherry + lin-15(+)*; *akEx3206, Pmyo-3::HA::glr-1::gfp + Pmyo-3::sol-1 + Pmyo-3::stg-1 + Pmyo-3::cnih-2 + Pmyo-3::mCherry + lin-15(+)*; *akSi17*, *Pflp-18::TagRFP::tram-1*; *akEx3184*, *Pmyo-3::sep::GluA1 + Pmyo-3::mCherry + lin-15(+)*; and *akEx3203*, *Pmyo-3::sep::GluA1 + Pmyo-3::cni-1 + Pmyo-3::mCherry + lin-15(+)*; *akEx3326*, *Prig::gfp::GluA1(flip) + Pflp-18::γ-8 + Pflp-18::cnih-1 + Pnmr-1::mCherry*, *akEx3327*, *Prig-3::gfp::GluA1(flip) + Pflp-18::γ-8 + Pflp-18::cni-1::TagRFP + Pegl-20::nls::dsRed*; *akEx3328*, *Prig-3::gfp::GluA1(flip) + Pflp-18::γ-8 + Pflp-18::cnih-2::mCherry + Pegl-20::nls::dsRed*; *akEx3329*, *Pcni-1::cni-1::gfp + Pglr-1::mCherry*; *akEx3331*, *Prig::gfp::GluA1(flip) + Pflp-18::γ-8 + Pnmr-1::mCherry*; *akEx3332*, *Prig-3::pHTomato::glr-1 + Pflp-18::cni-1::sep + Pegl-20::yfp*; *akEx3336*, *Pflp-18::cni-1 + Pegl-20::yfp*.

Supplemental text and figures: Brockie et al.

**Mutant alleles**. The mutant alleles used in this study were *glr-1(ky176)* (Maricq et al., 1995), *cni-1(tm4274)*, *sol-1(ak63)* (Zheng et al., 2004), *stg-2(ak134)* (Wang et al., 2008), *eat-4(ak75)* (Grunwald et al., 2004) and *lin-15(n765ts)* (Ferguson and Horvitz, 1985). Wild-type worms were the N2 Bristol ancestral strain.

**Quantification of fluorescence**. Synaptic puncta were identified by line-scan analysis of the fluorescence intensity using a criterion of 4 standard deviations above the interpunctal fluorescence. The portion of the linescan corresponding to a puncta was fit using a polynomial function to the natural logarithm of the data. The fluorescence of a synaptic puncta was determined by calculating the area under the curve of the fitted polynomial. The total fluorescence was calculated as the average synaptic puncta fluorescence multiplied by the puncta density.

**Supplemental references**

Ferguson, E.L., and Horvitz, H.R. (1985). Identification and characterization of 22 genes that affect the vulval cell lineages of the nematode Caenorhabditis elegans. Genetics *110*, 17-72.

Grunwald, M.E., Mellem, J.E., Strutz, N., Maricq, A.V., and Kaplan, J.M. (2004). Clathrin-mediated endocytosis is required for compensatory regulation of GLR-1 glutamate receptors after activity blockade. Proc Natl Acad Sci U S A *101*, 3190-3195.

Maricq, A.V., Peckol, E., Driscoll, M., and Bargmann, C.I. (1995). Mechanosensory signalling in C. elegans mediated by the GLR-1 glutamate receptor. Nature *378*, 78-81.

Wang, R., Walker, C.S., Brockie, P.J., Francis, M.M., Mellem, J.E., Madsen, D.M., and Maricq, A.V. (2008). Evolutionary conserved role for TARPs in the gating of glutamate receptors and tuning of synaptic function. Neuron *59*, 997-1008.

Zheng, Y., Mellem, J.E., Brockie, P.J., Madsen, D.M., and Maricq, A.V. (2004). SOL-1 is a CUB-domain protein required for GLR-1 glutamate receptor function in C. elegans. Nature *427*, 451-457.